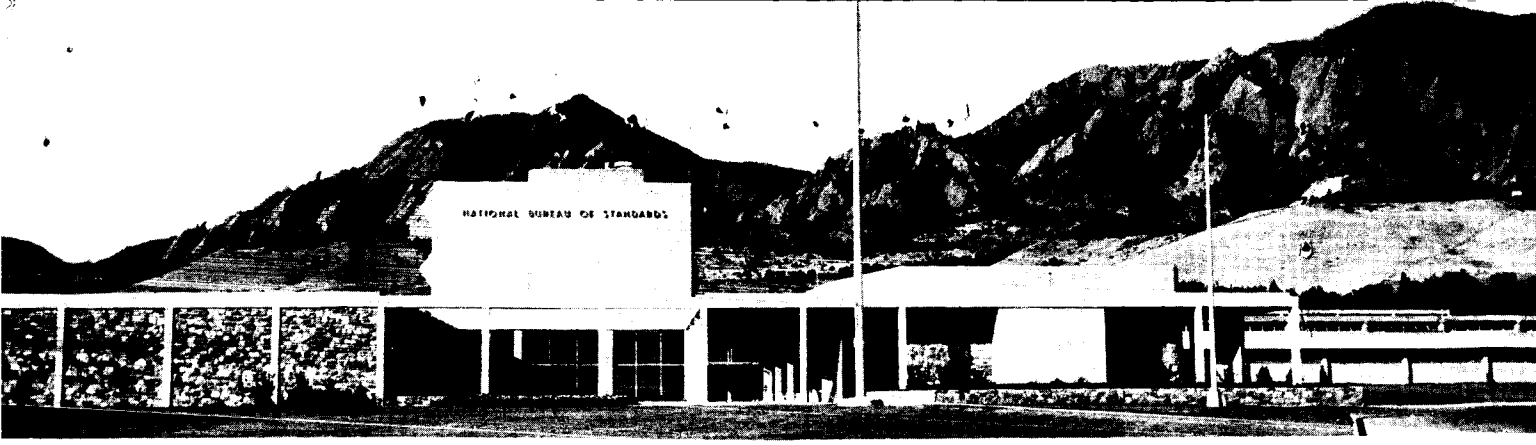

NBS REPORT

8497

STATISTICAL PATTERNS OF LARGE PARABOLIC ANTENNAS

by

D. E. Culnan and R. E. Skerjanec

U. S. DEPARTMENT OF COMMERCE
NATIONAL BUREAU OF STANDARDS
BOULDER LABORATORIES
Boulder, Colorado

THE NATIONAL BUREAU OF STANDARDS

The National Bureau of Standards is a principal focal point in the Federal Government for assuring maximum application of the physical and engineering sciences to the advancement of technology in industry and commerce. Its responsibilities include development and maintenance of the national standards of measurement, and the provisions of means for making measurements consistent with those standards; determination of physical constants and properties of materials; development of methods for testing materials, mechanisms, and structures, and making such tests as may be necessary, particularly for government agencies; cooperation in the establishment of standard practices for incorporation in codes and specifications; advisory service to government agencies on scientific and technical problems; invention and development of devices to serve special needs of the Government; assistance to industry, business, and consumers in the development and acceptance of commercial standards and simplified trade practice recommendations; administration of programs in cooperation with United States business groups and standards organizations for the development of international standards of practice; and maintenance of a clearinghouse for the collection and dissemination of scientific, technical, and engineering information. The scope of the Bureau's activities is suggested in the following listing of its four Institutes and their organizational units.

Institute for Basic Standards. Electricity. Metrology. Heat. Radiation Physics. Mechanics. Applied Mathematics. Atomic Physics. Physical Chemistry. Laboratory Astrophysics.* Radio Standards Laboratory: Radio Standards Physics; Radio Standards Engineering.** Office of Standard Reference Data.

Institute for Materials Research. Analytical Chemistry. Polymers. Metallurgy. Inorganic Materials. Reactor Radiations. Cryogenics.** Office of Standard Reference Materials.

Central Radio Propagation Laboratory.** Ionosphere Research and Propagation. Troposphere and Space Telecommunications. Radio Systems. Upper Atmosphere and Space Physics.

Institute for Applied Technology. Textiles and Apparel Technology Center. Building Research. Industrial Equipment. Information Technology. Performance Test Development. Instrumentation. Transport Systems. Office of Technical Services. Office of Weights and Measures. Office of Engineering Standards. Office of Industrial Services.

---

* NBS Group, Joint Institute for Laboratory Astrophysics at the University of Colorado.
** Located at Boulder, Colorado.

NATIONAL BUREAU OF STANDARDS REPORT

NBS PROJECT 58370-12-5830572

October 29, 1964

NBS REPORT 8497

STATISTICAL PATTERNS OF LARGE PARABOLIC ANTENNAS

by

D. E. Culnan and R. E. Skerjanec

U.S. DEPARTMENT OF COMMERCE

NATIONAL BUREAU OF STANDARDS

TABLE OF CONTENTS

Tables

Figures

ABSTRACT

15330

Antenna pattern measurements were made to examine the statistical distribution of relative gain for 18 meter diameter parabolic reflectors at 4.85 and 9.1 GHz. Such information is needed to predict the probability of interference from a frequency sharing transmitter being forward scattered into a space telecommunications antenna. Patterns were recorded on magnetic tape as the test antenna was rotated through all azimuth-elevation mount positions relative to a far field target exciter. Relative gain was analyzed in 2 db increments by random sampling data for each 5^{o} by 5^{o} block of the hemisphere. Weighting was applied to produce uniform spacing of data samples and to reject low elevation angles. Relative gain patterns for two antennas over four earth profiles are similar and gain is approximately normally distributed. The report includes statistical medians, stardard deviations, cumulative distributions, and patterns for vertical, horizontal, and cross polarization at both frequencies.

STATISTICAL PATTERNS OF LARGE PARABOLIC ANTENNAS

D. E. Culnan and R. E. Skerjanec

1. INTRODUCTION

Radio system propagation studies and interference evaluations require as one element the relative gain pattern of the antennas employed. Antenna parameters that are estimated or measured for large parabolic reflectors of the type employed in space vehicle telecommunications and tracking usually are limited to main-lobe relative gain and degree of suppression of primary side lobes. While such parameters are adequate for main-lobe path antenna gain considerations, estimates of interference probability require a description of minor lobes of the antenna and the effect of specified environmental factors upon the entire antenna gain pattern. Because the usual antenna environment involves the reflection, refraction, and absorption of microwaves by many complex time-varying factors, even the estimation of fine-grain backlobe characteristics by computer programming techniques is not presently available.

The antenna pattern measurements covered by this investigation include sets of patterns taken with two 18 m diameter parabolic reflectors over a total of four different typical terrain profiles. The purpose was to examine the statistical distributions of relative gain over all available azimuth and elevation angles to determine if general descriptions existed. An illustrative application of general statistical

pattern descriptions would be to estimate the probability that antenna relative gain would exceed the level of 60 db below main lobe gain for 50 percent of the sampled solid angle for given antenna elevations and azimuths. Such information is needed, for example, to predict the probability of interference due to unwanted signals from a distant source being forward scattered into a space telecommunications receiving antenna. Appendix A shows an application of the entire statistical distribution to an interference problem.

The general procedure followed included selection of exciter locations to provide suitable terrain profiles, measurement and recording of received power level at the antenna terminals as the antenna was driven through all available elevations and azimuth angles, and analysis of the recorded data. The data analysis segregated antenna gain into 2-db increments for each spherical 5^{o}-by-5^{o} area. Conventional antenna patterns plots are also available. Over 2900 single sweep patterns were required to record the data for the two frequencies, two or more polarizations, and four sites used.

2. MEASUREMENT METHODS

Methods for measuring the patterns of microwave antennas to examine main-lobe gain and principal side lobes are well established [Cutler, King, and Koch, 1947]. The preferred technique requires (1) an elevated range without significant ground or object reflections, (2) sufficient separation to provide a nearly plane incident wave front, (3) a suitable target exciter, (4) an azimuth-elevation mount and position recorder, and (5) a stable receiver with calibrated power levels and data recording equipment. In the case of an 18 m diameter parabolic antenna, a separation of 21 km is required to produce an incident

wave-front plane to within $\lambda/16$ at the frequency of 9.1 GHz. Adequate elimination of ground reflections at this range can be obtained only by use of an airborne exciter, which was not available for these measurements.

Since the purpose of this project was to determine antenna gain for unwanted signals from ground-based sources, the most available pattern measurement involved combination of ground terrain effects and antenna gain. Surrounding ground environment is an important factor in the pattern of an antenna of this size, and the antenna pattern as measured on an antenna range which controls or minimizes ground reflections, if available, would still require measurement or estimation of factors such as multipath coupling loss, height gain function, and obstacle gain [Campanella, et al., 1962]. Fortunately, a variety of terrain profiles were available so that typical line-of-sight, several grazing paths, and an obstacle path were provided. For most interference problems, one or more of these test profiles should be similar enough for estimation of antenna pattern and gain. Measurements were made at 4.85 and 9.1 GHz to provide descriptions that can be used in the 3-to-12 GHz frequency allocations reserved for space telecommunications.

Gain measurement of microwave antennas is usually accomplished by comparisons to a standard gain horn. In the case of large antennas, these comparisons are only of qualitative value, because height gain functions affect both the horn and the other antenna, but in different ways because the horn beamwidth is considerably wider. The present pattern measurements are referenced to main-lobe gain when the receiver and the exciter antennas are directed toward each other and adjusted for maximum signal. This method provided a stable basis for side-lobe measurement.

In measuring a statistical pattern, sufficient data points are needed to describe the frequency of occurrence of components of gain as the antenna is rotated. While the antennas tested can be rotated at very low angular rates, wind forces and mechanical tolerances did not permit a uniform distribution of data at speeds of less than 30' per second. A practical limit for taking the quantity of patterns needed also prohibited the use of very low angular rates. A rate of 36^{o} per minute, the maximum available speed, was tried and proved to be satisfactory for information bandwidth requirements. The theoretical main-lobe beam width between half-power points for an 18-meter parabolic antenna at 9.1 GHz is 7.8', although the actual measured beam width was about 15'. Considering the lobes as being sinusoidal, a sweep rate of 36^{o} per minute would require a digital information rate of about 6 Hz to retain all data, as the smallest lobes and nulls were about 9' wide. Since the magnetic tape recording used has a bandwidth in excess of 100 Hz and the pen recorders are capable of 20 Hz, the maximum sweep rate proved to be satisfactory for recording the fine-grain details of the patterns.

Stability of signals during pattern measurement is affected by mechanical vibration of the antennas, electrical stability of the exciter and receiver equipment, and by propagation attenuation and multipath phase changes. If a signal fluctuation exists, there is a choice of rejecting the data or attempting to average out the unwanted variations. An averaging technique was considered which would sample the analog data at invervals of 1.3' of azimuth and take the mean of four adjacent samples. During preliminary tests, it was found that the signal stability could be held to better than ±1 db over the time required to record a pattern. It was decided to avoid the complexity of averaging during

data processing by monitoring pattern quality and operating only when signal stability was acceptable. Serious delays were encountered from signal fluctuation only during unusual atmospheric conditions in midwinter and on a few days when high winds caused severe mechanical vibration of both exciter and receiver antennas.

Data sampling for statistical antenna patterns can be either time distributed or spaced at uniform azimuth intervals. Because the antennas being measured do not rotate at sufficiently uniform angular rates under even moderate wind conditions, data sampling at equal azimuth intervals was selected. This was done by placing pulses on a magnetic tape channel at intervals of 1.3' of aximuth which could be used for data sample triggers. This rate was consistent with the expected lobe width and used the full resolution capacity of the antenna servo system. Other azimuth marks at 5^{o} intervals were planned so that the pattern data could be segregated in 5^{o} arcs, each of which provided an effective random sample over a $5^{o} \times 5^{o}$ block for analysis. It is possible to break the data into a larger number of blocks in azimuth, but this does not appear warranted except at the main lobe and two principal back lobes. To obtain a true statistical distribution of antenna gain, data sampling points must be completely random in spacing. Either time or angle spaced sample points will meet this requirement providing that lobe spacing does not happen to coincide with a series of chosen sample spaces. The measurement limits of 0^{o} and 90^{o} elevation require special attention. No problems are involved with this parabolic reflector at 90^{o} elevation as the pattern shows the data points to be random samples. At 0^{o} elevation, the main lobe is encountered and antenna gains of less than 24 db below main lobe level are given undue weight in the sampling. This can be corrected by

considering the main lobe as a symmetrical pencil beam and a new sample space synthesized which adds data points at many elevations near 0^{o}.

In planning these pattern measurements it was soon apparent that a set of general patterns could not include all the factors that will be important to specific interference calculations. Two practical approaches are available for specific problems which require more refined antenna patterns. If the antenna is available, additional statistical patterns could be measured using the proper wavelength, polarization, and ground environment. The area of a signal source can be simulated by summation of groups of adjacent sample points during data processing. Some elevated angles of arrival can be obtained by locating a target generator on a captive balloon or mountain peak. In most instances it will be impractical to make such measurements and theoretical estimates must be used. Signal sources of any desired angular area can be simulated with the magnetic tape data, and areas of $5^{o} \times 5^{o}$ or its multiples can be summed directly from the punched cards. Low angles of arrival will not produce as large a variation from horizon signals as are caused by the unknown height gain function inherent in each site. Lacking complete knowledge of all antenna and propagation factors, it will be necessary to include an uncertainty factor of 5 or 10 db in resulting interference estimates.

3. MEASUREMENT SYSTEM DESCRIPTION

3.1 General Requirements

For far-field measurements, the antenna range is commonly dictated by the relation $R = D^{2}/\lambda$, where R is the range between the transmitter and receiver, D is the largest antenna aperture dimension,

and λ is the wavelength. In this case, at 9.1 GHz, the minimum length is 21 km. Transmission loss for this length of free space range may be calculated by well known methods.

$$L_{bf} = 32.45 + 20 \log f_{MHz} + 20 \log d_{km},$$

where f_{MHz} is frequency in MHz, and d_{km} is antenna range in kilometers.

Target transmitter power must be sufficient to provide the required signal-to-noise ratio and null measurement dynamic range at the receiver. A system "gain-loss" chart similar to Fig. 1 is helpful. In choosing a target transmitter antenna, several compromises have to be made. The antenna should have as narrow a beam as possible to provide maximum gain and eliminate reflections from nearby obstacles and the ground surface. However, if the transmitting antenna is too large, uniform illumination across the test antenna aperture will be difficult to obtain. Once the antenna is chosen, the gain should be measured and calculations verified.

The receiver system is composed of the test antenna, RF transmission line, waveguide precision attenuator, superheterodyne receiver, and recording circuits. The test antennas and receivers are described in subsequent sections. Graphical records were obtained on an automatic pattern recorder and a two-channel rectilinear recorder. An external servo system driven by the antenna synchro provided positional drive for the automatic pattern recorder and position information for the magnetic tape recorder and rectilinear recorder. Signal level of both receiver frequencies, time, waveguide attenuator settings, and antenna position were recorded on a 14-channel magnetic tape recorder.

The basic measurement apparatus list included the following items:

A. At Target Site

1) CW transmitter with variable output power

2) Transmitting antenna and mount

B. At Test Antenna

3) Motor-operated antenna pedestal, remotely controlled

4) Synchro repeaters for angular position

5) Servo-driven position readouts for recording equipment

6) Servo-driven automatic pattern recorder

7) Precision-calibrated attenuator

8) CW Superheterodyne receiver

9) Strip-chart recorder

10) 14-channel magnetic tape recorder

Photographs of the receiver equipment are shown in Figs. 2 and 3. If patterns of more than one large antenna are to be measured, receiver equipment must be suitable for installation in a mobile van. When a variety of profiles are to be used, the transmitter must be mobile and preferably use an engine-driven power source. For these measurements, all equipment was mobile when needed.

3.2 Antennas and Environment

The antennas measured were 18 m parabolic reflectors on an azimuth-elevation mount. The reflector has a focal length of 7.5 m and is constructed of perforated aluminum with maximum opening diameter of 6.4 mm. The specified maximum deviation from true parabolic shape was ±6.4 mm when the antennas were erected in 1958. While the antennas were intended for use in the 200 MHz to 3 GHz frequency range, satisfactory operation was obtained at 4.85 and 9.1 GHz

with reduced antenna efficiency. The feed assembly is supported by three fiberglass spars and will accommodate a variety of feeds. Waveguides and coaxial lines are attached to the spars and can be routed through rotary joints. For multiple frequency use above 2 GHz, flexible waveguides around the rotary joints were used. The antennas are motor driven and remotely controlled with a maximum azimuth slew rate of 36^{o} per minute. Antenna positions are synchro repeated. The specified precision of the servos is 2' for tracking and position indication.

The reflector feed is a dual-frequency assembly employing a small X-band horn with two C-band H-plane slots, one on each side of the horn, and backed by a small ground plane as shown in Fig. 4. The feed at 9.1 GHz has a gain of 5 db and provides edge illumination assymetrically down 5 to 10 db. At 4.85 GHz the gain is 8 db and edge illumination is down 12 db symetrically.

The antenna environment was left in its previous operational state. No attempt was made to clear the nearby area of obstacles such as maintenance towers, communication antennas, and other such structures. The antenna at Haswell, Colorado, Fig. 3, is located on smooth terrain in a bowl-shaped area. The one large obstacle that could alter incident plane waves was a 500' tower located about 600' from the antenna. The antenna at the T-22 site, Boulder, Colorado, is located on a corner of a large mesa.

3.3 Receiver System

3.3.1 Receiver (9.1 GHz)

A complete block diagram of the receiver is shown in Fig. 5. Basically, it is a conventional double-conversion superheterodyne receiver with a first IF of 9.9 MHz and a second IF of 100 kHz. The receiver has a bandwidth of 850 Hz, which requires a high degree of

frequency stabilization of the first local oscillator klystron. The latter is accomplished by a phase-type AFC loop consisting of a 10 MHz reference oscillator, a X10 balanced multiplier, a X91 multiplier, and a phase discriminator. The 10 MHz reference oscillator is a crystal-controlled oscillator with a 24-hour frequency stability of 5 parts in 10^{10}. The phase discriminator output is applied as an error signal to the repeller of the klystron and in this manner the local oscillator frequency is held to the approximate stability of the reference oscillator.

The first IF amplifier consists of two amplifier stages, each with feedback for gain stability. The second mixer and IF amplifier are feedback coupled for best gain stability. The 850 Hz bandwidth is established with tuned circuits in the second IF stages and provided with an optional crystal filter with 50 Hz bandwidth, which was not used in these measurements.

The input of the receiver is provided with a 0-50 db calibrated variable attenuator, plus a 0-10 db calibrated attenuator at the target transmitter. This signal attenuation and the usable dynamic range of the receiver proper of approximately 25 db give an over-all measurement dynamic range of 85 db.

Also at the input, as an in-line component, is a 9.1 GHz calibrated noise source to establish a reference signal level. This tube is a small gaseous noise generator of the argon type with a very low VSWR in the extinguished state. When fired, it provides a broad-band noise spectrum of a fixed excess noise ratio of 14.6 db. The excess noise level and receiver noise level provide constant reference levels for daily receiver system calibration which is not dependent on critical frequency matching.

More detailed information on this receiver is available [Hubbard and Cateora, 1961].

Following is a list of receiver specifications:

1) Operating frequency - 9.1 GHz
2) Receiver type - double-conversion superheterodyne
3) Bandwidth - 850 Hz
4) Noise figure - 14 db
5) Sensitivity (measured 3 db above excess noise) - 121 dbm
6) Dynamic Range - 85 db: 25 db receiver; 60 db in-line attenuators
7) Local Oscillator Stability - $\approx$ 5 parts in 10^{10} per day
8) Intermediate Frequencies - First: 9.9 MHz; Second: 100 kHz.

3.3.2 Receiver (4.85 GHz)

A complete block diagram of the receiver is shown in Fig. 6. The receiver is a modified commercial troposcatter receiver. Basically, it is a double-conversion superhetrodyne receiver with a first IF of 70 MHz and a second IF of 99 kHz. The receiver has a bandwidth of 3600 Hz which requires a high degree of frequency stabilization of the first local oscillator. This is accomplished by a phase-type AFC loop consisting of 4 MHz reference oscillator, a X12 solid-state multiplier, a X3 vacuum tube multiplier, a X33 disc planar triode multiplier, and a phase discriminator. The 4 MHz reference oscillator is a crystal-controlled oscillator with a stability of 1 part in 10^8 per day. The phase discriminator output is applied through a current amplifier as an error signal to the resonator of the oscillator tube. The planar triode multiplier, the AFC mixer, and LO tube are mounted on a microwave block.

The first IF mixer, also mounted on the above-mentioned microwave block, employs a balanced pair of microwave crystal mixer diodes and a five-stage broadband pre-amp. The microwave block contains waveguide filters to suppress the image frequency. The 70

MHz IF amplifier is a five-stage broadband amplifier. The second local oscillator, at 3.88 MHz, is multiplied and mixed with the 70 MHz IF. The second mixer and 99 kHz IF amplifier are feedback coupled for maximum gain stability. The 3600 Hz bandwidth is established with tuned circuits in the second IF stages.

The receiver input is provided with a 0-50 db variable calibrated attenuator and the target transmitter contains a 0-10 db calibrated attenuator. This total of 60 db with a 25 db usable dynamic range of the receiver proper gives an overall measurement dynamic range of 85 db.

Also at the input is a 4.85 GHz waveguide-mounted calibrated noise source of the argon gas type. In the fired state, it provides a broadband noise spectrum at a fixed excess noise ratio of 15.2 db.

Following is a list of receiver specifications:

1) Operating frequency - 4.855 GHz
2) Receiver Type - double-conversion superhetrodyne
3) Bandwidth - 3600 Hz
4) Noise Figure - 13 db
5) Sensitivity (measured 3 db above excess noise) - 117 dbm
6) Dynamic range - 85 db: 25 db receiver; 60 db in-line attenuators
7) Local Oscillator Stability - $\approx$ 1 part in 10^8 per day
8) Intermediate Frequencies - First: 70 MHz; Second: 99 kHz.

3.4 Target Generator

The target generators were installed in a small trailer house and powered by a small diesel-powered generator. (See Fig. 7). The transmitter system was made as portable as possible to minimize moving time from site to site. The trailer also housed communications equipment at 41.34 MHz for operations contact with the receiver site.

A complete block diagram of the 9.1 GHz CW transmitter is shown in Fig. 8. The transmitter is essentially the local oscillator from the 9.1 GHz receiver as described in Section 3.3. The transmitter consists of a 40 mW klystron phase locked to a stable reference oscillator with a 24-hour frequency stability of 5 parts in 10^{10}.

The 4.85 GHz, CW transmitter is shown in Fig. 9 in block diagram form. The transmitter consists of a 125 mW heil tube mounted in a waveguide block and phase locked to a stable reference oscillator with a stability of 1 part in 10^{8} per day. The transmitter is essentially the same as the receiver local oscillator circuit described in Section 3.3. The transmitters are shown in Fig. 10.

The 9.1 GHz antenna used an 0.46 m parabolic reflector with a gain of 27 db and a 3-db beamwidth of 5.1°. The 4.85 GHz antenna used a 1.22 m parabolic reflector with gain of 30 db and a beamwidth of 3.6°. The antennas (Fig. 11) were mounted on a table and guyed securely for mechanical stability. The antennas were individually adjustable over a 60° azimuth range and a 10° elevation range. The antennas were aligned manually to provide for maximum signal at the receiver.

4. DATA COLLECTION PROCEDURE

4.1 Site Selection

Preliminary site selection, with the restrictions of a minimum distance of 21 km and line-of-sight paths, was done on topographic maps. Upon satisfactory field inspection, each site-to-receiver profile was plotted from topographic maps on special graph paper using 4/3 earth radius to compensate for standard atmospheric refraction. Inconsistencies were found using some topographic maps and if more precise profiles are needed, surveys should be made over the paths.

Pertinent data for each profile was measured or computed. These include R, the antenna range in kilometers; h_t and h_r, the transmitter and receiver heights in meters above mean sea level; θ_{et} and θ_{er}, the transmitter and receiver take-off angles in minutes; and $L_{bf(x)}$ and $L_{bf(c)}$, the 9.1 GHz and 4.85 GHz path losses. Figures 12 and 13 show the target locations for each site.

The Firestone-to-T-22 profile (Fig. 14) is a line-of-sight path. The Matterhorn-to-T-22 profile (Fig. 15) is nearly line-of-sight with grazing incidence across the level area where the receiver is located. The E-1-to-Haswell profile (Fig. 16) is slightly beyond optical line of sight, and possibly an obstacle path. The E-2-to-Haswell profile (Fig. 17) is a typical grazing incidence path. Site locations are shown in Table 1. For most interference conditions, one or more of these four profiles may be used for an estimation of antenna directive gain distributions. Figures 3, 18, and 19 show the ground environment surrounding the test antennas.

Table 1

	Latitude	Longitude
Boulder, Colorado		
Receiver Site		
Boulder	40° 08' 53.76" N	105° 13' 53.19" W
Transmitter Site		
Matterhorn	39° 56' 7.4 " N	105° 14' 12.3 " W
Firestone	40° 07' 53.5 " N	104° 53' 32.3 " W
Haswell, Colorado		
Receiver Site		
Haswell	38° 22' 51" N	103° 9' 21.15" W
Transmitter Site		
E-1 Haswell	38° 21' 36" N	103° 32' 36" W
E-2 Haswell	38° 33' 36" N	103° 30' 12" W

4.2 Pattern Parameters

Pattern data were taken for horizontal and vertical polarizations from all sites and cross polarization from one site. Full azimuth patterns were taken for 0° to 5° elevations in 1° increments, and from 5° to 90° elevation in 5° increments. A typical pattern at a given elevation consisted of several azimuth passes. These include 360° passes with 0 db and 20 db line attenuation, and 12° passes at main lobe with 20 db, 40 db, and 60 db line attenuation. The 12° passes were made only in the 0° -to-5° elevation interval where main lobe detail was required. Antenna azimuth position was based on 0° at true north with azimuth angle increasing in the clockwise direction. Main lobe azimuths for the four sites were 94° for Firestone, 181° for Matterhorn, 265° for E-1 Haswell, and 303° for E-2 Haswell.

Typical patterns taken on the automatic pattern recorder are shown in Figs. 20-41. The 360° passes with 0 db and the 12° passes at main lobe were recorded for both frequencies. Patterns were placed on the recorder chart by removing attenuation at the recorder to a corresponding amount of attenuation that was added at the RF input line, thus making it possible to overlay successive sweeps of a pattern, to obtain a complete pattern.

Patterns were recorded on a strip-chart recorder as shown in Fig. 42 so that both frequencies could be monitored simultaneously. The two signal channels, a 5° azimuth marker, a good data indicator, and time were recorded. Signal data for statistical analyses were recorded on a 14-channel FM tape recorder. The following data items were FM tape recorded at 500 Hz ± 40% deviation:

Channel No.	Data	Scale Factor	Range
1	Time Marks	1 sec. intervals (AM)	------
2	Ant. El. (Coarse)	1^{o}/2 Hz	100^{o}
3	Ant. Az. (Coarse)	1^{o}/2 Hz	360^{o}
4	Ant. Az. (Fine)	0.75'/1 Hz	5^{o}
5	Ant. Az. (Digital)	1.3'/bit (AM)	5^{o}
6	4.85 GHz Attenuator	1 db/8 Hz	50 db
7	4.85 GHz Signal	1 db/16 Hz	25 db
8	9.1 GHz Attenuator	1 db/8 Hz	50 db
9	9.1 GHz Signal	1 db/16 Hz	25 db
10	Recorder Compensation	----------	------
11	Good Data Indication	On-Off	------

4.3 Calibrations and Data Evaluation

Receiver calibrations were made using the target transmitter as the signal generator. Knowing the bandwidths of the receivers, the KTB level may be calculated for each receiver. An argon gas tube is then fired and the change in receiver output level noted. The target generator is then turned on and the CW signal increased to match the output level of the noise tube. Calculating the KTB level and knowing the excess noise ratio of the gas tube, with appropriate corrections for spurious image response, a db level can be assigned to the matched level. The attenuator is then reduced in steps from the matched excess noise level to complete the calibration.

The primary requisite for good calibrations was a steady signal from the target transmitter. On occasion, unusual atmospheric conditions or mechanical vibration caused by high winds caused a delay in the calibrations, which was a prerequisite to beginning pattern measurements.

Calibration curves for setting analog-to-digital data conversion were plotted as power level against FM tape frequency. Curves were constructed from all calibrations made from one target site. A mean of the curves was then used for calibrating the analog-to-digital converter when sufficiently constant calibrations existed. A separate mean calibration curve was made for each target site, and in a few of the cases where the deviation between daily calibrations was greater than 2 db, separate curves were made for each day. Since the main lobe signal level was used as the reference at frequent intervals, small changes in absolute calibration level were not critical.

Hourly checks of signal level at main lobe were made to monitor signal stability and provide a level for data reduction. Received signal level was held to 1 db variation during the 10 minute period required to record a 360^{o} pattern as the criteria for reliable data.

Main lobe relative gains were measured from several target sites by using the standard gain horn substitution method. The 4.85 GHz standard gain horn had a calibration of 15.2 db, and the 9.1 GHz standard gain horn had a calibration of 21.8 db. The standard gain horns were positioned both at the antenna feed horn ring and on the antenna pedestal. Height gain function contributed by terrain in front of the antenna prevents true free space gain measurement. Table 2 shows the results of the main lobe relative gain measurements.

Table 2

Main Lobe Relative Gain

	Horizontal Polarization	Vertical Polarization
4.85 GHz	46 db	46 db
9.1 GHz	52 db	52 db

5. DATA ANALYSIS

5.1 Analog-to-Digital Conversion

Since each 360^{o} sweep of the antenna produces a recorded signal that contains hundreds of backlobes and nulls at either frequency, some mechanization of data reduction and analysis is mandatory. After giving consideration to characteristics to sample pattern data and the available equipment, the following data parameters were chosen:

1) Recording format-analog
2) Tape carrier frequency - 500 Hz
3) Deviation - ± 40%
4) Signal total dynamic range - 25 DB
5) Analysis dynamic range - 20 DB
6) Sampling trigger interval - 1.35'
7) Sample width - 20 μ sec.
8) Recording tape speed - 0.6 in. per sec.
9) Analysis tape speed - 2.4 in. per sec

System gain was adjusted during calibration so that receiver thermal noise was slightly above the recording threshold, at about 310 Hz. The analysis dynamic range of 20 db covered the deviation frequencies of about 320 Hz to 670 Hz. The tape recording and discriminator characteristics permitted nonlinear recording of an additional 10 db of signal, but the 20 db range chosen proved more stable. To accomodate the 70 db of signal range that exists in the main lobe area, attenuation was added in 20 db increments. When a signal saturated the recording system, that part of the sweep was repeated with 20 db attenuation added. During analysis, each 20 db portion of the data was analyzed separately and the sample space totals were combined.

The chosen form for antenna description and evaluation is a cumulative distribution plot of antenna relative gain levels. Increments of 2 db between levels were dictated by the objective of obtaining as much information on minor lobe structure as possible and the limitation dictated by recording system drift. During periods of stable propagation when usable data were obtained, the recording system exhibited a stability of ± 0.5 db. Data analysis equipment stability was somewhat better than this.

Data analysis was performed by playing back pattern sweeps into a Digital Analyzer (DASY) with a tape transport of the same model used in recording. The DASY automatically segregated data samples into 10 levels covering 20 db of signal range and printed out the number of samples which exceeded each of the levels for each block of data. Block diagrams of the data analysis system are shown in Figs. 43 and 44. The DASY sampled the discriminated analog signal for each azimuth trigger at 1.33' intervals. Each sample is the maximum signal value present during the 20 μ second sampling period, which is 0.2 percent of the data sample space represented.

The procedure followed in digitizing the pattern data included these steps: First, a calibration chart was constructed so that the most favorable 20 db range could be selected between receiver noise and tape saturation levels. The DASY thresholds were then set at 2 db increments to these analog levels using a signal generator. A main lobe absolute calibration record was then located and analyzed with the DASY. These data usually had 60 db of attenuation and the maximum signal established the main lobe reference point. An antenna pattern was then selected from the data log and was identified by the time channel indication and by comparison with the strip chart real time

record. The analog pattern was again recorded on a strip chart from the magnetic tape during analysis, along with the 5^{o} azimuth marks and DASY gate signal to aid in monitoring data quality. This gave a positive record of the analog pattern that was being digitized.

Several passes through the tape were required to allow for DASY printout time after each 5^{o} azimuth block. When a printout indicated that signals in excess of the 20 db range were present, an adjacent recording with 20 db attenuation was also analyzed. A typical DASY printout record is shown in Fig. 45. Relative power values were assigned to each DASY level based on the attenuation used and the value of main lobe maximum signal. During recording, the main lobe calibrations were repeated several times a day. In most instances, it was not necessary to determine which main lobe calibration applied, as these calibrations remained very constant for several days of pattern data. Data on the DASY printout record were transferred to punch cards for further processing.

5.2 Computer Program

After editing the DASY tapes for correct printing and reasonable continuity of the data from the 0 db attenuation to 20 db attenuation and higher, the azimuth blocks were numbered and the calibration value written on the identification to each tape. The data were then punched on IBM cards with one card for each 5^{o} azimuth block. The data card format is shown in Fig. 46. After completion of punching of a group, the cards were verified and then sorted according to azimuth block number, elevation, and attenuation.

The computer program was written in Fortran language. An IBM 1401 electronic data processor prepared the program and data for the large scale computer, an IBM 7090. The computer converted each sampling level to db below main lobe. A summation was made of the

sampling counts for each sampling level and a percentage taken for each attenuation level and each elevation.

As a subroutine, a summation was made for each sampling level for each elevation. The summations were then weighted and percentages calculated for each sample level for all elevations.

The weighting procedures were applied as stated below.

Weight No. 0

This is a non-weighting subroutine that sums the values for all attenuation levels and all elevations as recorded at equal azimuth intervals and the elevations chosen.

Weight No. 1

This weighting procedure was used to obtain an even distribution of data points with elevation. All data are weighted according to the elevation angle as follows:

Angle	Weight
0° or 91°	0.1
1°, 2°, 3°, 4°	0.2
5°	0.6
10° to 85°	1.0
90°	0.5

The total sampling count and the number of sampling counts at each power level are multiplied by these weighting factors before being combined with other elevations.

Weight No. 2

The data were weighted to eliminate the effect of the main lobe and large ground reflections. All data below 10° elevation were disregarded. Data from 10° to 85° elevation received a weight of unity, and at 90° a weight of 0.5.

Weight No. 3

The following weighting procedure was used to produce a uniform distribution of data points over the celestial sphere by modifying the 5^{o} azimuth blocks. An azimuth-elevation antenna mount which is methodically oriented in its two motions inherently produces a congestion of point angles around the elevation axis. This can be adjusted by assigning the proportional area of the sphere that each data point represents. The 72 azimuth blocks were renumbered so that the main lobe block became block No. 1. The weighting factors were then applied to block no. as follows:

Block Nos.	Weight
1, 37	$\cos 2.5^{o}$
2, 36, 38, 72	$\cos 5^{o}$
3, 35, 39, 71	$\cos 10^{o}$
4, 34, 40, 70	$\cos 15^{o}$
5, 33, 41, 69	$\cos 20^{o}$
- - - -	-
- - - -	-
- - - -	-
- - - -	-
18, 20, 54, 56	$\cos 85^{o}$
19, 55	$\cos 87.5^{o}$

The number of sampling counts at each power level are multiplied by these weighting factors before being combined with other azimuth blocks.

The program output was in printed tabular form, giving the identification and the percentages at each 2 db level below main lobe. A sample output is shown in Table 3.

Table 3

WEIGHT 0 GENERAL DISTRIBUTION

SITE 1 POLARIZATION 1 BAND 9

DB	PERCENT	DEL PERCENT	DATA COUNT
0	0.003	0.	4.
2	0.006	0.001	7.
4	0.006	0.	8.
6	0.006	0.001	8.
8	0.007	0.001	9.
10	0.008	0.	10.
12	0.008	0.001	10.
14	0.009	0.002	11.
16	0.011	0.002	14.
18	0.014	0.002	17.
20	0.016	0.006	20.
22	0.023	0.010	28.
24	0.032	0.014	40.
26	0.046	0.015	57.
28	0.061	0.027	76.
30	0.089	0.050	110.
32	0.138	0.034	172.
34	0.172	0.058	214.
36	0.230	0.070	286.
38	0.300	0.126	373.
40	0.427	0.151	530.
42	0.577	0.151	717.
44	0.728	0.339	904.
46	1.067	0.824	1325.
48	1.891	1.785	2349.
50	3.676	2.853	4566.
52	6.530	3.316	8110.
54	9.846	4.078	12229.
56	13.924	5.180	17294.
58	19.105	6.924	23728.
60	26.028	8.835	32327.
62	34.863	10.320	43300.
64	45.184	10.017	56118.
66	55.200	9.112	68559.
68	64.312	9.560	79876.
70	73.873	-73.873	91750.
72	0.	0.	0.
74	0.	0.	0.
76	0.	0.	0.
78	0.	0.	0.

6. DISCUSSION

The primary useful results of these pattern measurements and the reduction of the data lie in the areas of (1) an aid in predicting vulnerability to unwanted signals for similar antennas, and (2) evaluating effects of ground environment on the pattern of this antenna. The methods used for these patterns can be used on other antenna installations as desired. The equipment is mobile and can be used with any antenna which has standard synchro outputs. The data for these patterns are stored on magnetic tapes and punched cards so that further data processing is possible for other purposes.

Figures 47 through 54 show the summary of statistical pattern data for horizontal and vertical polarizations for both frequencies at all four sites. Figures 55-90 are relative gain cumulative distribution plots for individual sites. The distribution curves are limited at low percentages by the number of data points available about the main lobe and by the dynamic range of the system at high percentages. While it would be interesting to examine the percentage distribution of very deep nulls, this would require 20 db more exciter power or lower noise level. Since the balance of the distribution is normal (Gaussian) this curve is likely to extend to the 99.99% extremity.

A curve fitted to the data would intercept the .01% ordinate at about the 15 db level, giving an apparent upward bend to the distribution. For example see Fig. 63. This results from the arbitrary selection of 0^{o} and 1^{o} elevation as data sampling lines. Random sampling of data is required to produce a theoretical normal distribution. Analysis of the main lobe area shows that the .01% is crossed at the 25 db ordinate by the normal curve when a circular beam is assumed and random sampling is synthesized. No actual elevation sweeps were taken through the

main lobe. However, weight 2 eliminates the main lobe area, along with the 0° -5° sweeps, and also produces a nearly straight line on the normal distribution graph used. The 1° and 5° elevation increments gave an adequate random sampling of the pattern except in the main lobe area. This is shown by the close similarity of patterns at adjacent elevation increments.

The nature of the back lobes for this parabolic reflector antenna is important to space vehicle or satellite tracking with similar antennas. Figure 23 shows back lobes at 210° and 340° elevation, and as elevation is increased these lobes broaden and then merge. When the antenna was at an elevation of about 70°, the dominant back lobes were most prominent. These back lobes have been termed spillover lobes because they are caused by illumination from the feed that is diffracted over the edge of the reflector. The importance of these lobes is that they are over 60° wide with few deep nulls. These lobes can be an important entrance for interference at a level of 40 db below main-lobe level. Means to minimize this type of back lobe should be considered in the design of space vehicle tracking antennas. However, edge illumination does not appear an important factor as the lower edge illumination at 4.85 GHz did not materially reduce the spillover lobes.

In using data from these pattern measurements, weight 3 is recommended as the most general description. This weighting removes from the data two distortions that were introduced by the AZ-El mount mechanics and the additional elevation sweeps needed below 5° to effectively sample rapid changes in ground reflection contribution. The usual AZ-El mount points its axis at a ground-based target twice on each azimuth sweep without regard to the elevation angle used. This results in the same area of the pattern being included in the data more often than

would be obtained with a random sample. When an Az-El mounted antenna is being considered, the weight 1 plots are appropriate. If a restriction is placed on this Az-El antenna so that it will never be used below 7° in elevation, weight 2 is the description that applies. Since the data on punched cards are in 5° -by-5° blocks, other weightings can be applied if desired by a slight modification in the Fortran program.

Cross-polarization measurements were made only from the Matterhorn exciter site. The shape of the distribution curve shown in Fig. 74 is generally similar to straight horizontal or vertical polarization except that the mean is 10 to 15 db lower. Cross-polarization patterns were measured with vertical polarization at the exciter and the main antenna feed set for horizontal polarization, because this orientation caused greater phase shift in reflected rays.

Table 4 shows the medians taken from Figs. 55-90 and Table 5 shows standard deviations taken from Figs. 51-54 which have been determined from the distributions on the basis of a line fitted to the 16% and 50% points. While a binormal distribution could be fitted to some of the curves [CCIR, 1962b], the break in these normal distributions occurs near the 5% point rather than at the median as required for a binormal distribution. Another advantage to a normal approximation is to facilitate combinations with other normally distributed functions in a system.

Table 4

Medians of the Distributions

(in decibels)

Site	Band	Polarization	Wgt. 0	Wgt. 1	Wgt. 2	Wgt. 3
1	5	1	67.0	69.3	66.7	76.6
1	5	2	66.5	69.2	66.2	71.6
1	9	1	65.0	68.8	66.0	71.2*
1	9	2	65.6	68.5*	65.3	70.5*
2	5	1	70.0	73.0	71.0	74.8*
2	5	2	69.0	72.2	68.4	81.3*
2	9	1	70.4*	74.0*	72.0*	76.2*
2	9	2	70.2	72.8	70.2	72.0
3	5	1	69.2	72.0*	70.0	75.0*
3	5	2	68.5*	71.0*	66.0*	72.7*
3	9	1	74.0*	71.0*	70.0*	79.0*
3	9	2	73.0*	71.0*	68.0*	72.7*
4	5	1	65.8	69.0	65.8	73.5
4	5	2	66.1	70.3	66.0	70.5
4	9	1	66.1	68.8	65.8	72.0*
4	9	2	66.3	71.0	66.8	74.0*
4	5	3	52.8	60.4	54.0	67.0*
4	9	3	51.5	53.5	43.0	59.0*

*Extrapolated value

Key:

Site No.
1 Firestone
2 E-2 Haswell
3 E-1 Haswell
4 Matterhorn

Polarization No.
1 Horizontal
2 Vertical
3 Cross

Table 5

Statistical Distribution Gains

Weight 3

	Mean Relative Gain	Standard Deviation
4.85 GHz		
Horizontal Polarization	-73 db	10 db
Vertical Polarization	-75 db	13 db
Cross-Polarization	-58 db	15 db
9.1 GHz		
Horizontal Polarization	-74 db	10 db
Vertical Polarization	-73 db	12 db
Cross-Polarization	-51 db	12 db

The results of these measurements at two frequencies are comparable to previous statistical patterns at 1040 GHz [CCIR, 1962b]. The larger standard deviation for 4.85 GHz appears to be a function of wavelength with the decreasing standard deviation for 9.1 GHz probably resulting from low antenna efficiency at this higher than design frequency.

7. CONCLUSIONS

The measurements made from four target sites indicate that a large parabolic reflector has a normally distributed statistical gain pattern. Nearly identical distributions were obtained at 4.85 and 9.1 GHz and both polarizations. Patterns for the four sites for which complete data were reduced and two additional sites for which only preliminary patterns were taken show sample means which are reasonably well

grouped. Table 5 shows the mean statistical distributions from the four sites for a uniform density of samples. For prediction purposes, it is recommended that a standard error of 4 db be allowed in estimating a mean gain value for a similar antenna. Appendix A shows one way in which these statistical distributions can be used for interference prediction purposes.

8. ACKNOWLEDGEMENTS

The measurements reported here were supported by the National Aeronautics and Space Administration. The experiment planning, field measurements, and data analysis were performed by personnel of the Troposphere and Space Telecommunications Division of the Central Radio Propagation Laboratory. Many specialized individual contributions were necessary to the completion of this experiment.

9. REFERENCES

Campanella, A. J., C. F. Douds, and R. E. Wolfe (1962), Feasibility study of a high performance antenna test range, RADC-TDR-62-301. Prepared by HRB-Singer, Inc.

CCIR (1962a), Sharing of radio frequency spectrum by earth space communication links, Study Group IV, Document No. 45.

CCIR (1962b), Measured cumulative distributions of the directive gain of an 18.3 meter diameter parabolic antenna at a frequency of 1040 Mc/s, Study Group V, Document No. 89.

Cutler, C. C., A. P. King, and W. E. Koch (1947), Microwave antenna measurements, Proc. IRE 35, 1462-1471.

Hubbard, R. W., and J. V. Cateora (1961), A fixed frequency 9.1 Gc field intensity recording receiver with extremely narrow bandwidth, NBS Technical Note No. 107.

GAIN - LOSS DIAGRAM

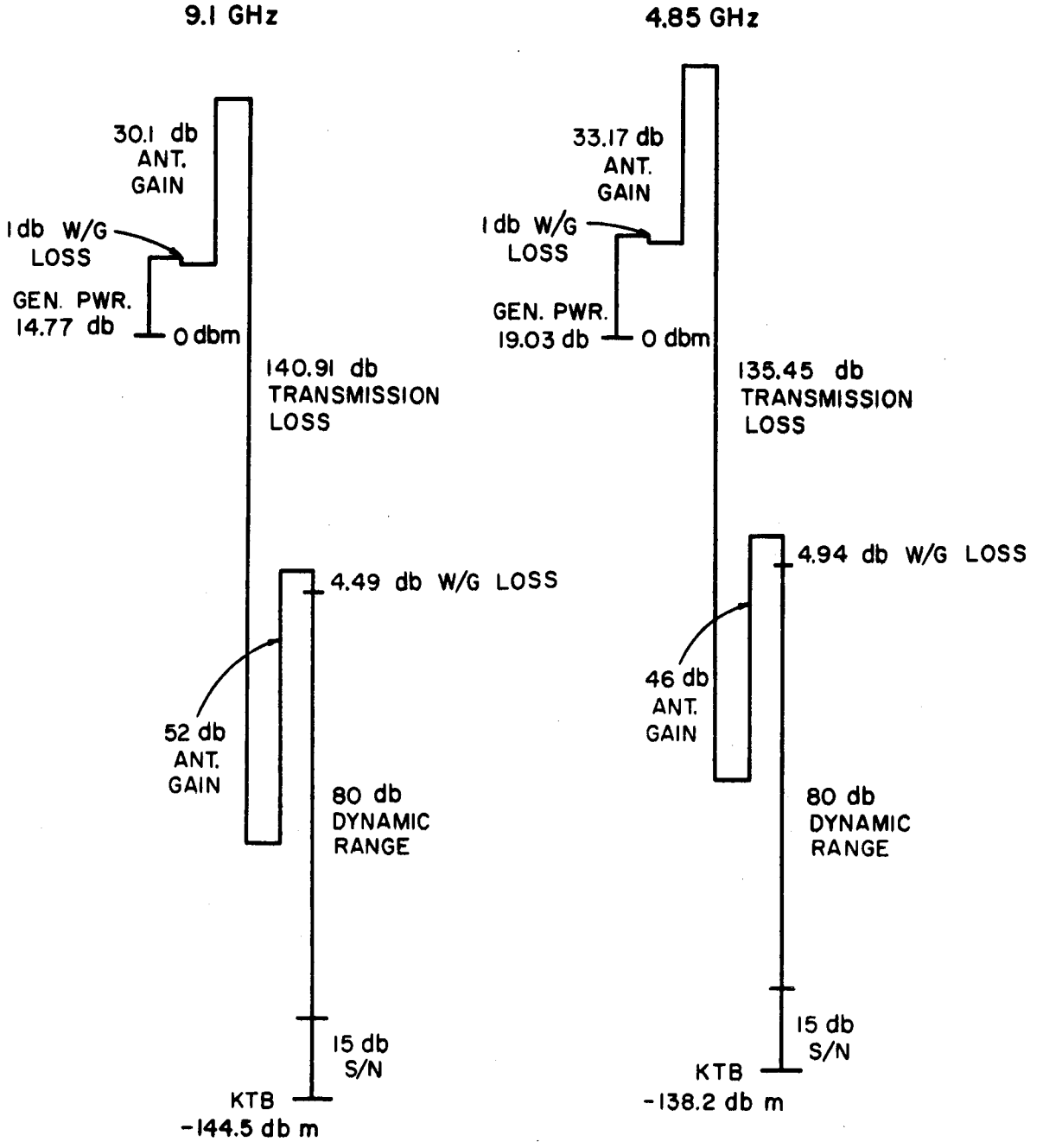

Figure 1

B-48846

Figure 2

HASWELL, COLORADO, 18 m ANTENNA (AT RIGHT)

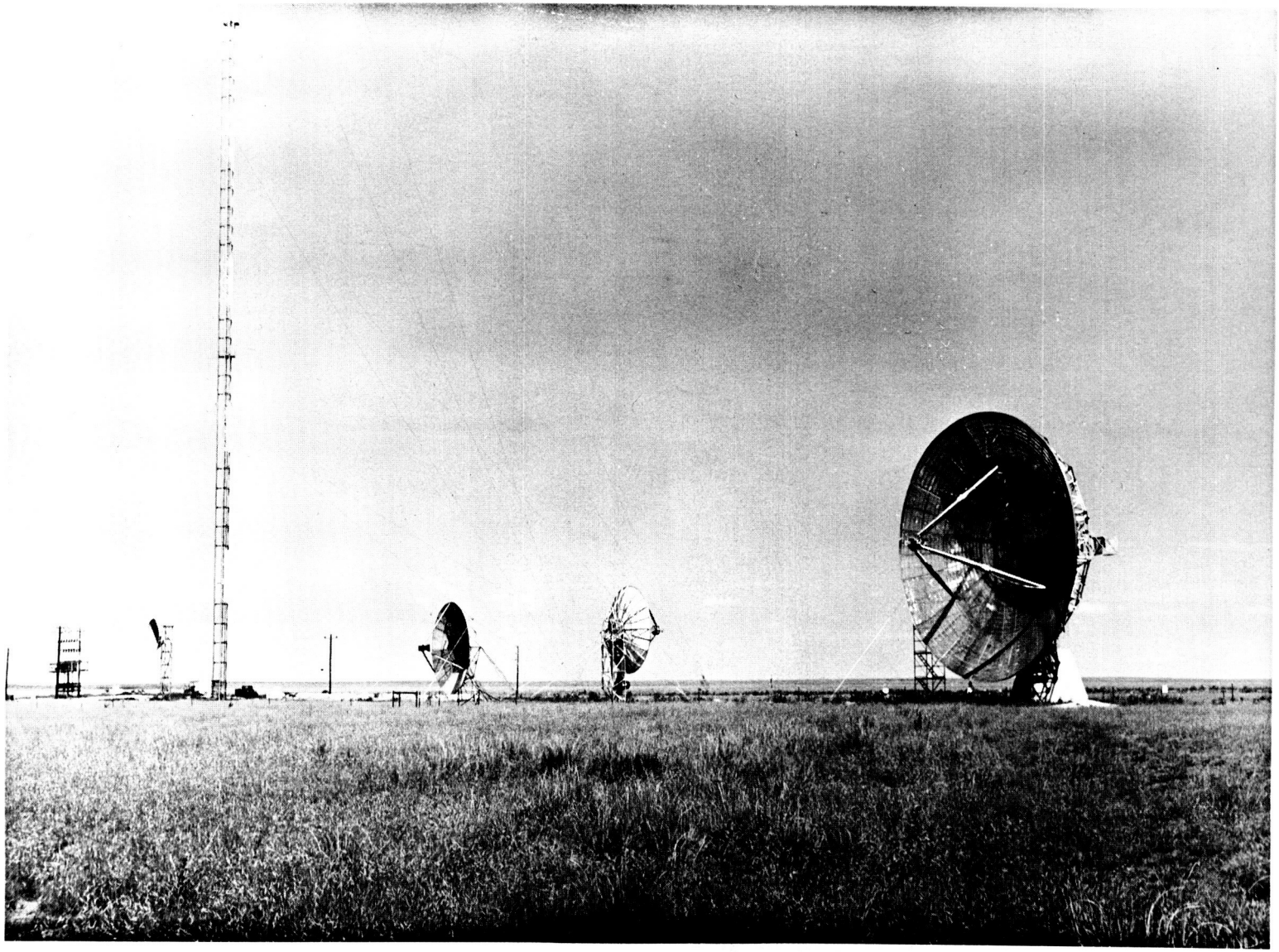

Figure 3

DUAL FREQUENCY FEED FOR 18 m ANTENNA

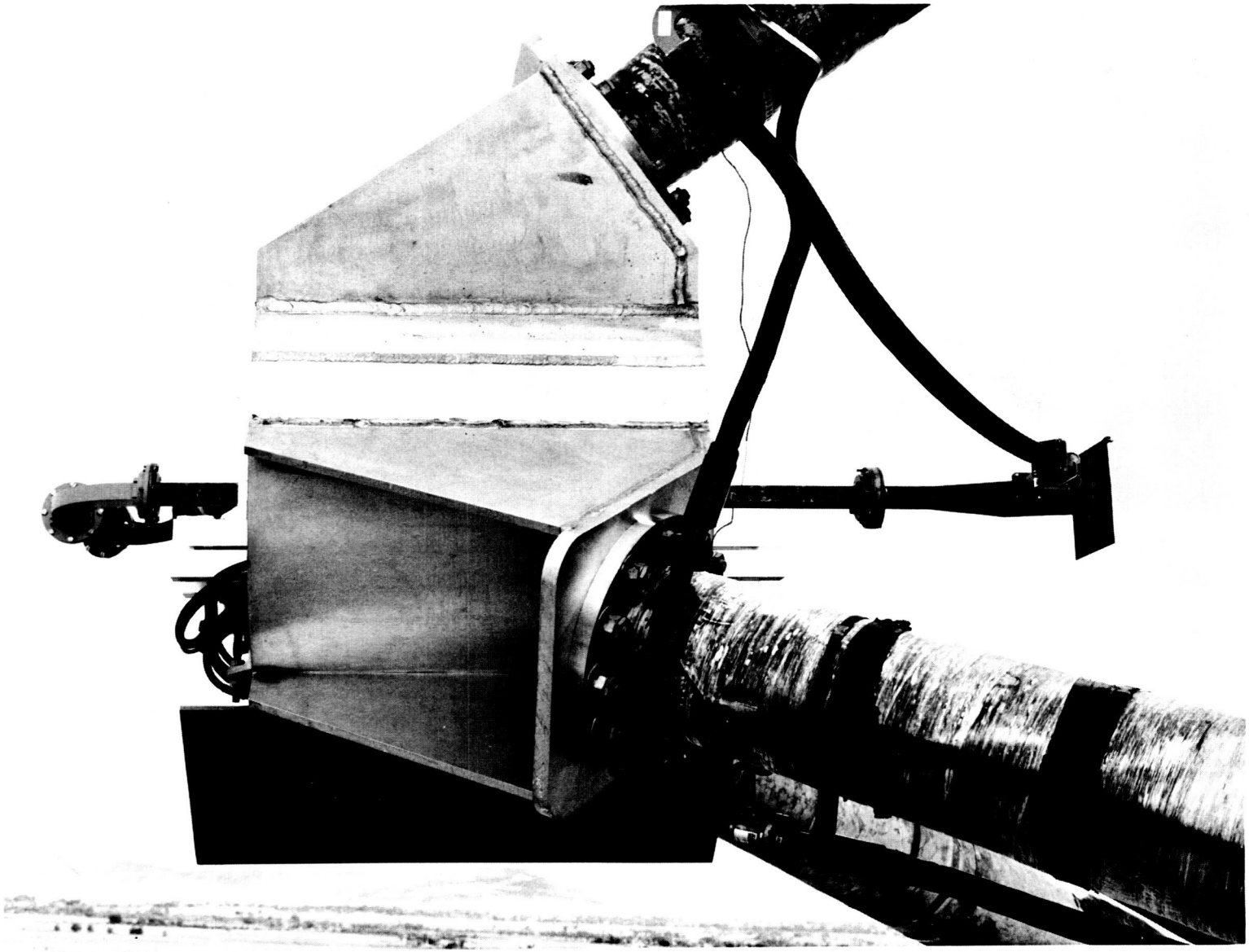

Figure 4

9.1 GHz RECEIVER

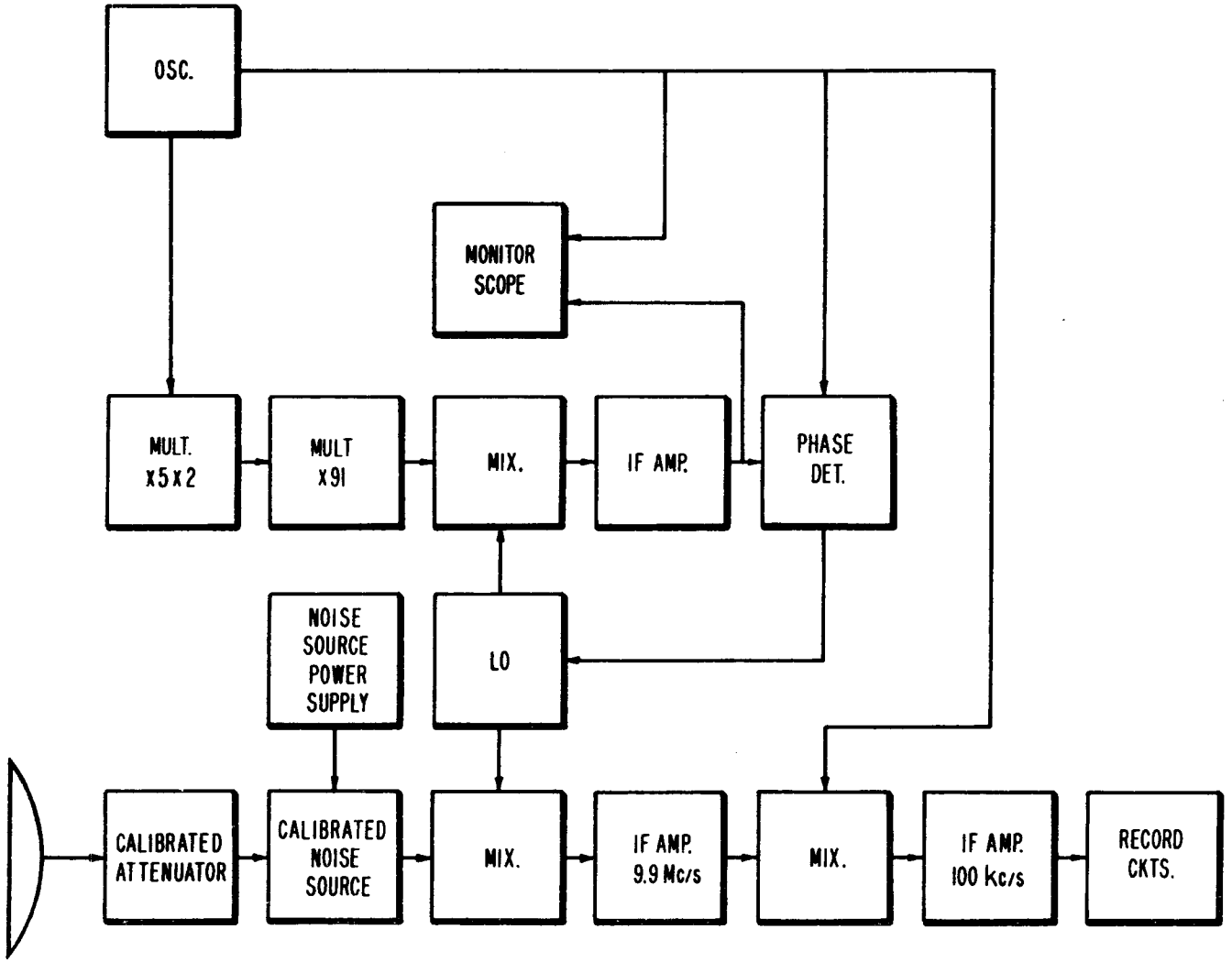

Figure 5

4.8 GHz RECEIVER

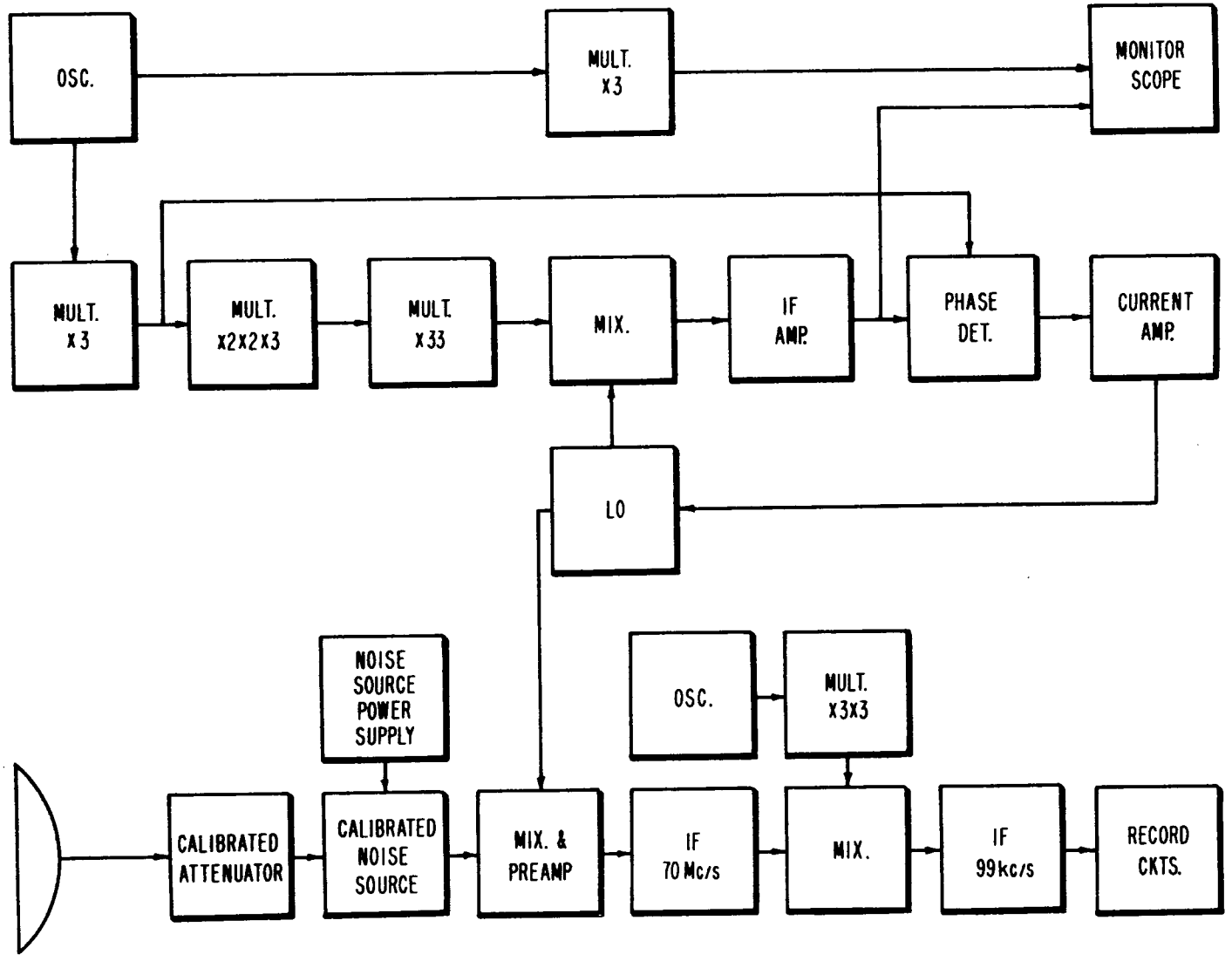

Figure 6

B- 48859

TARGET GENERATOR TRAILER

Figure 7

9.1 GHz TARGET GENERATOR

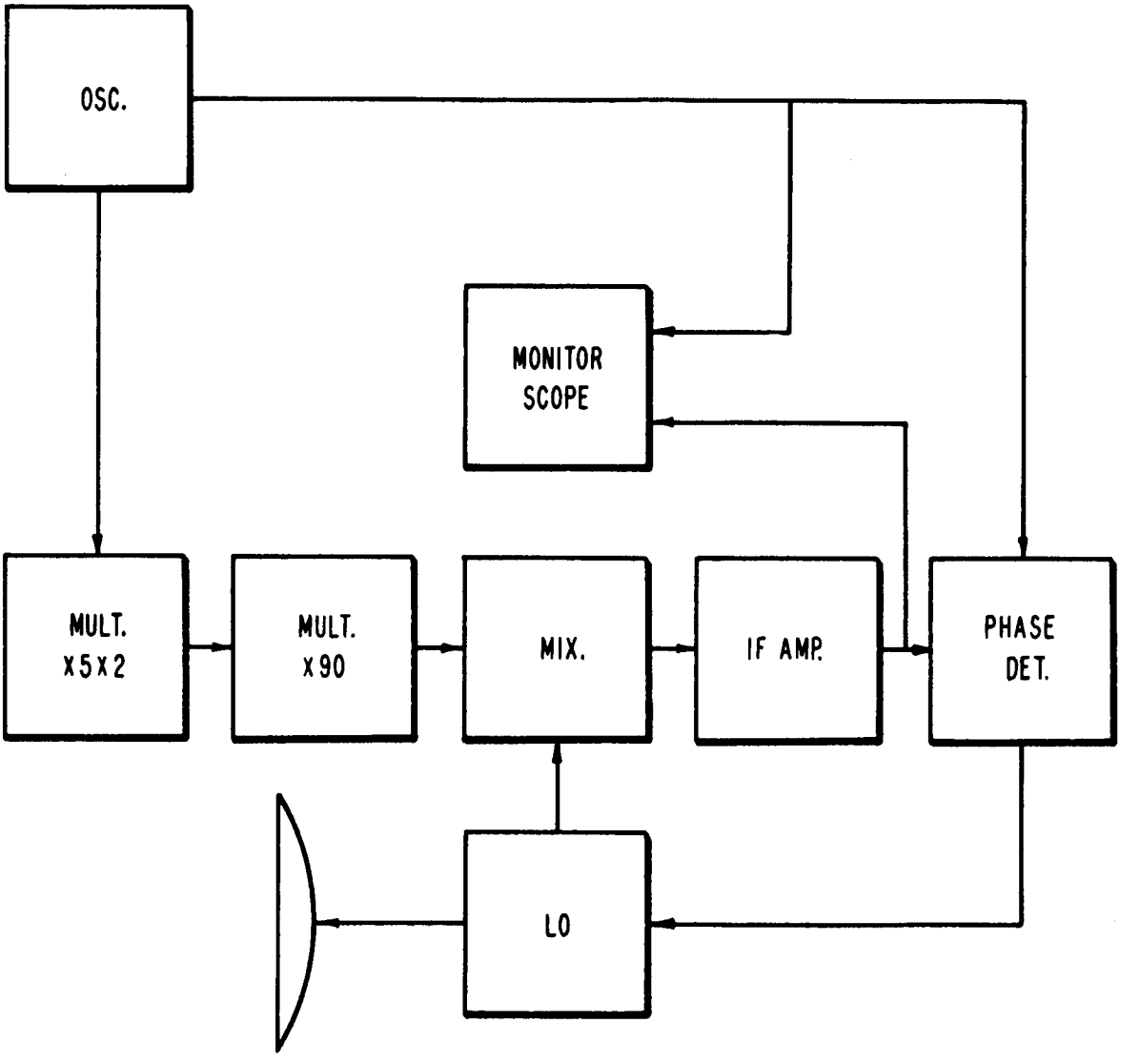

Figure 8

4.8 GHz TARGET GENERATOR

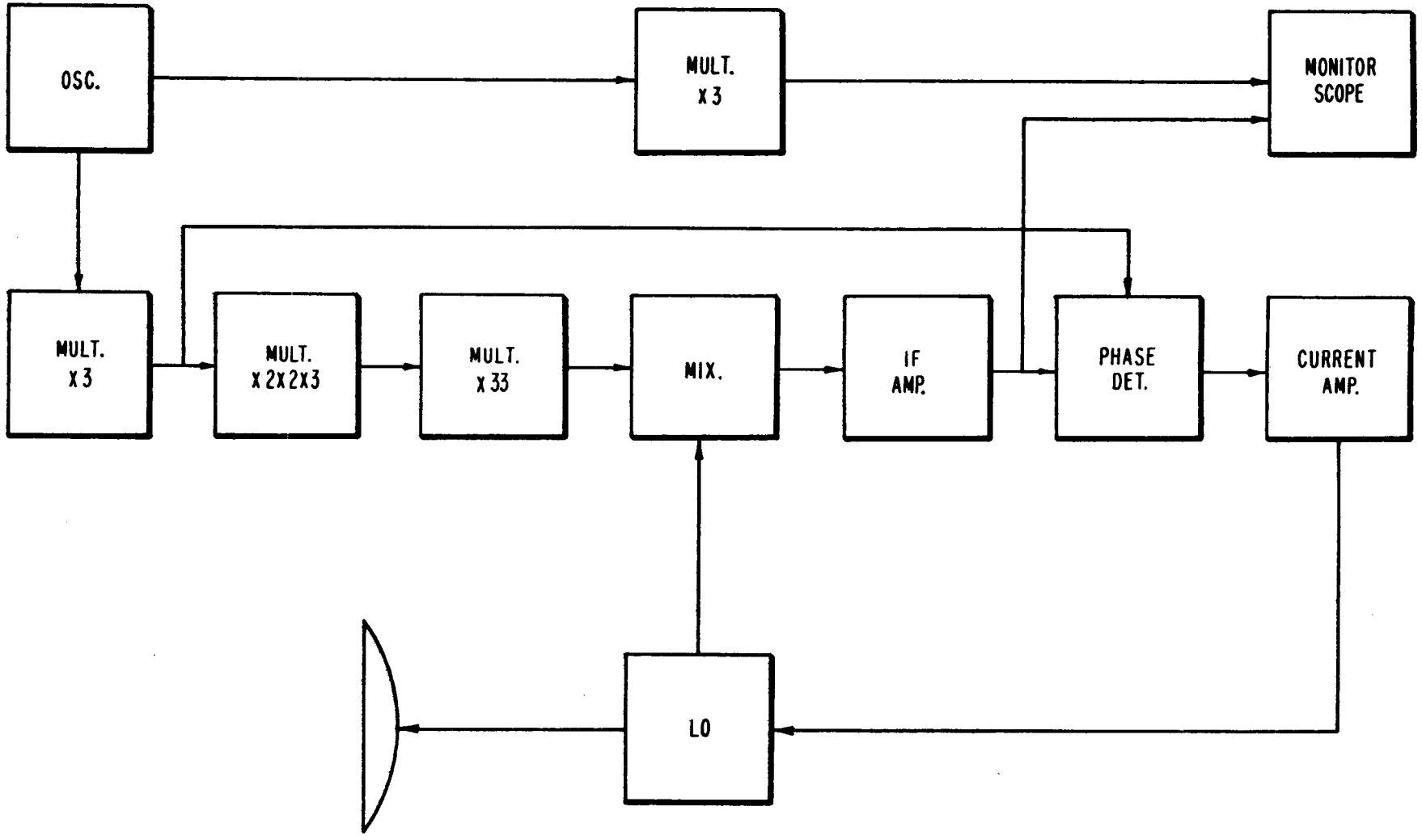

Figure 9

B- 48858

TARGET GENERATOR TRANSMITTERS

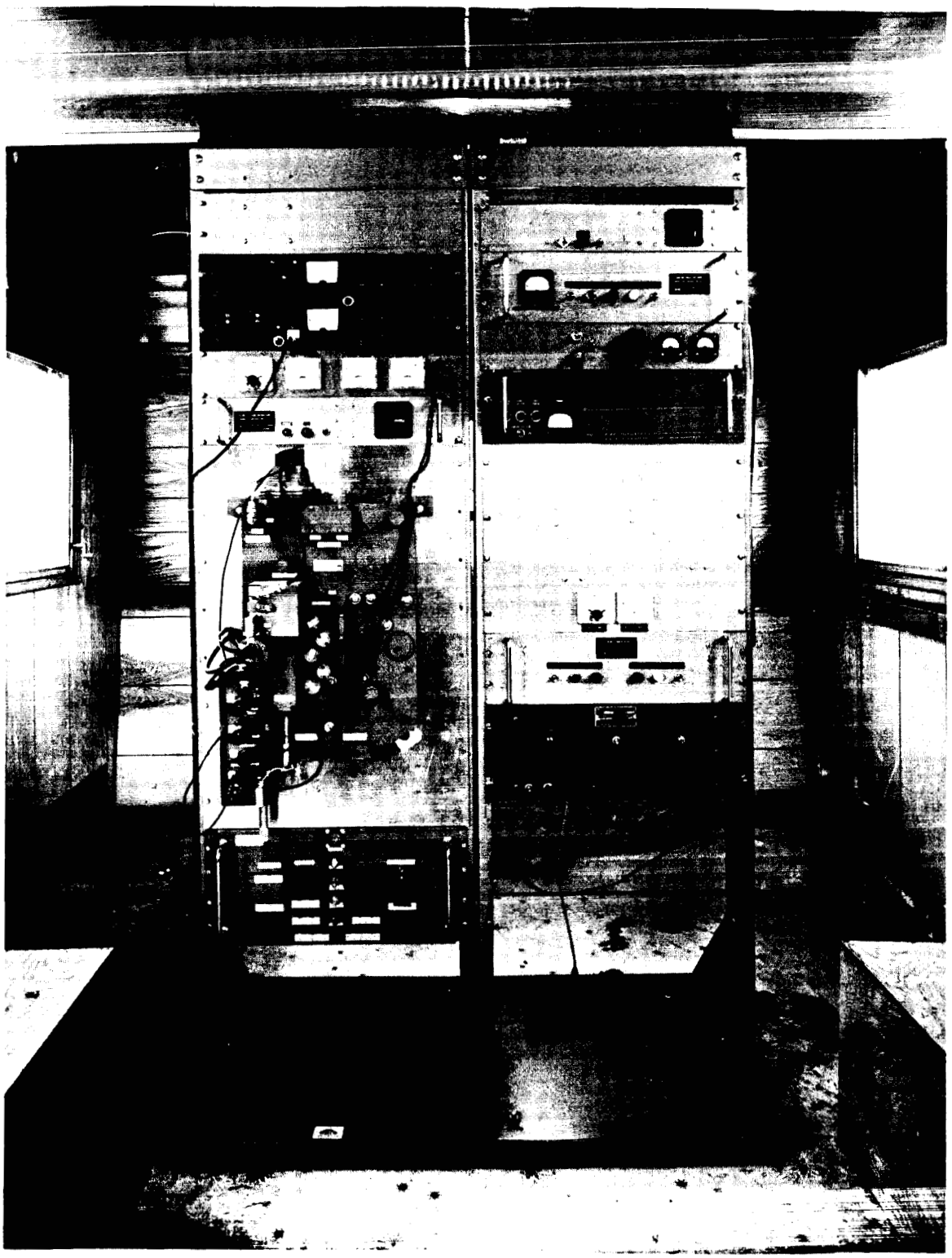

Figure 10

TARGET GENERATOR ANTENNAS

Figure 11

BOULDER, COLORADO T-22 SITE

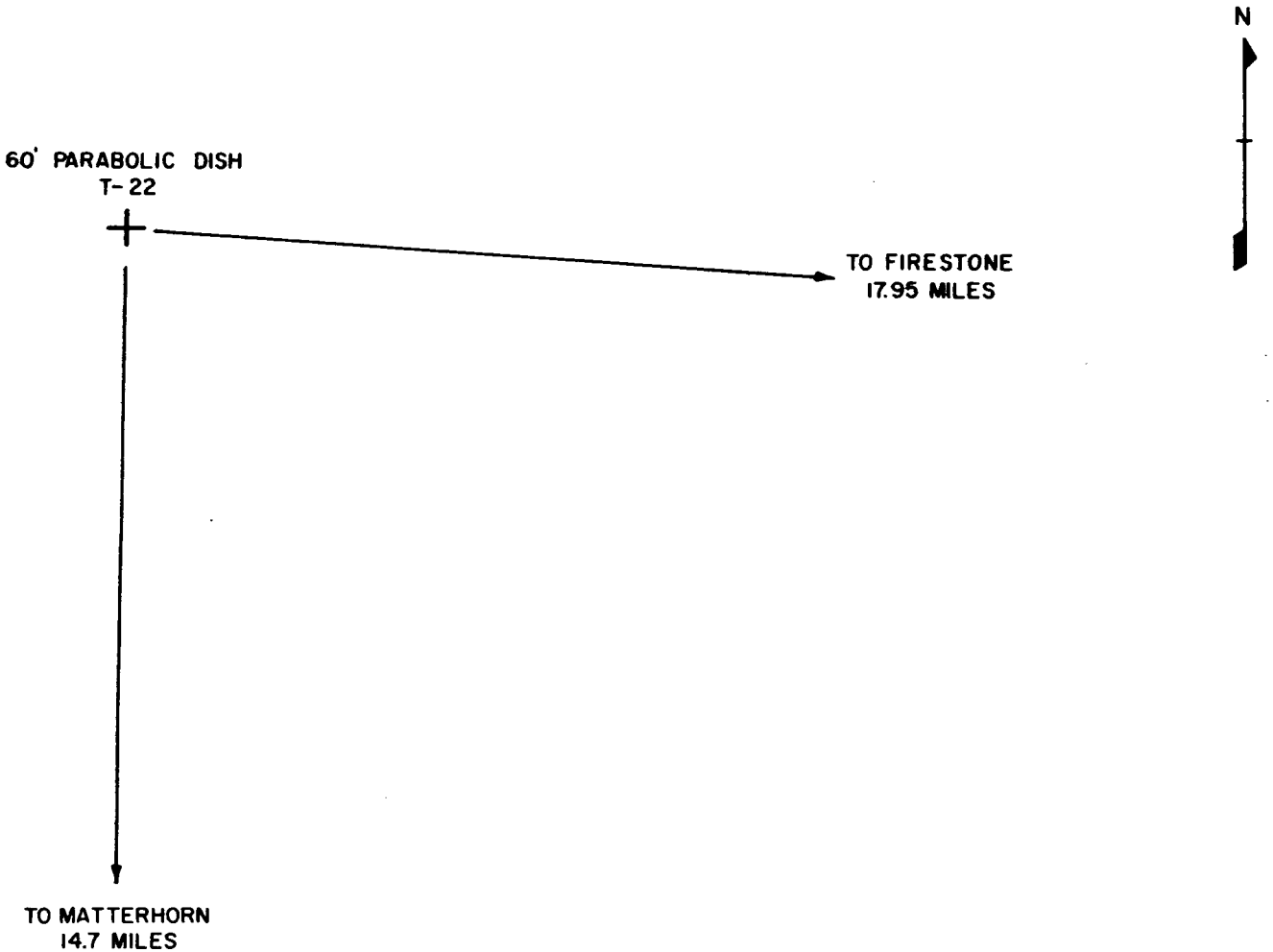

Figure 12

B-48844

HASWELL, COLORADO SITE

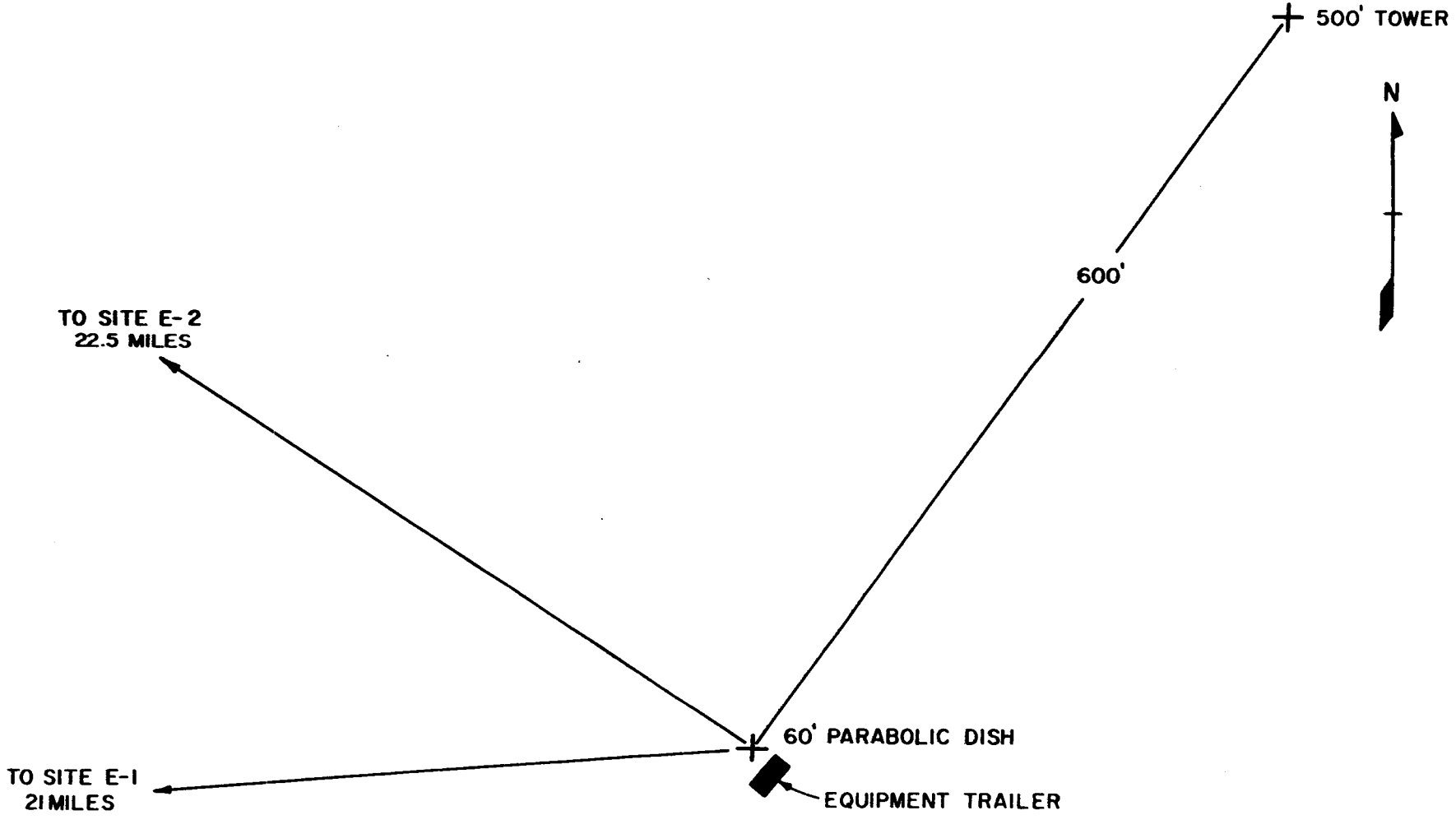

Figure 13

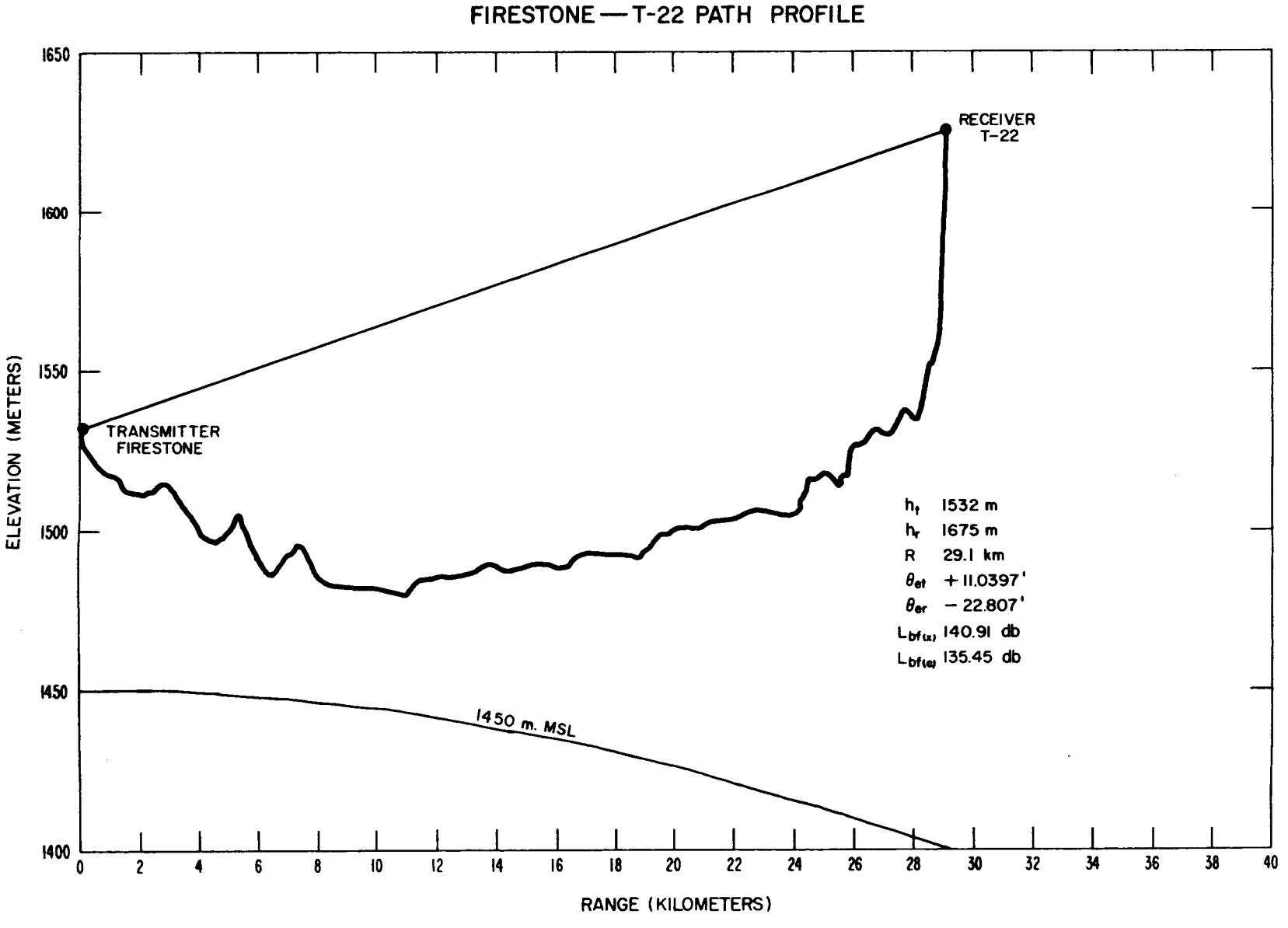

Figure 14

B- 49659

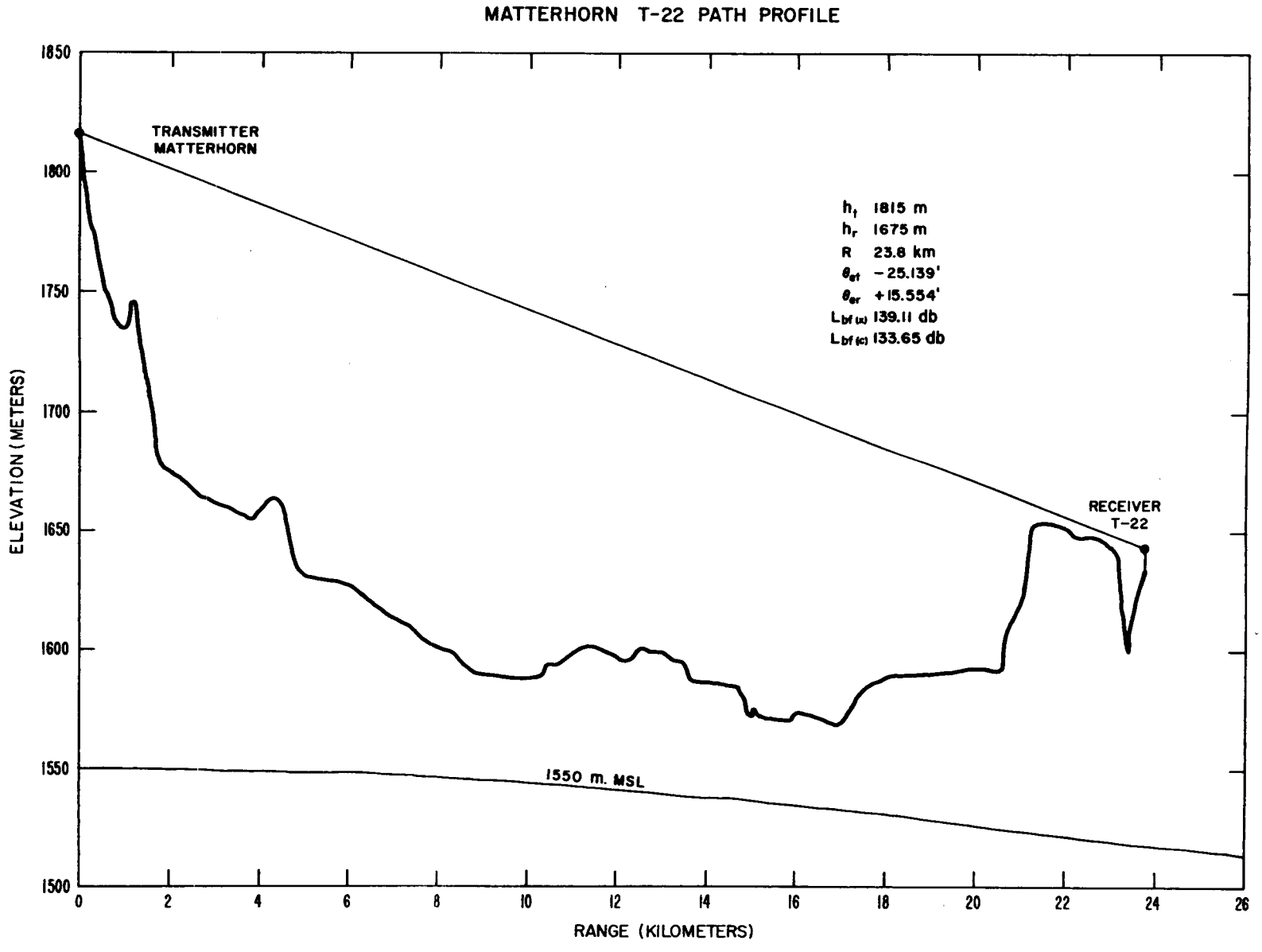
MATTERHORN T-22 PATH PROFILE
TRANSMITTER
MATTERHORN
RECEIVER
T-22
h_t 1815 m
h_r 1675 m
R 23.8 km
θ_{et} −25.139'
θ_{er} +15.554'
$L_{bf(u)}$ 139.11 db
$L_{bf(c)}$ 133.65 db
1550 m. MSL
ELEVATION (METERS)
RANGE (KILOMETERS)
1850
1800
1750
1700
1650
1600
1550
1500
0
2
4
6
8
10
12
14
16
18
20
22
24
26

Figure 15

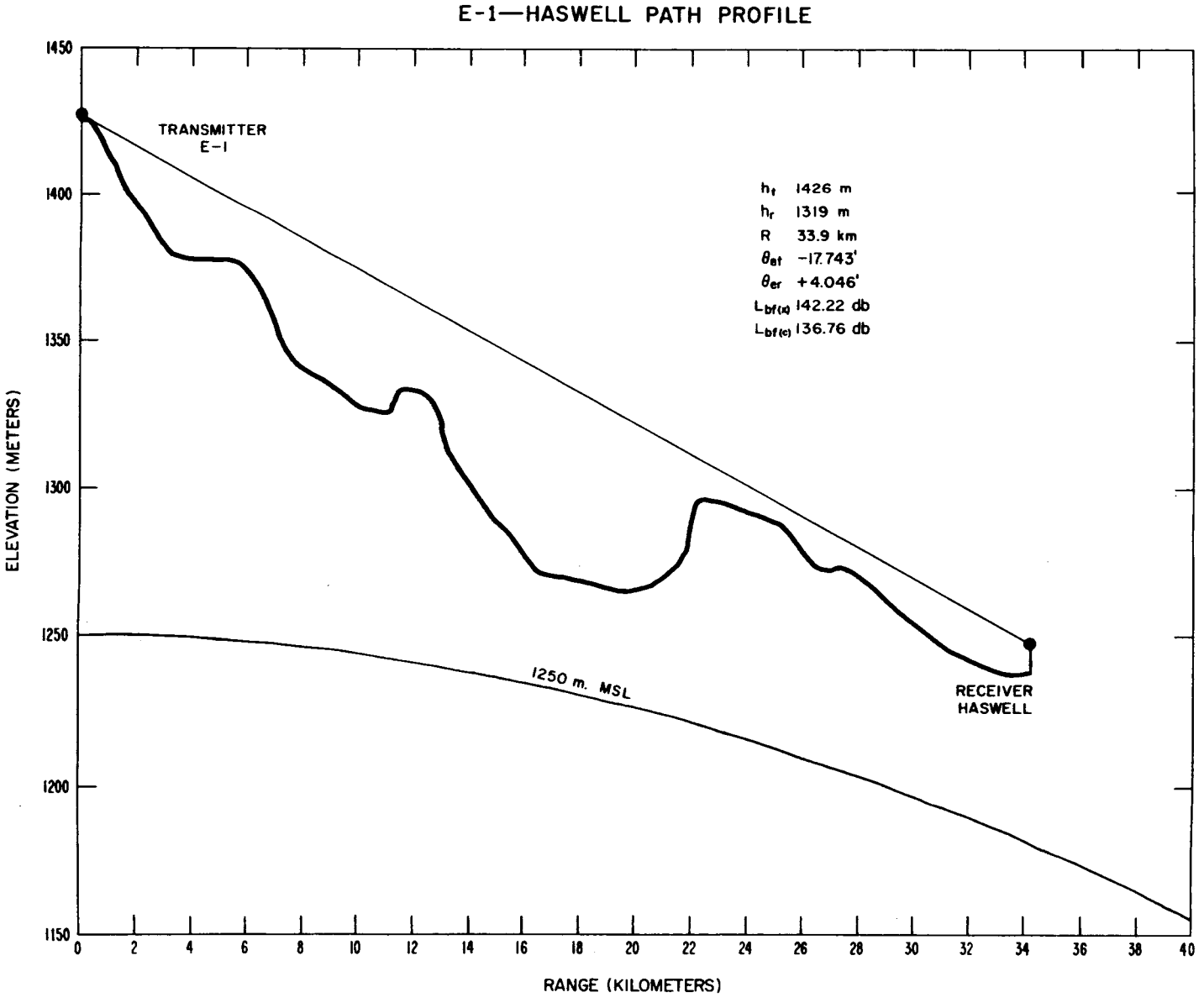

Figure 16

B- 48848

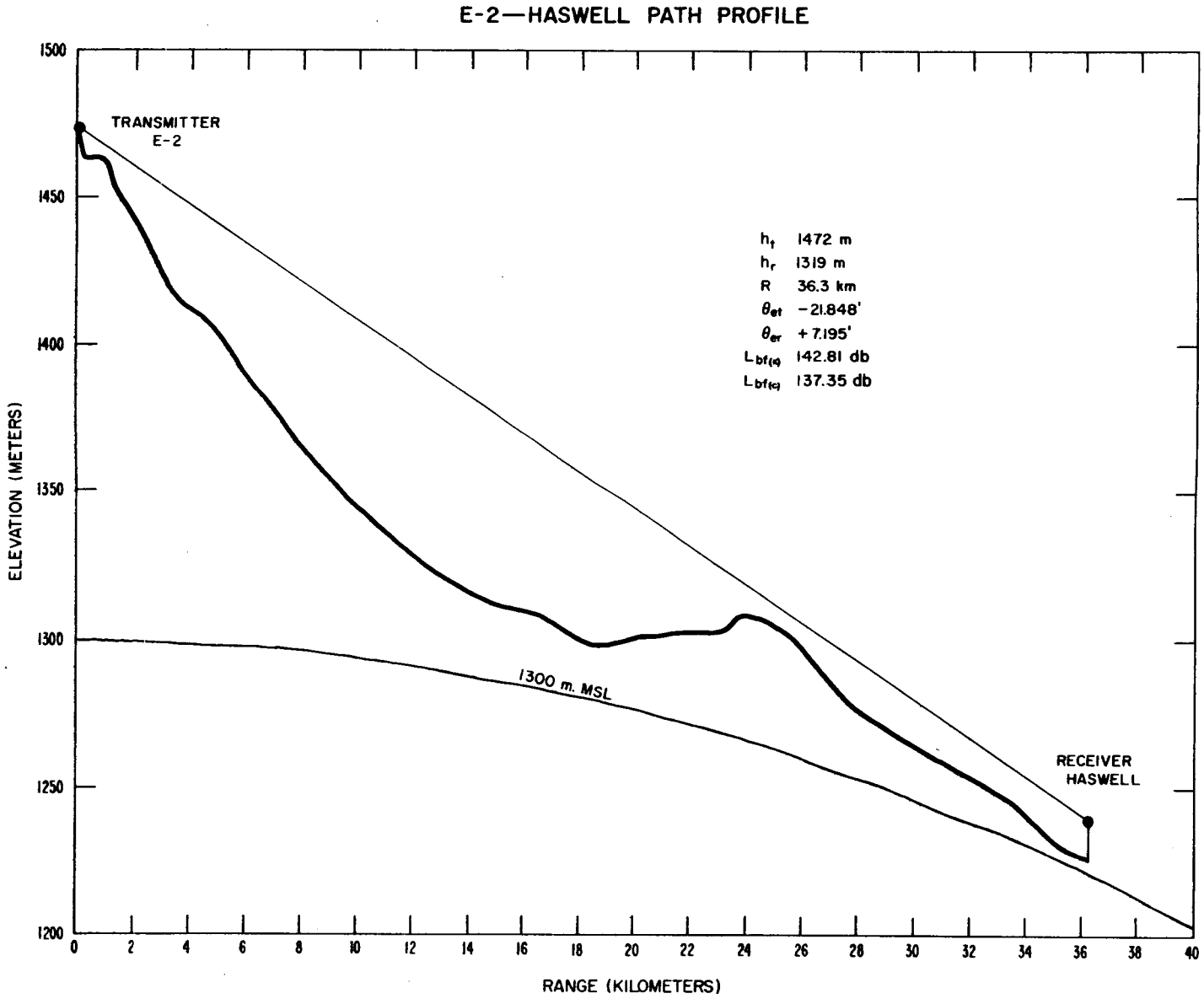

Figure 17

B- 49658

T-22 TERRAIN LOOKING TOWARD FIRESTONE

Figure 18

T-22 TERRAIN LOOKING TOWARD MATTERHORN

Figure 19

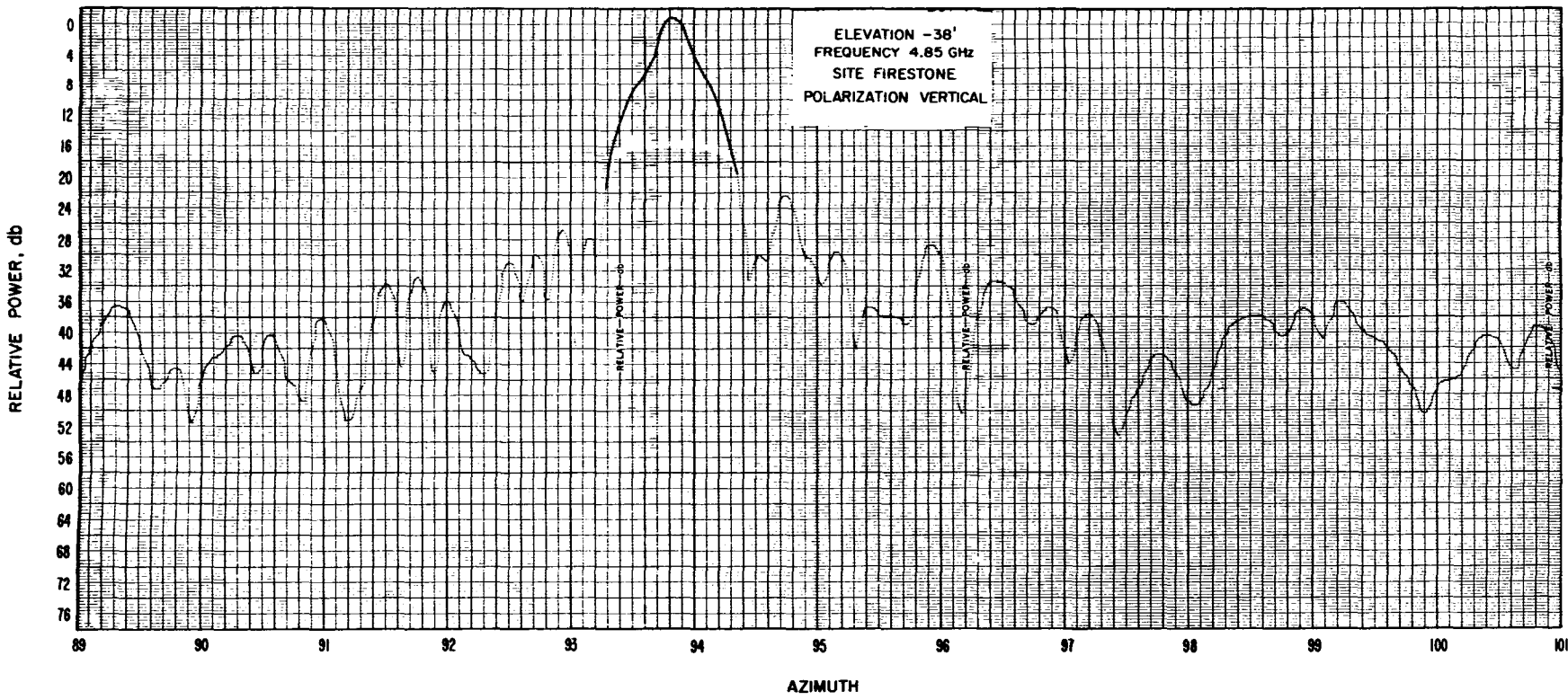

Figure 20

B-49320

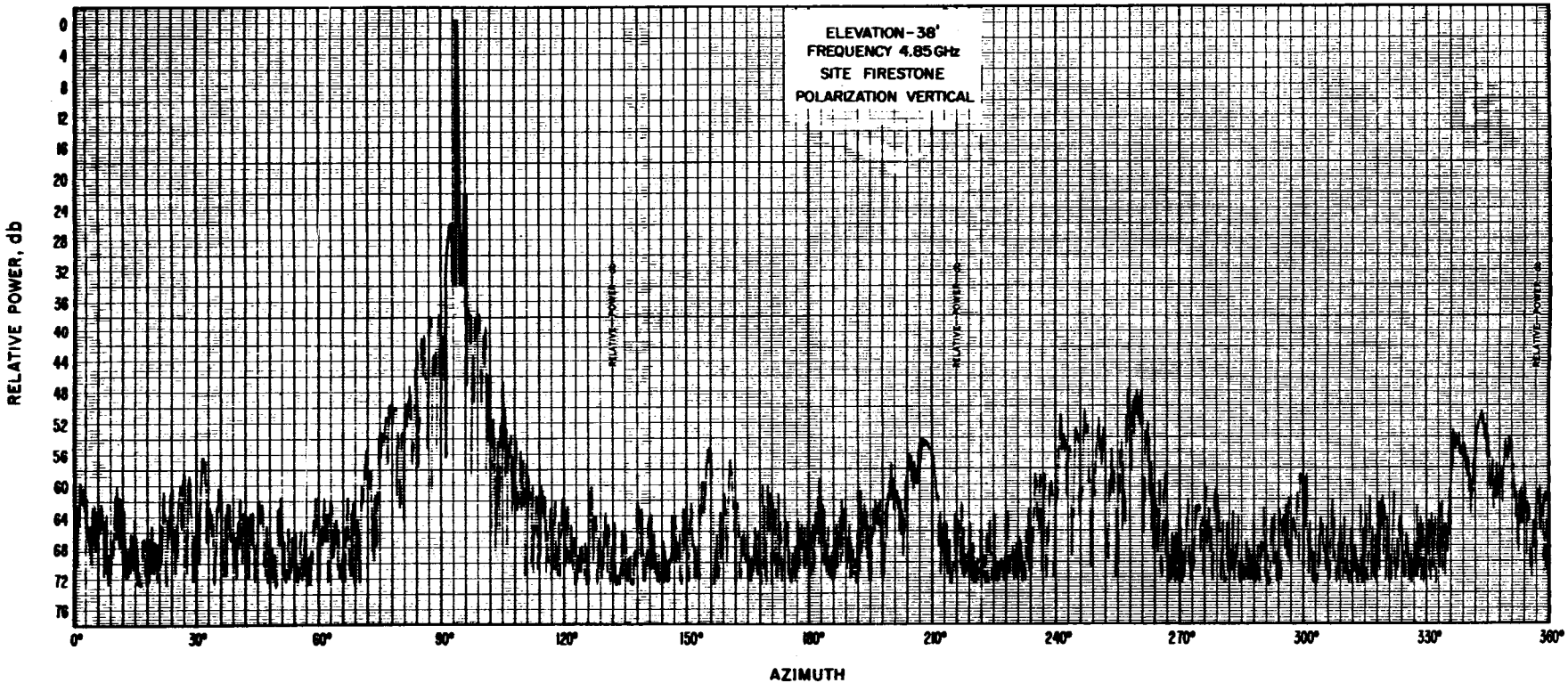
ELEVATION - 38°
FREQUENCY 4.85 GHz
SITE FIRESTONE
POLARIZATION VERTICAL
RELATIVE POWER, db
0
4
8
12
16
20
24
28
32
36
40
44
48
52
56
60
64
68
72
76
0°
30°
60°
90°
120°
150°
180°
210°
240°
270°
300°
330°
360°
AZIMUTH

Figure 21

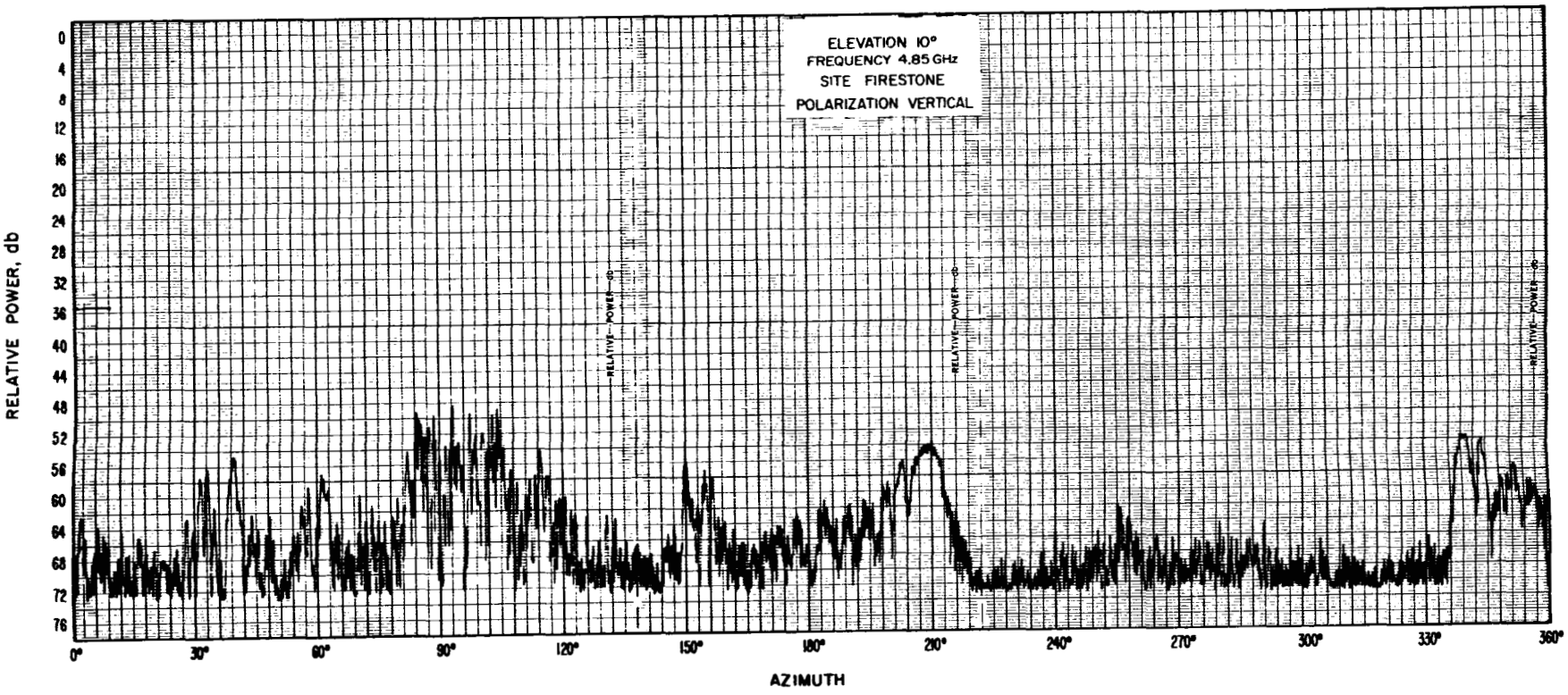

Figure 22

B-49319

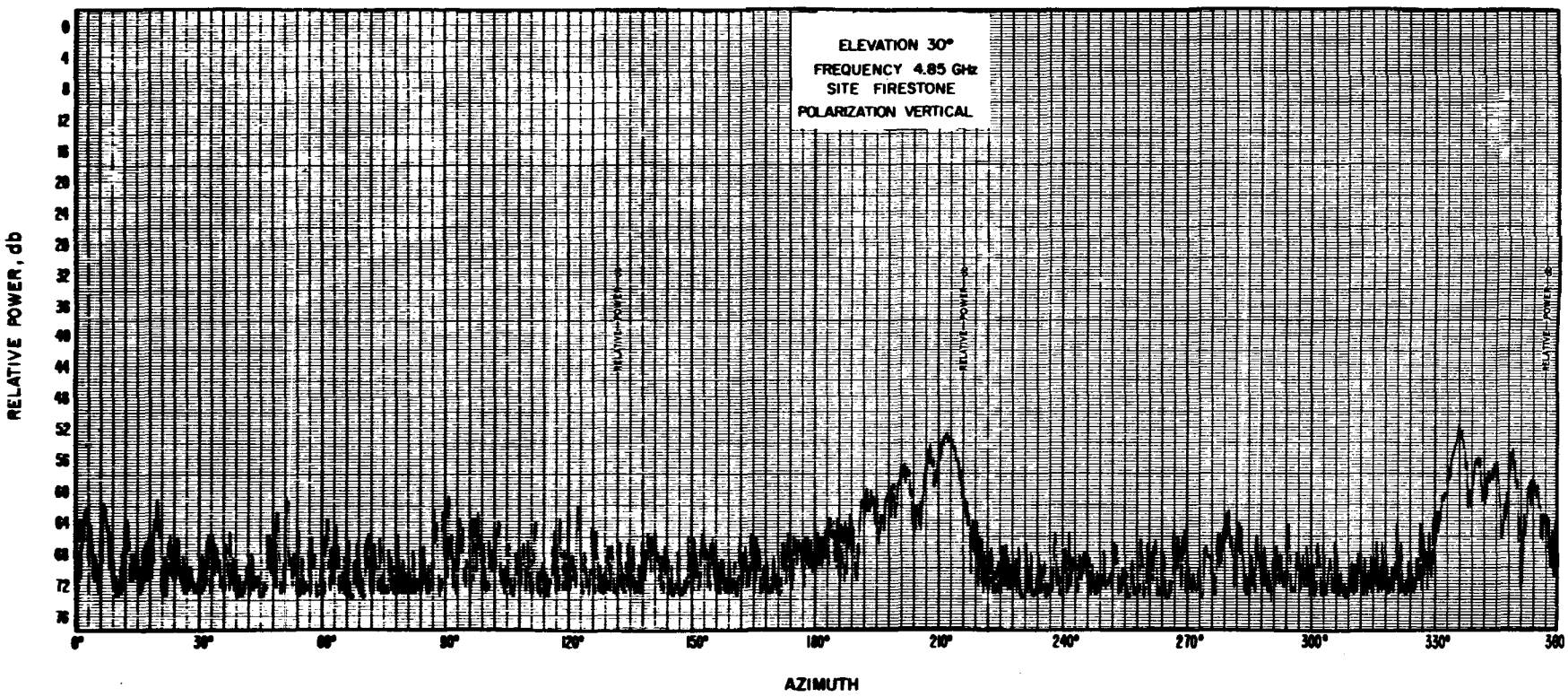
ELEVATION 30°
FREQUENCY 4.85 GHz
SITE FIRESTONE
POLARIZATION VERTICAL
RELATIVE POWER, db
AZIMUTH
0°
30°
60°
90°
120°
150°
180°
210°
240°
270°
300°
330°
360

Figure 23

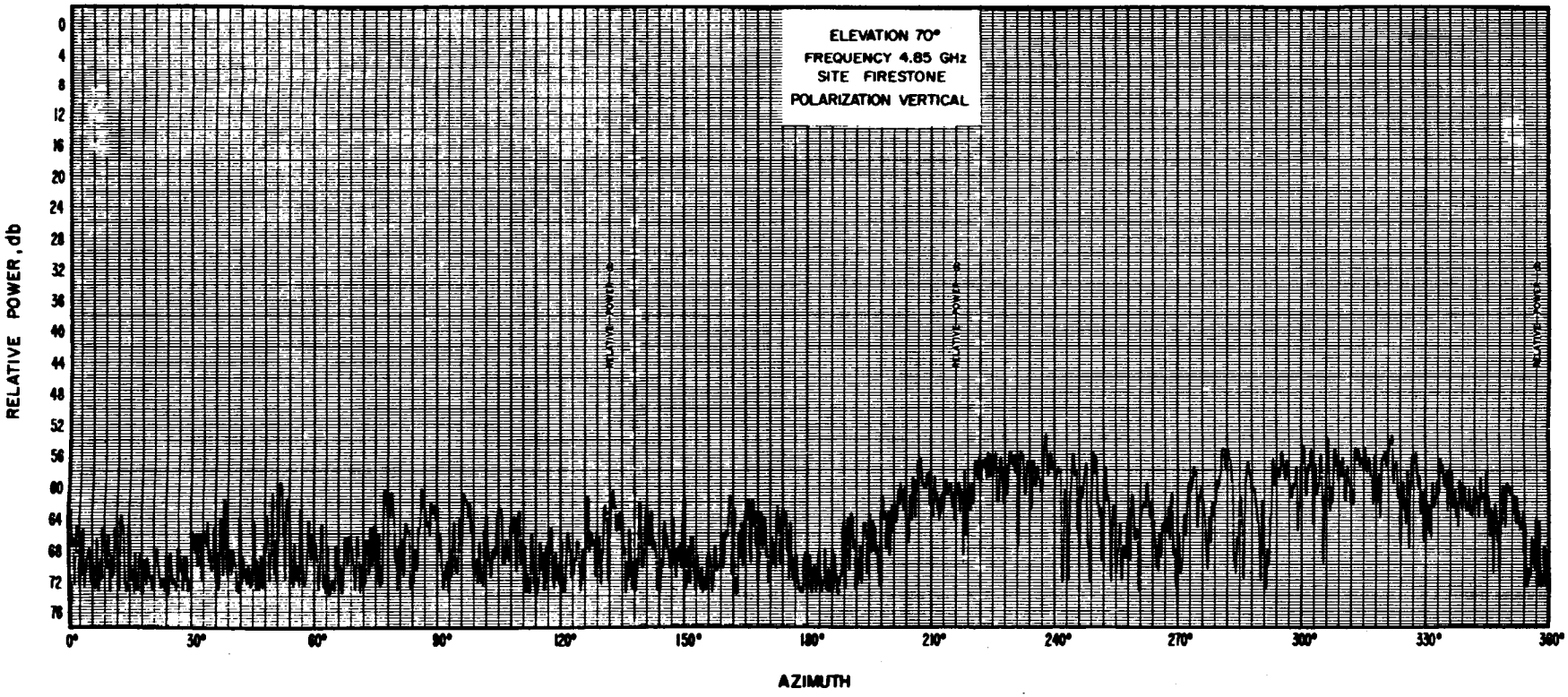

Figure 24

B-49317

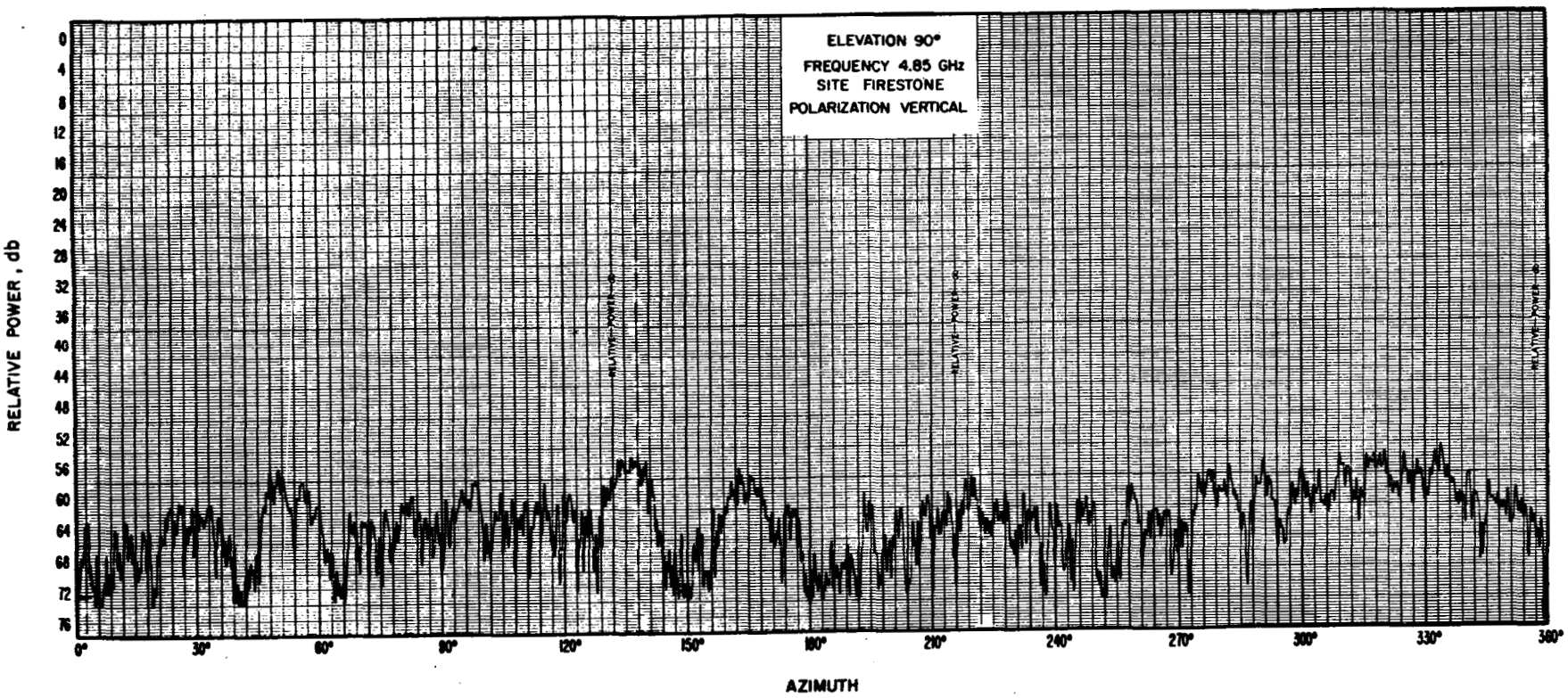

Figure 25

B- 49323

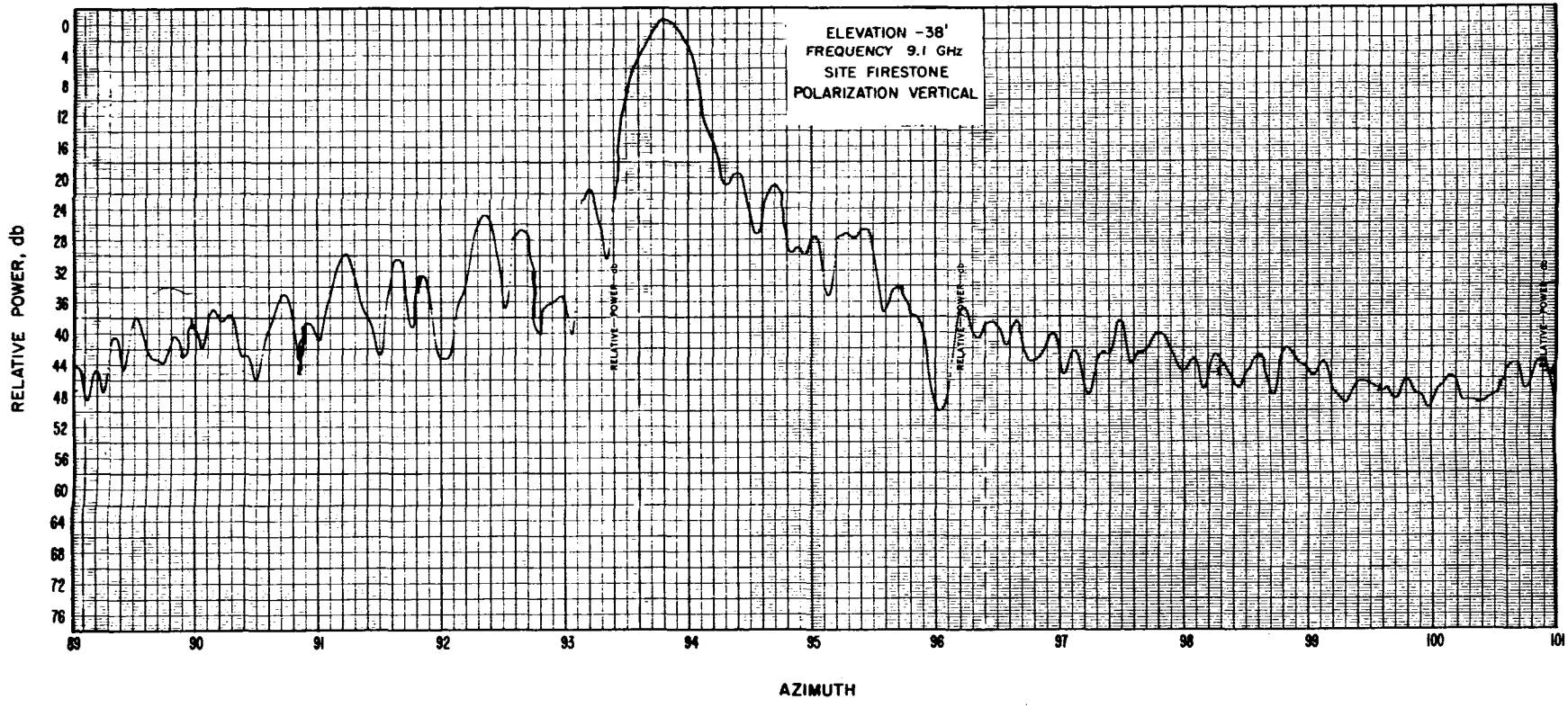

Figure 26

B-49321

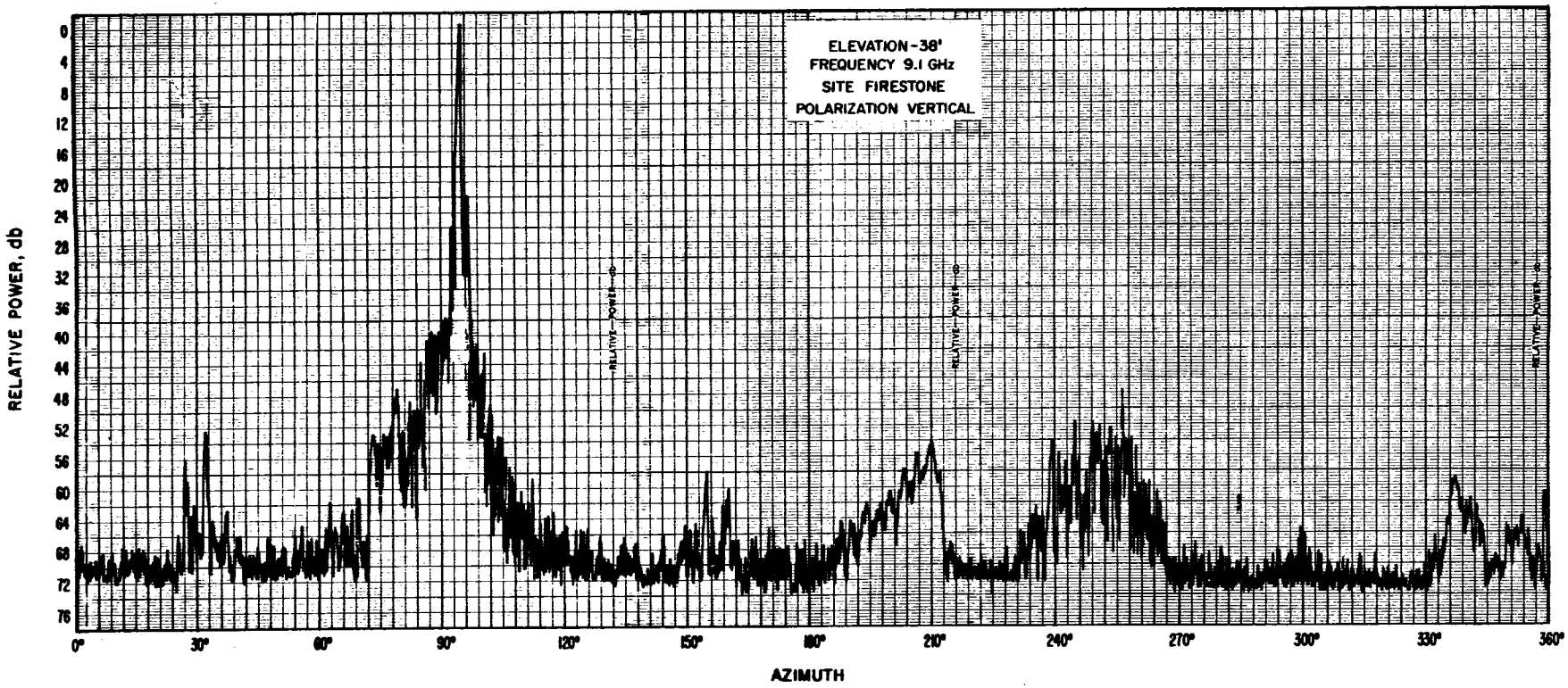
ELEVATION-38'
FREQUENCY 9.1 GHz
SITE FIRESTONE
POLARIZATION VERTICAL
RELATIVE POWER, db
0
4
8
12
16
20
24
28
32
36
40
44
48
52
56
60
64
68
72
76
0°
30°
60°
90°
120°
150°
180°
210°
240°
270°
300°
330°
360°
AZIMUTH

Figure 27

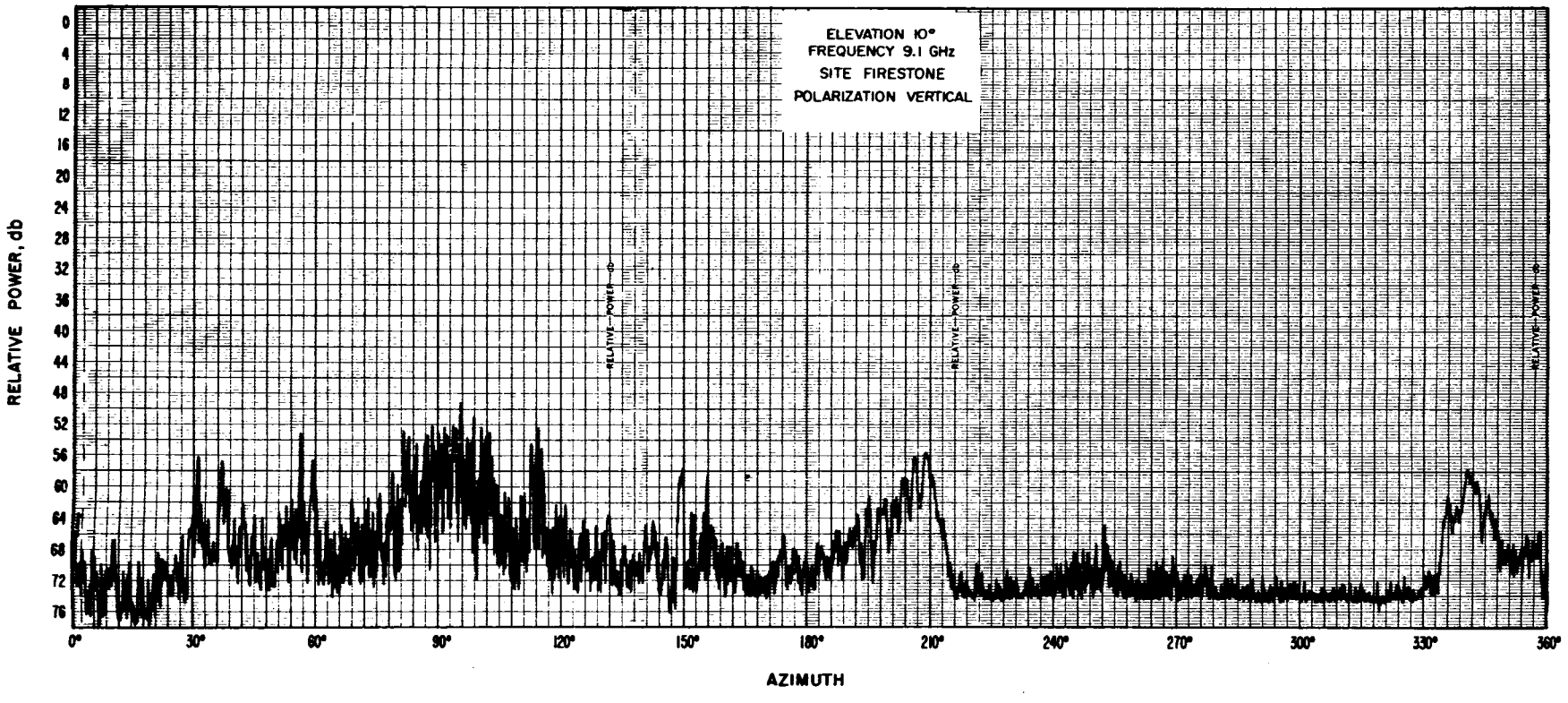

Figure 28

B- 49328

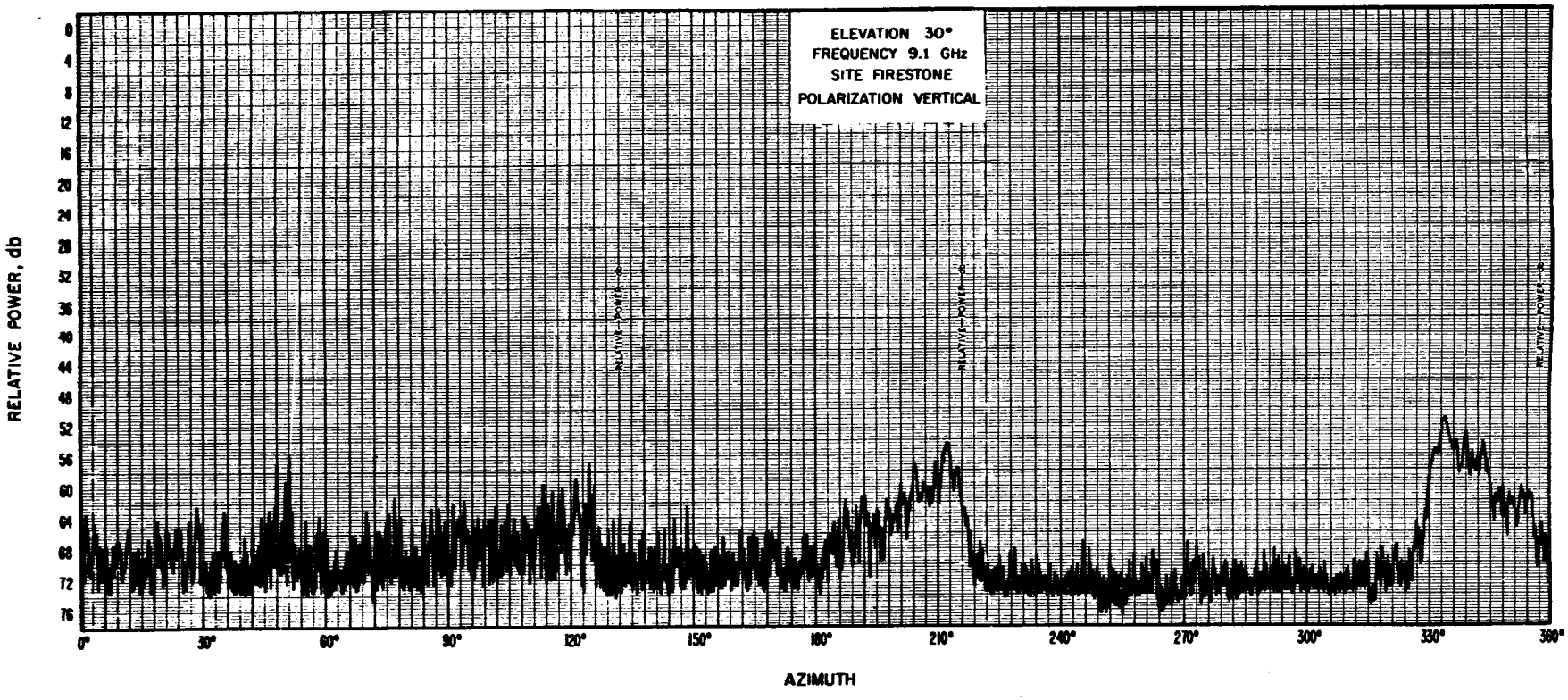

Figure 29

B- 49334

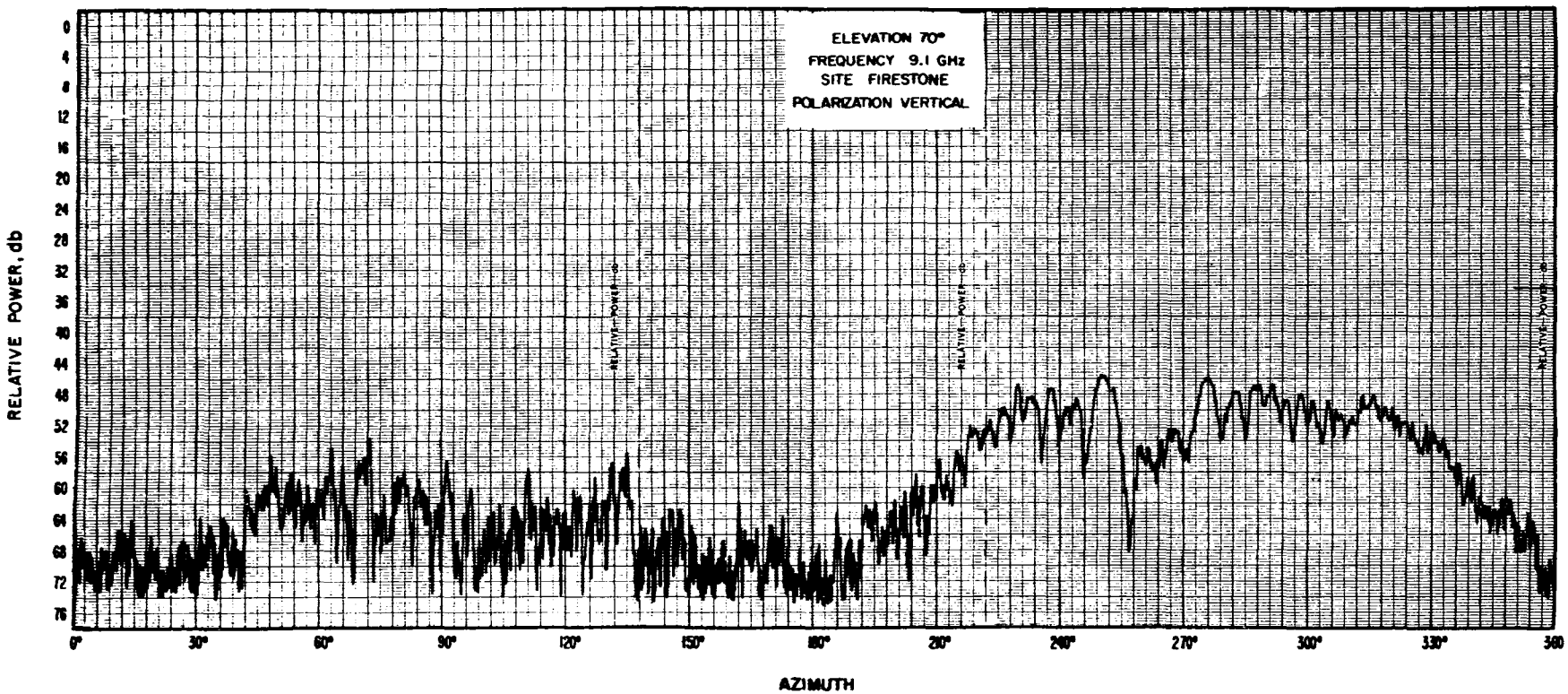
ELEVATION 70°
FREQUENCY 9.1 GHz
SITE FIRESTONE
POLARIZATION VERTICAL
RELATIVE POWER, db
0
4
8
12
16
20
24
28
32
36
40
44
48
52
56
60
64
68
72
76
0°
30°
60°
90°
120°
150°
180°
210°
240°
270°
300°
330°
360
AZIMUTH

Figure 30

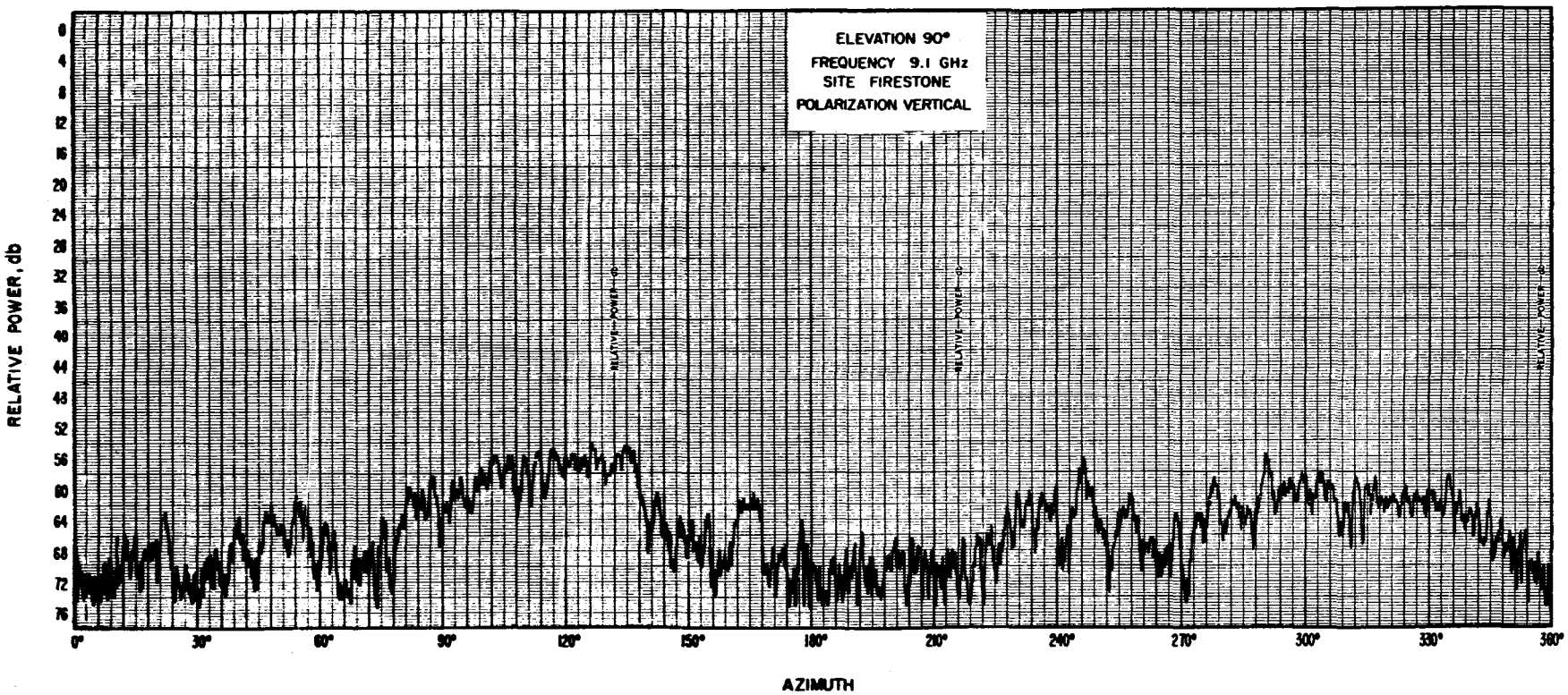
ELEVATION 90°
FREQUENCY 9.1 GHz
SITE FIRESTONE
POLARIZATION VERTICAL
RELATIVE POWER, db
0
4
8
12
16
20
24
28
32
36
40
44
48
52
56
60
64
68
72
76
0°
30°
60°
90°
120°
150°
180°
210°
240°
270°
300°
330°
360°
AZIMUTH

Figure 31

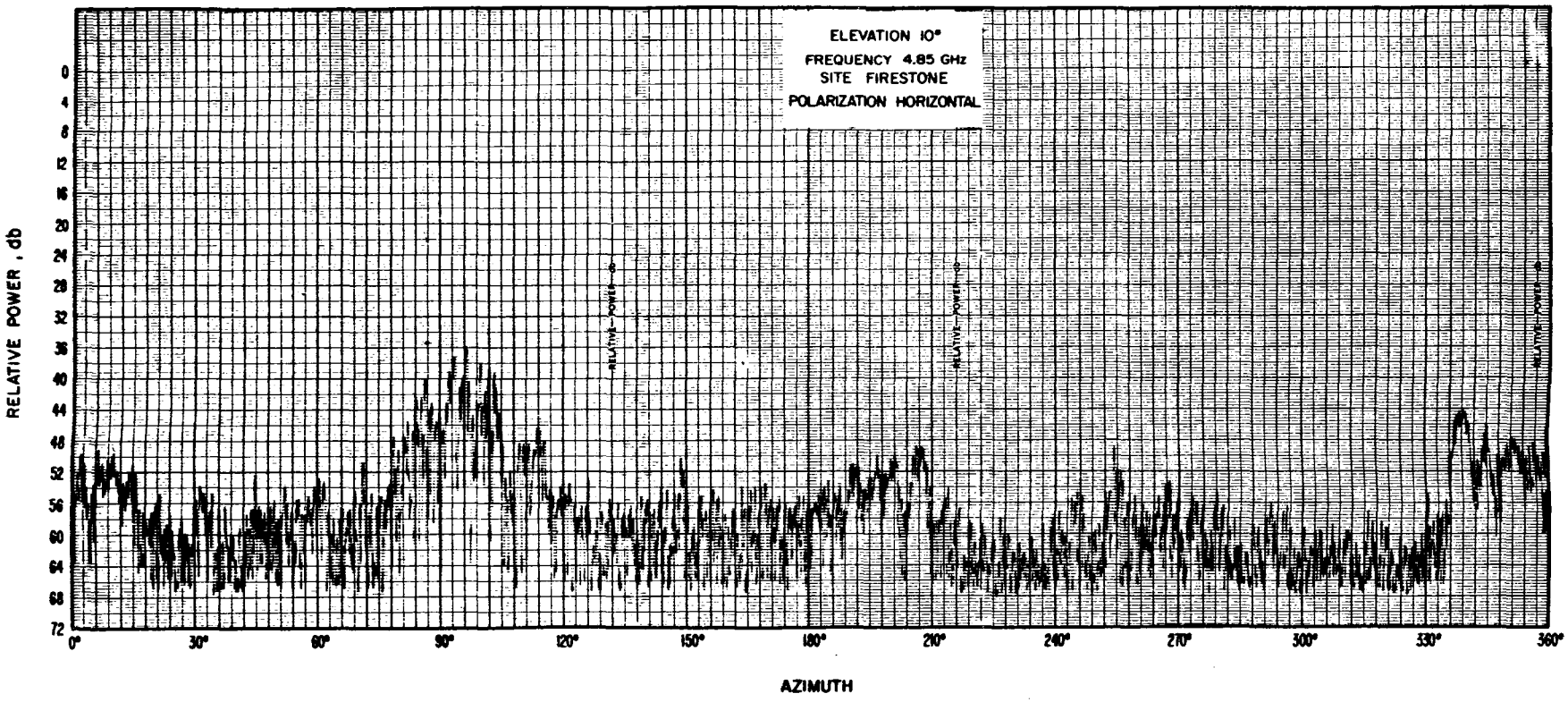

Figure 32

B- 49326

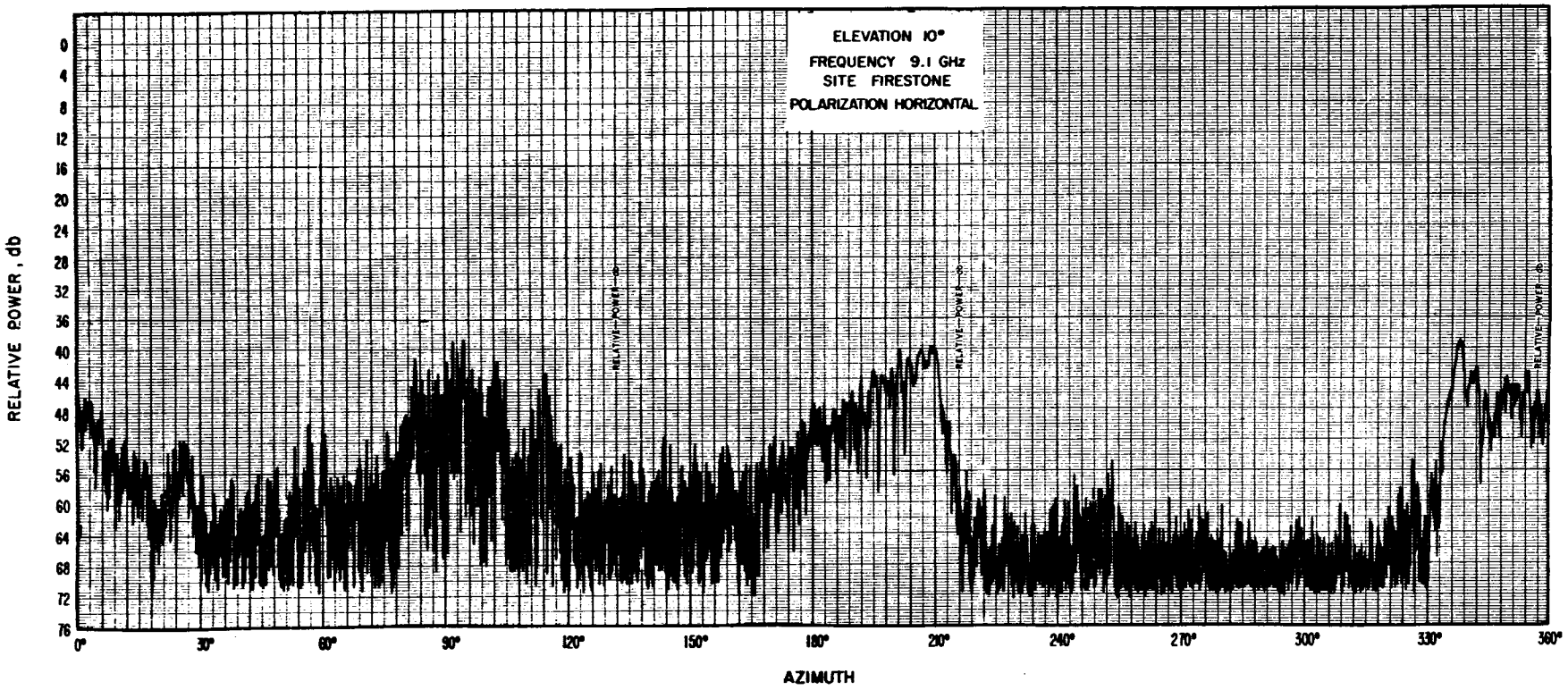

Figure 33

B- 49324

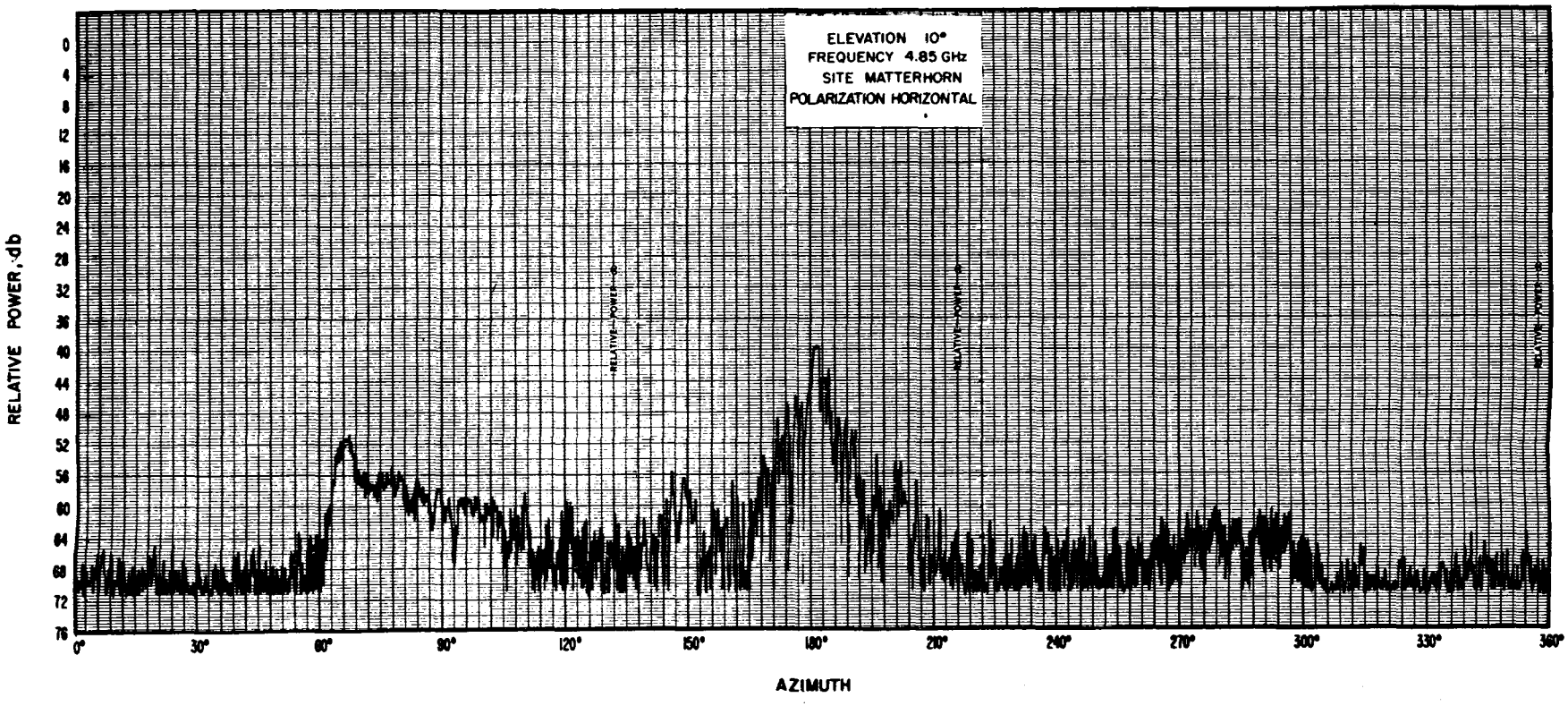

Figure 34

B-49338

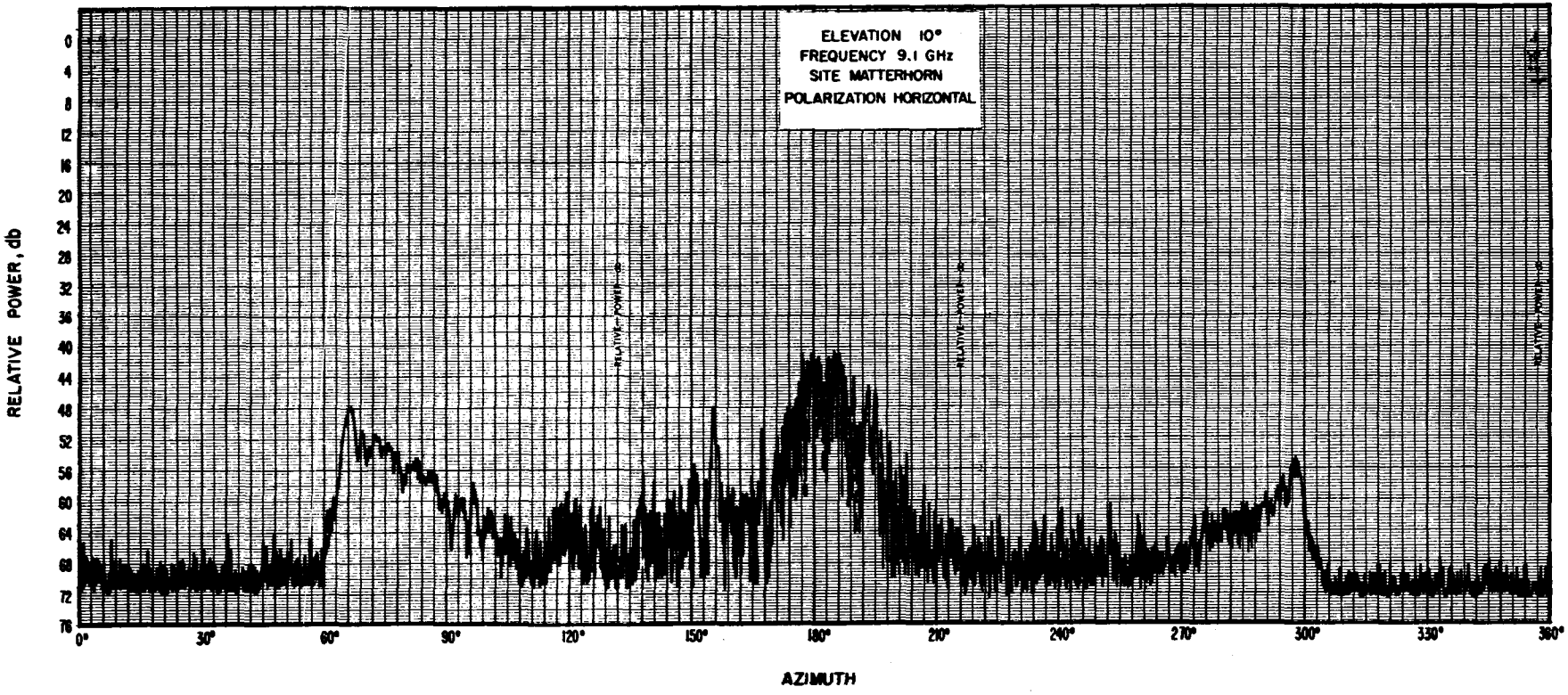
ELEVATION 10°
FREQUENCY 9.1 GHz
SITE MATTERHORN
POLARIZATION HORIZONTAL
RELATIVE POWER, db
0
4
8
12
16
20
24
28
32
36
40
44
48
52
56
60
64
68
72
76
0°
30°
60°
90°
120°
150°
180°
210°
240°
270°
300°
330°
360°
AZIMUTH

Figure 35

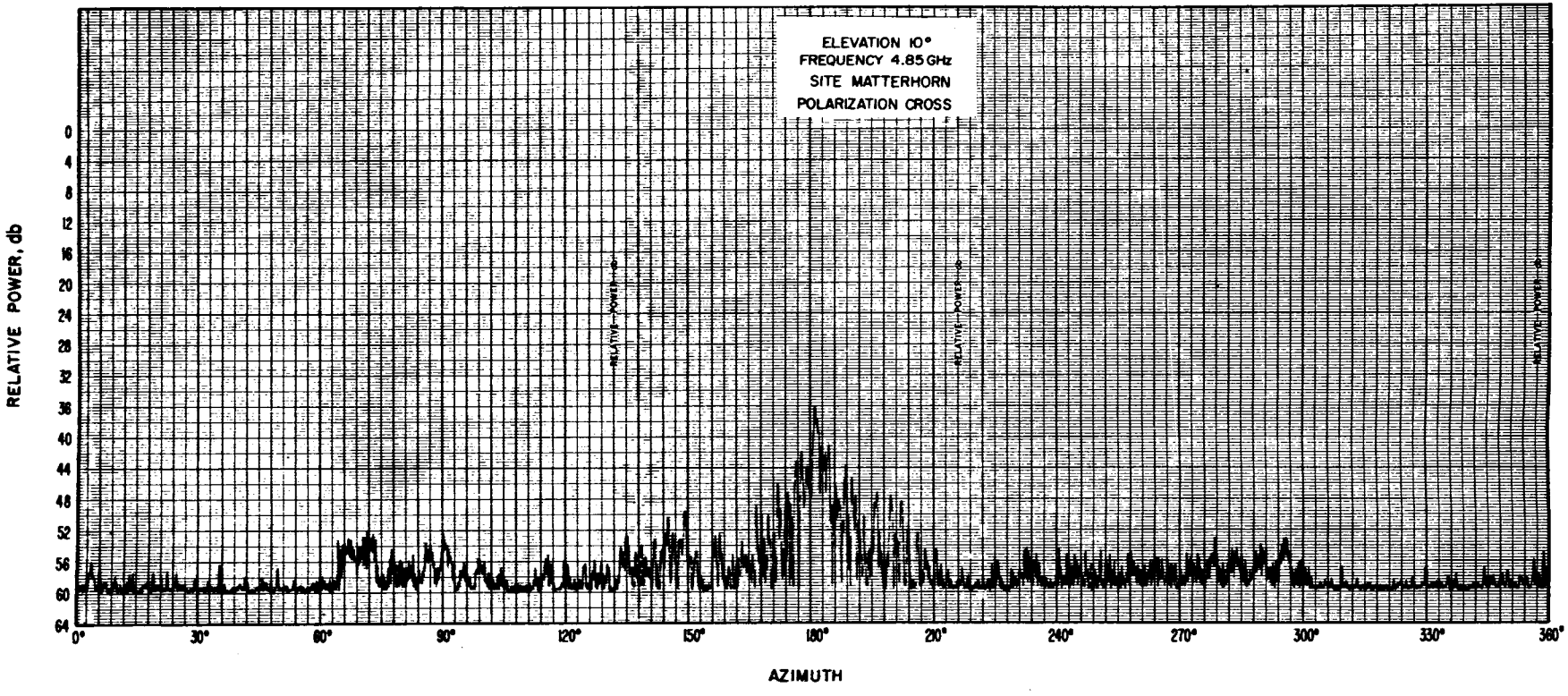

Figure 36

B- 49332

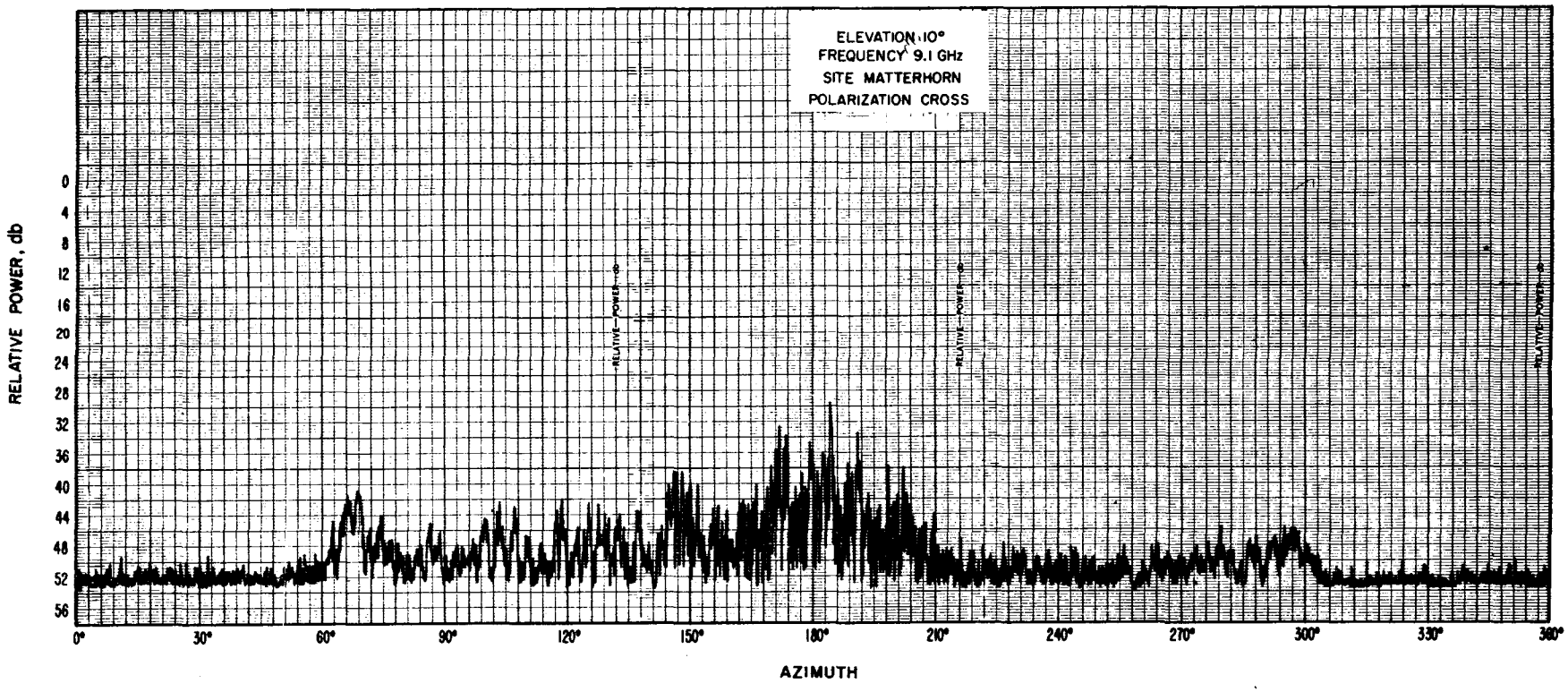

Figure 37

B- 49327

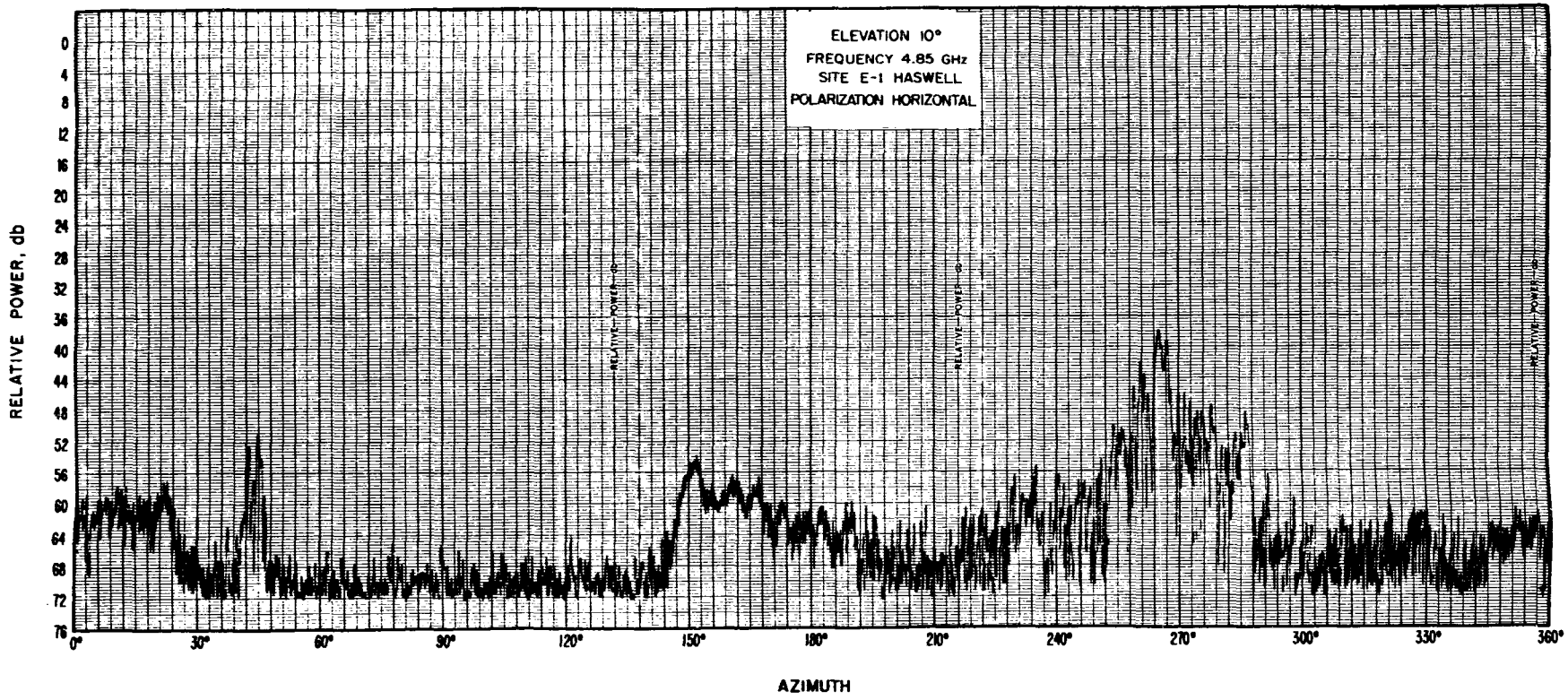

Figure 38

B- 49331

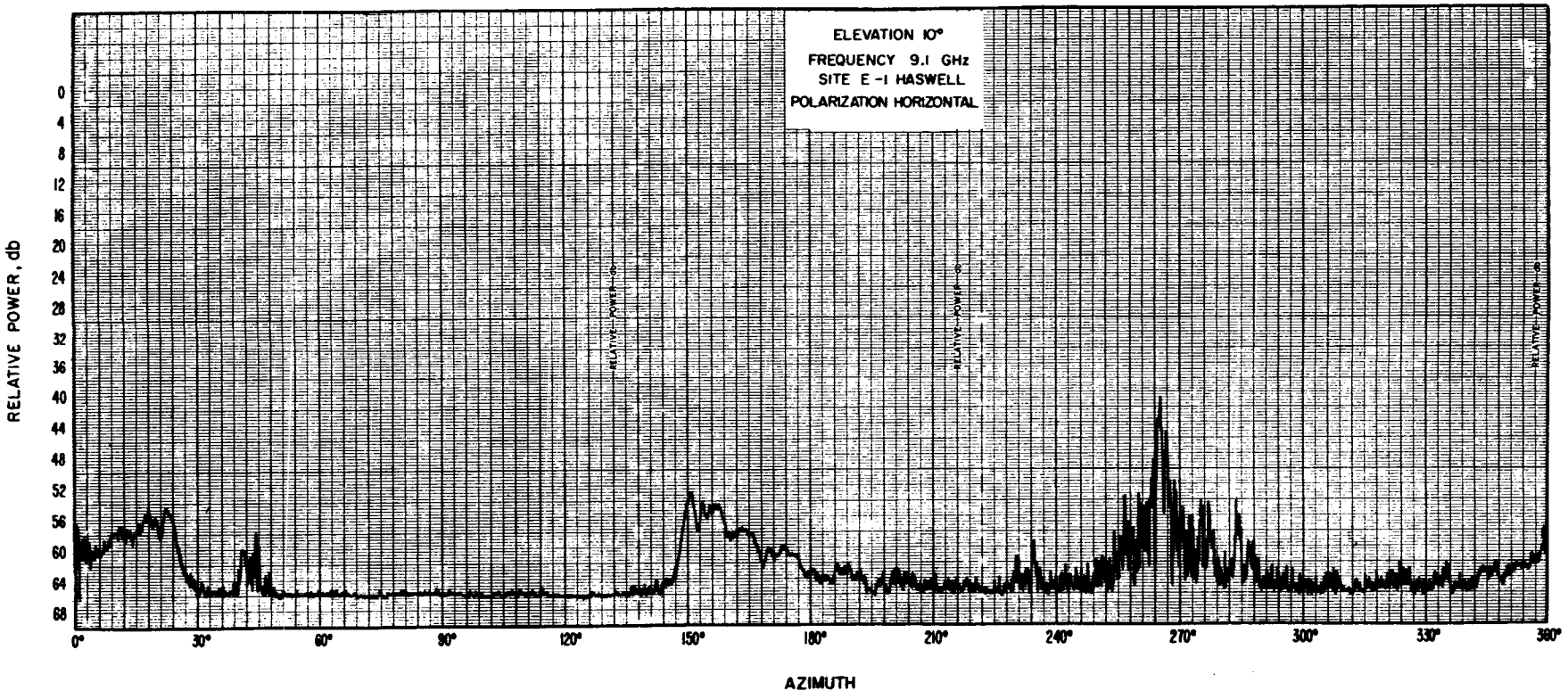
ELEVATION 10°
FREQUENCY 9.1 GHz
SITE E-1 HASWELL
POLARIZATION HORIZONTAL
RELATIVE POWER, db
0
4
8
12
16
20
24
28
32
36
40
44
48
52
56
60
64
68
0°
30°
60°
90°
120°
150°
180°
210°
240°
270°
300°
330°
360°
AZIMUTH

Figure 39

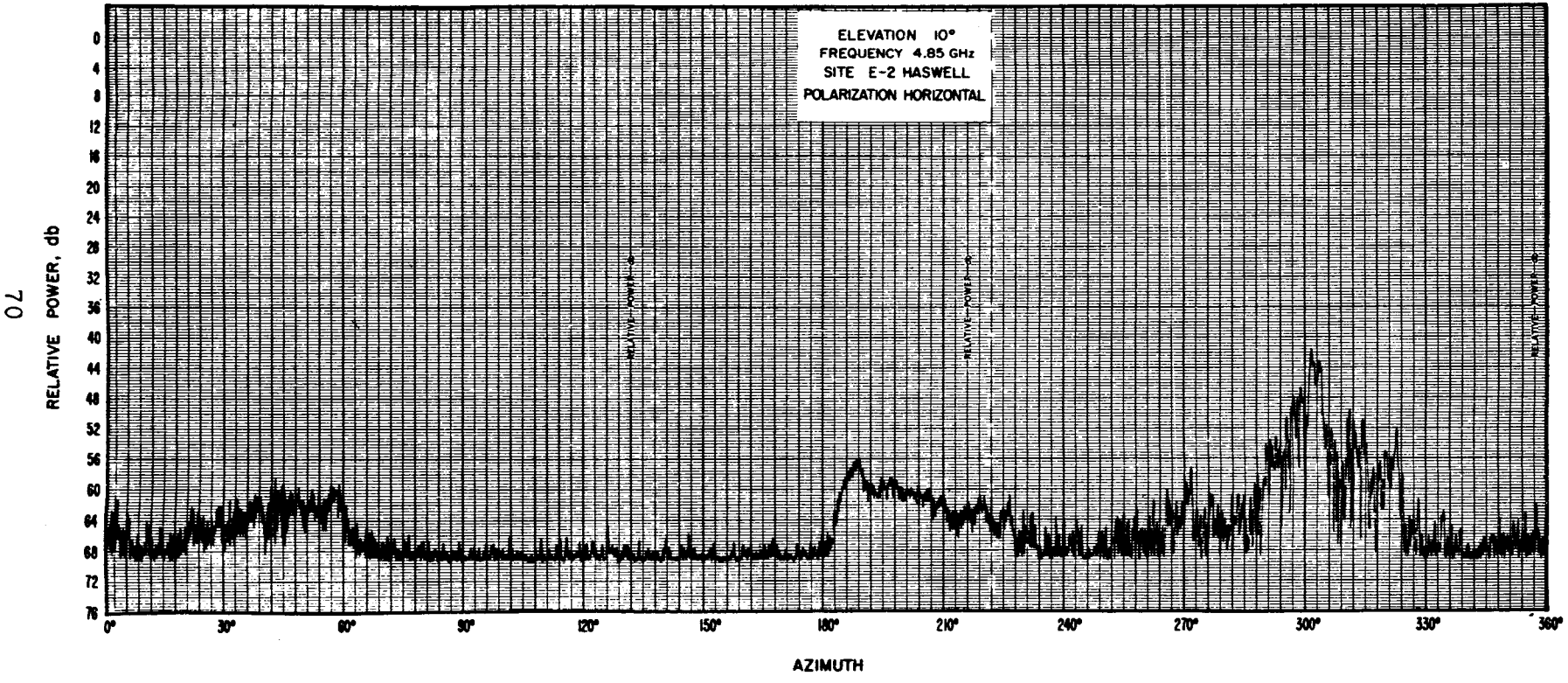

Figure 40

B- 49336

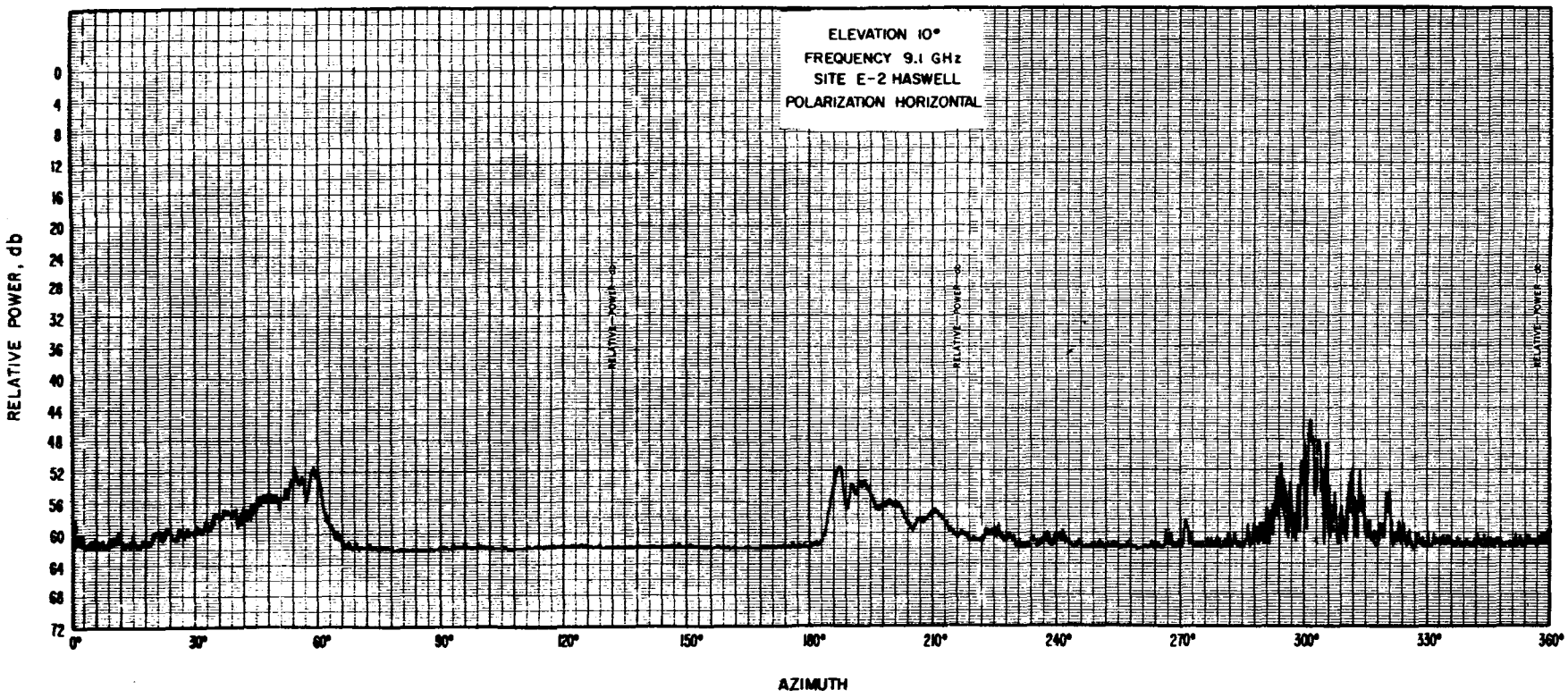
ELEVATION 10°
FREQUENCY 9.1 GHz
SITE E-2 HASWELL
POLARIZATION HORIZONTAL
RELATIVE POWER, db
0
4
8
12
16
20
24
28
32
36
40
44
48
52
56
60
64
68
72
0°
30°
60°
90°
120°
150°
180°
210°
240°
270°
300°
330°
360°
AZIMUTH

Figure 41

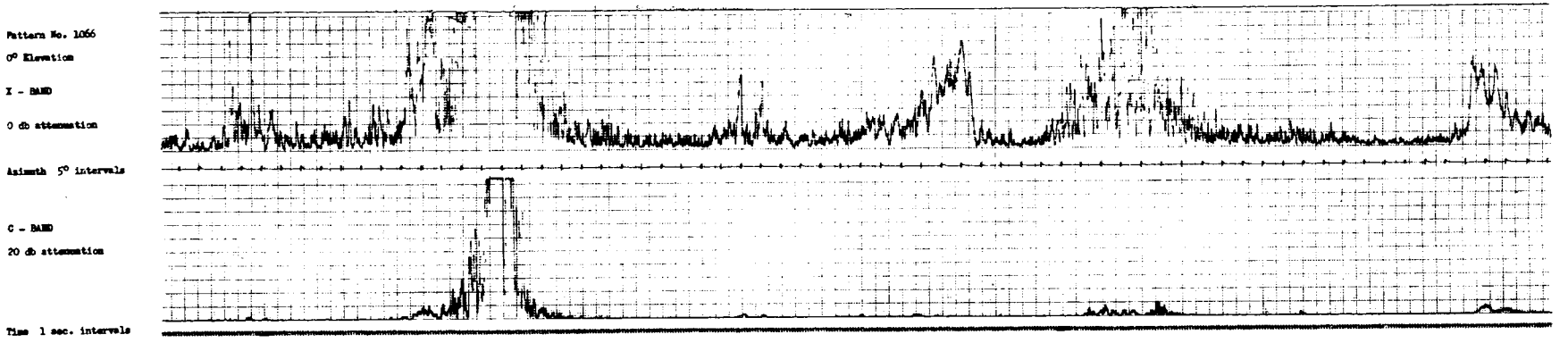
Pattern No. 1066
0° Elevation
X - BAND
0 db attenuation
Azimuth 5° intervals
C - BAND
20 db attenuation
Time 1 sec. intervals

Figure 42

ANTENNA PATTERN ANALYSIS DIAGRAM

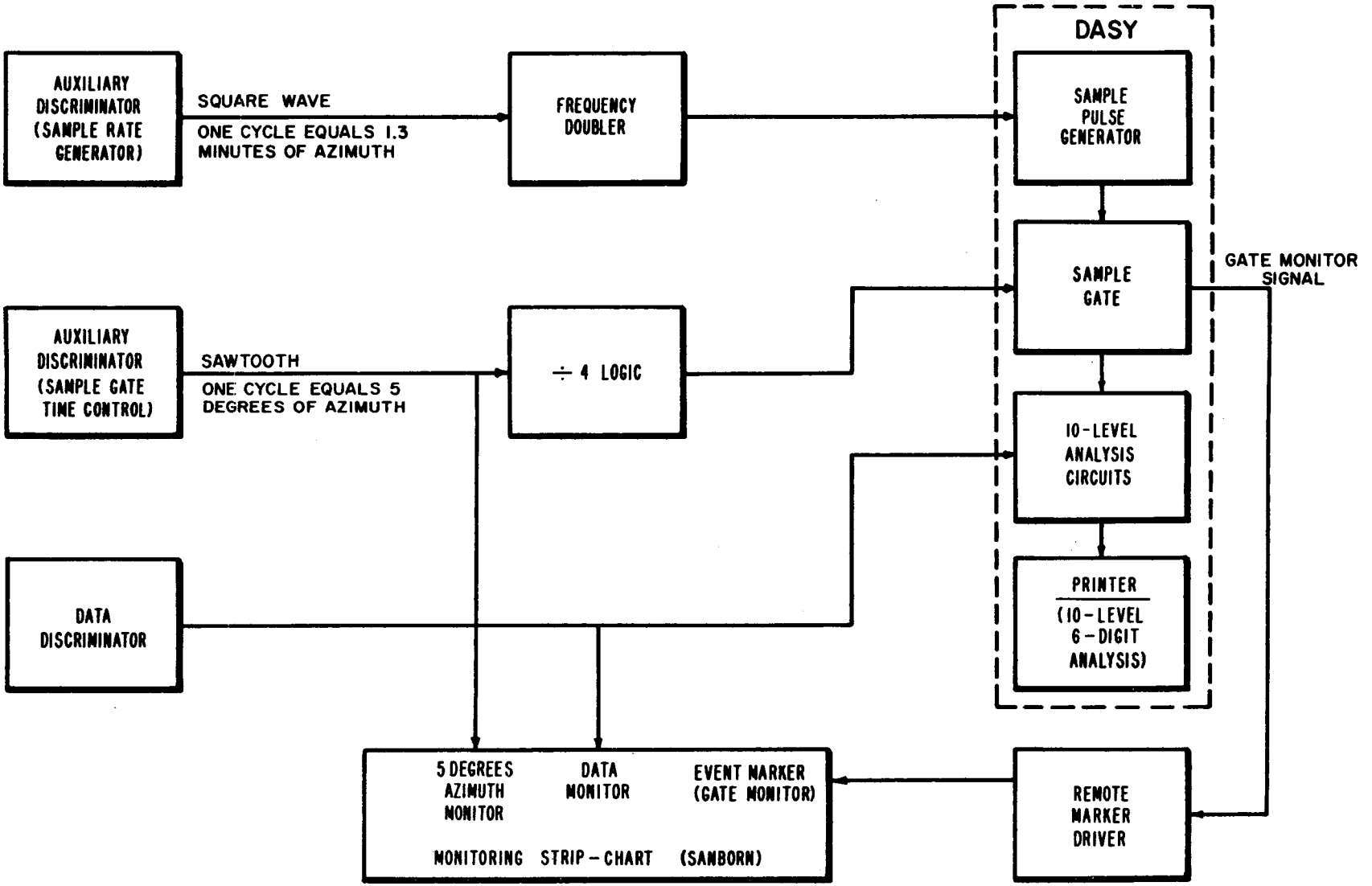

Figure 43

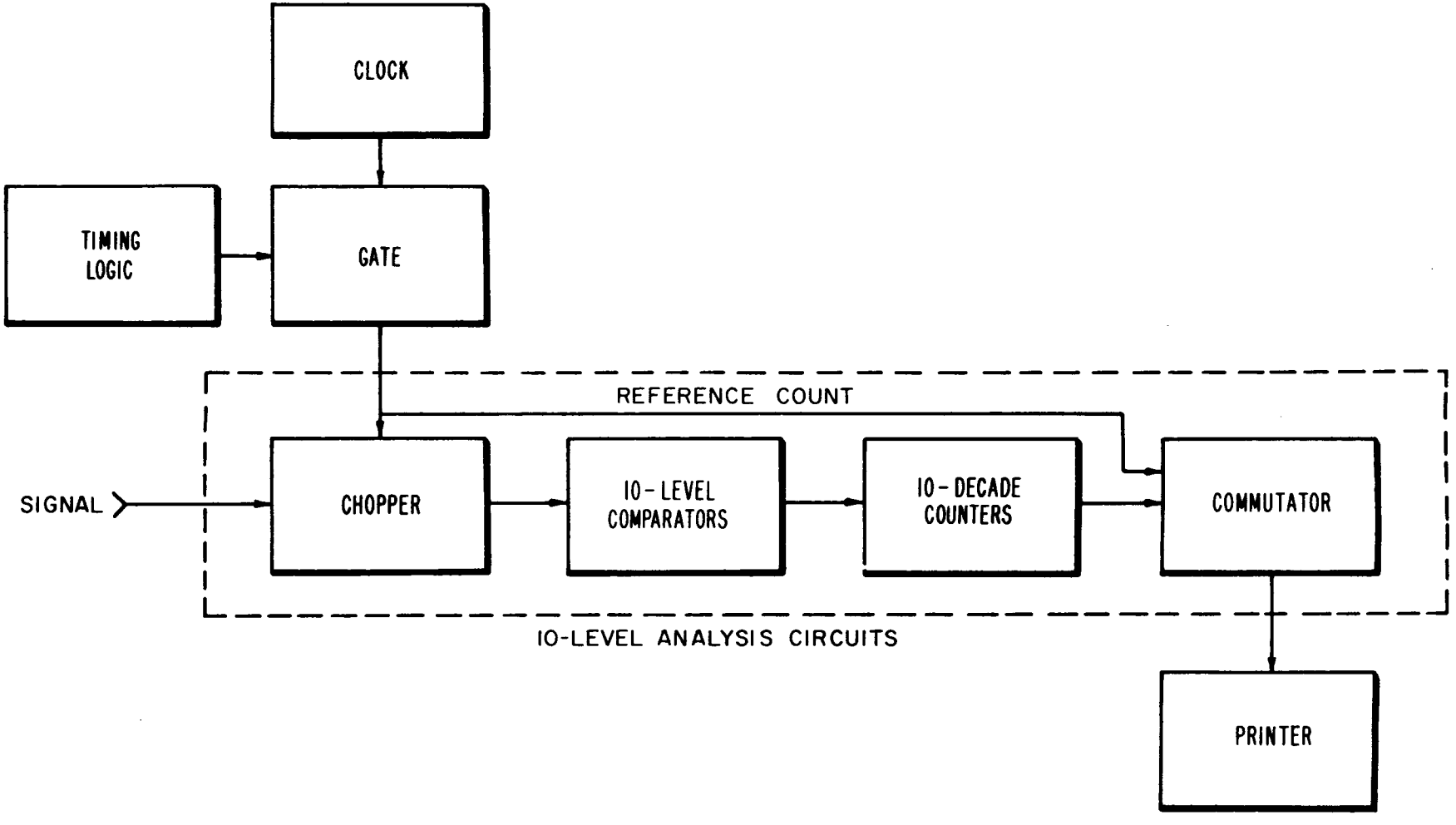

Figure 44

B-48845

Block No.	Level No.	Data Sample Count
1	10	000170
	09	000150
	08	000120
	07	000093
	06	000048
	05	000024
	04	000004
	03	000001
	02	000000
	01	000000
	00	000219

PROJECT 83453

Pattern 1255 Site 4

Polarization 1

Elev. 1 Band 9 Pad 0

Figure 45

Sample of digital data on folding paper tape.

Punched Card Format

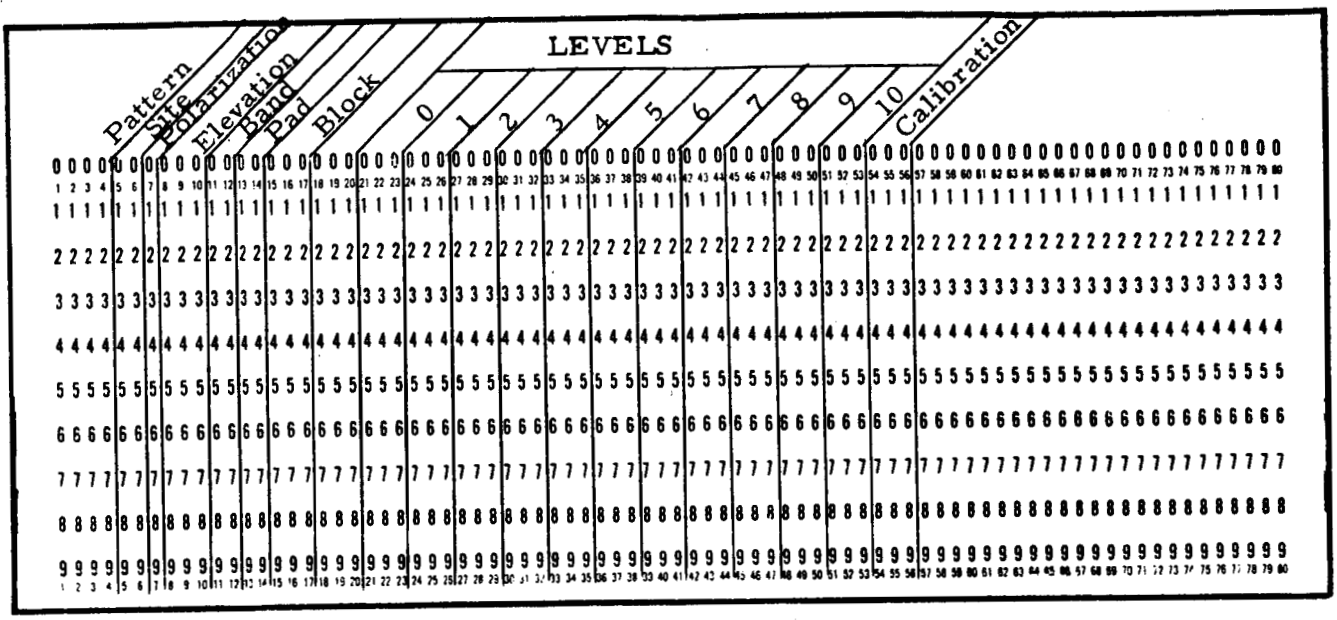

Card Column	Description	Remarks
1-4	Pattern Number	
5-6	Site Number	#1=Firestone;#2=E-2;#3=E-1;#4 Matterhorn
7	Polarization	#1=Horizontal; #2=Vertical;
8-10	Elevation	Elevation is in degrees; minus degrees coded as 91.
11-12	Band	#5 for 4.85 GHz; #9 for 9.1 GHz
13-14	Attenuation	Attenuation codes as 0, 2, 4... etc for 0, 20, 40... db attenuation
15-17	Block Number	Block number corresponds to every 5^{o} of the Azimuth
18-20		Blank (empty)
21-23	Level 0	Data Count
24-26	Level 1	Data Count
27-29	Level 2	Data Count
30-32	Level 3	Data Count
33-35	Level 4	Data Count
36-38	Level 5	Data Count
39-41	Level 6	Data Count
42-44	Level 7	Data Count
45-47	Level 8	Data Count
48-50	Level 9	Data Count
51-53	Level 10	Data Count
54-56	Calibration	First Card only of each elevation and each pad

Figure 46

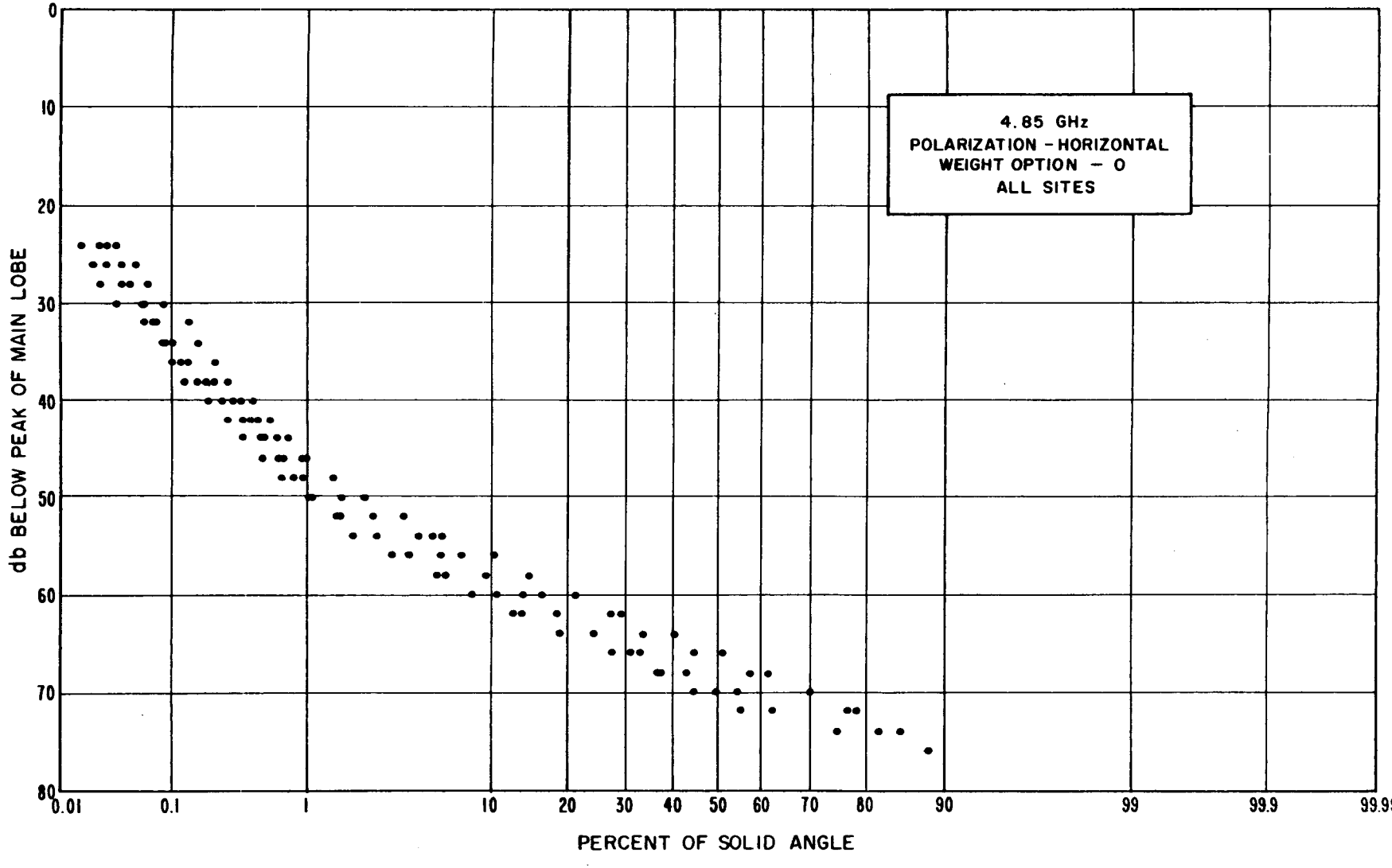
4.85 GHz
POLARIZATION - HORIZONTAL
WEIGHT OPTION - 0
ALL SITES
db BELOW PEAK OF MAIN LOBE
0
10
20
30
40
50
60
70
80
0.01
0.1
1
10
20
30
40
50
60
70
80
90
99
99.9
99.99
PERCENT OF SOLID ANGLE

Figure 47

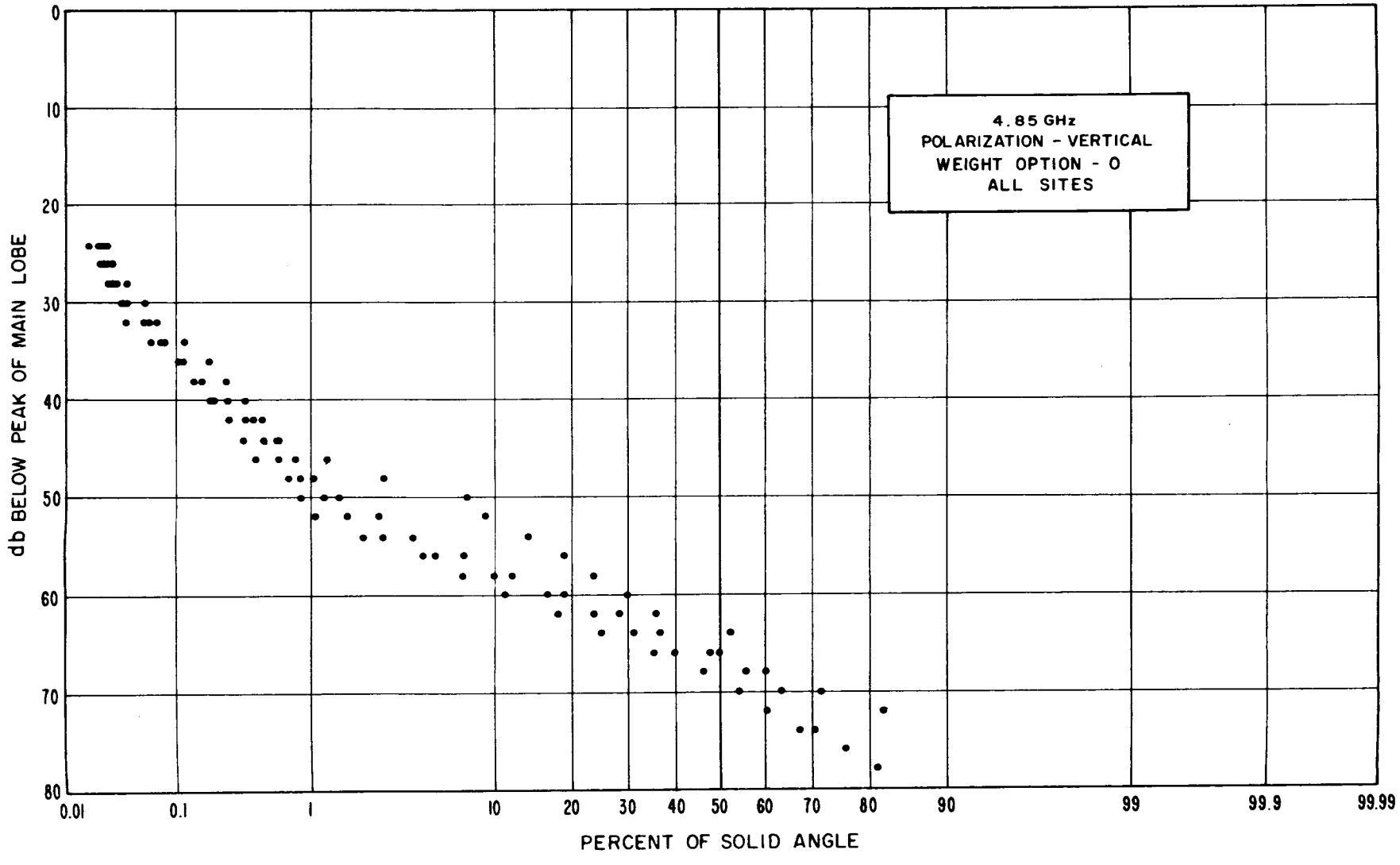
4.85 GHz
POLARIZATION - VERTICAL
WEIGHT OPTION - 0
ALL SITES
db BELOW PEAK OF MAIN LOBE
0
10
20
30
40
50
60
70
80
0.01
0.1
1
10
20
30
40
50
60
70
80
90
99
99.9
99.99
PERCENT OF SOLID ANGLE

Figure 48

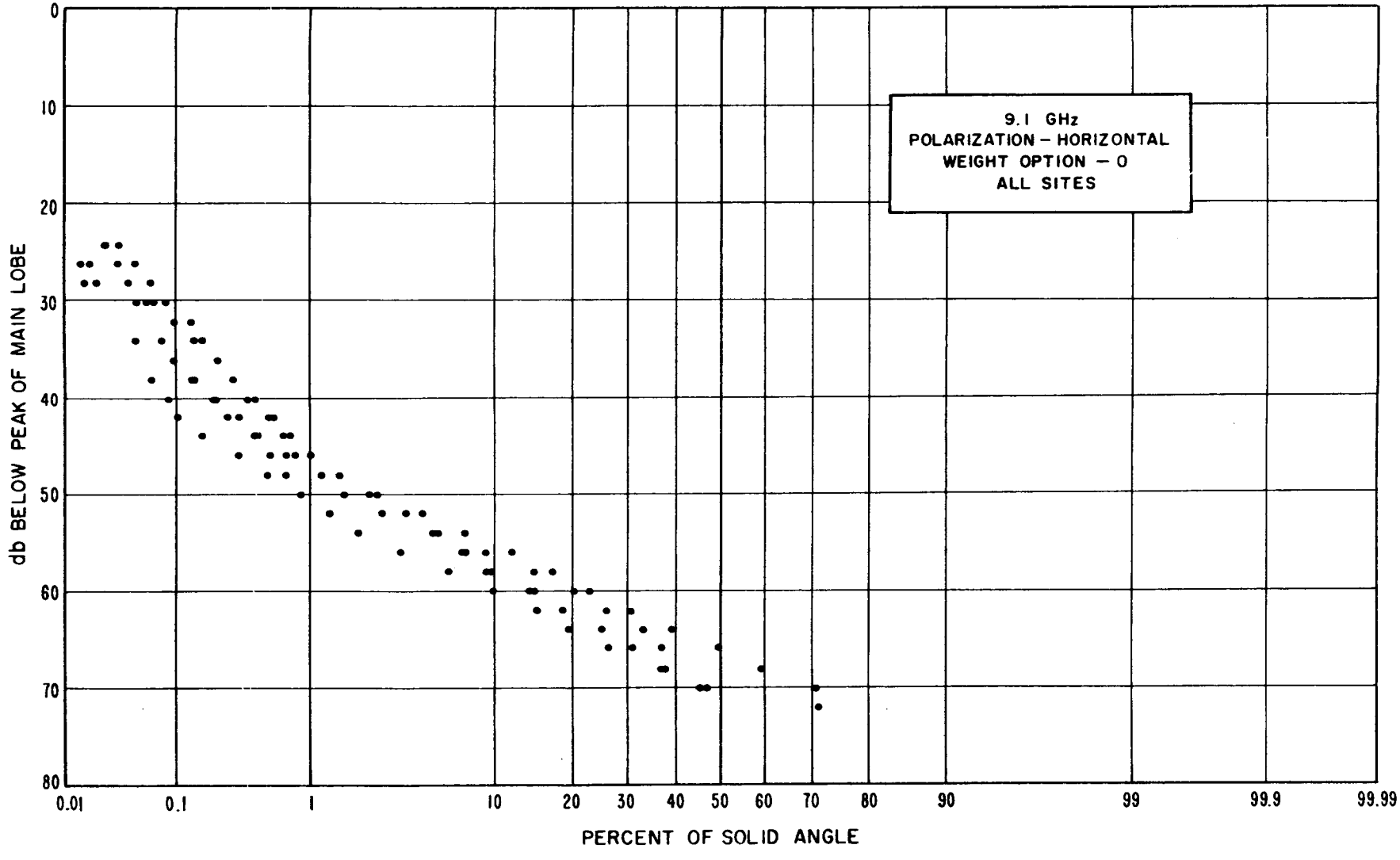
9.1 GHz
POLARIZATION – HORIZONTAL
WEIGHT OPTION – 0
ALL SITES
db BELOW PEAK OF MAIN LOBE
0
10
20
30
40
50
60
70
80
0.01
0.1
1
10
20
30
40
50
60
70
80
90
99
99.9
99.99
PERCENT OF SOLID ANGLE

Figure 49

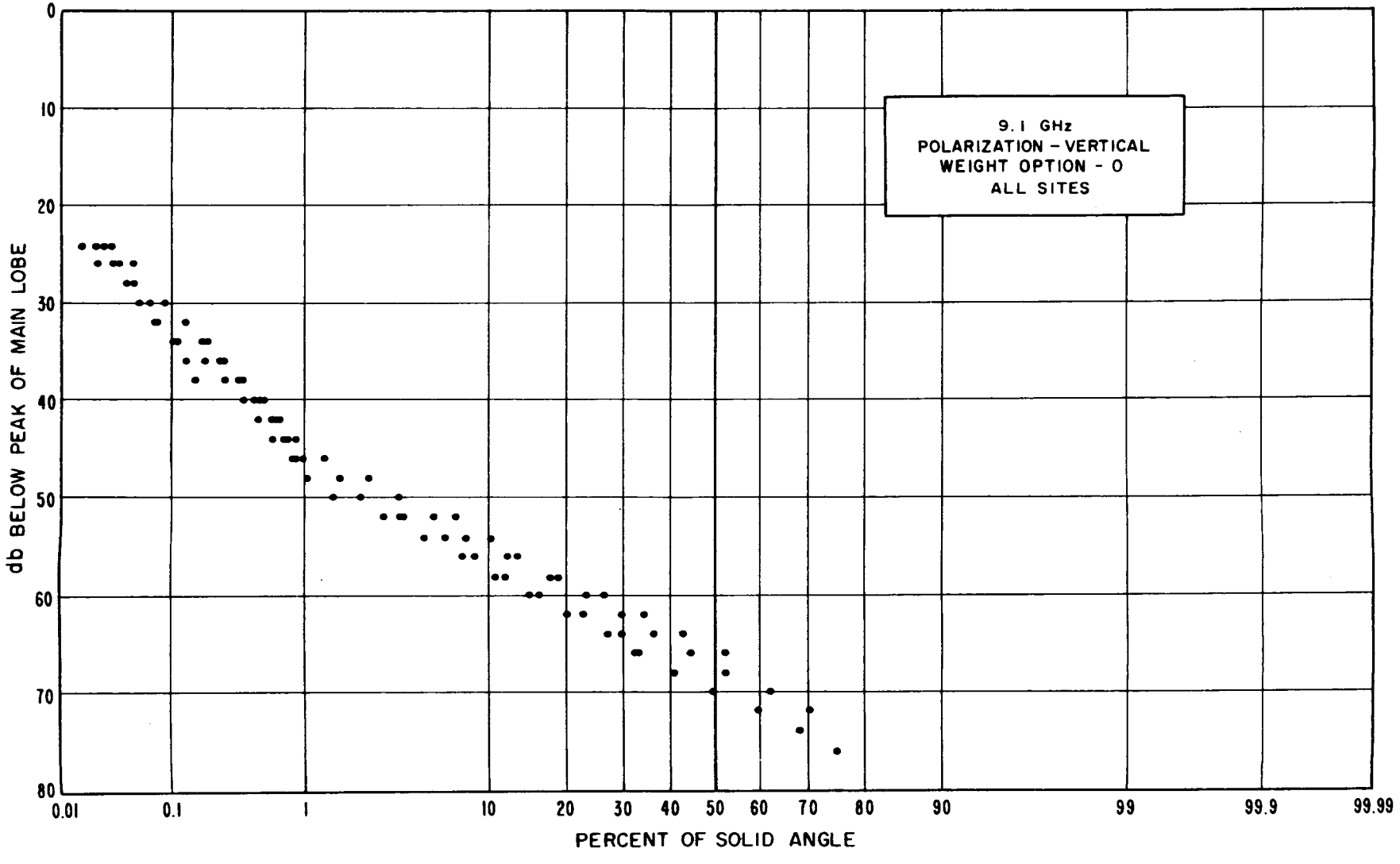
9.1 GHz
POLARIZATION - VERTICAL
WEIGHT OPTION - 0
ALL SITES
db BELOW PEAK OF MAIN LOBE
0
10
20
30
40
50
60
70
80
0.01
0.1
1
10
20
30
40
50
60
70
80
90
99
99.9
99.99
PERCENT OF SOLID ANGLE

Figure 50

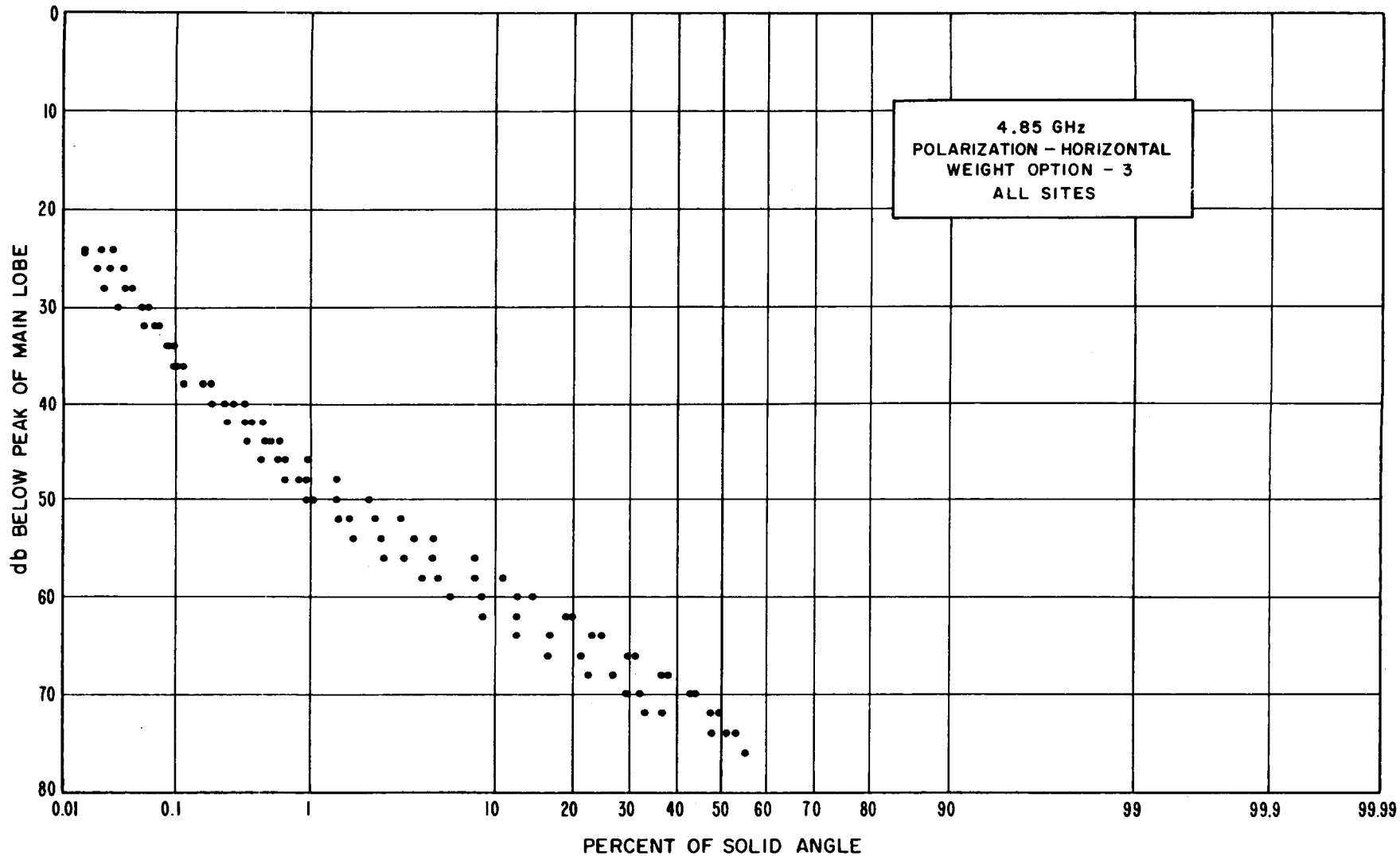
4.85 GHz
POLARIZATION – HORIZONTAL
WEIGHT OPTION – 3
ALL SITES
db BELOW PEAK OF MAIN LOBE
0
10
20
30
40
50
60
70
80
0.01
0.1
1
10
20
30
40
50
60
70
80
90
99
99.9
99.99
PERCENT OF SOLID ANGLE

Figure 51

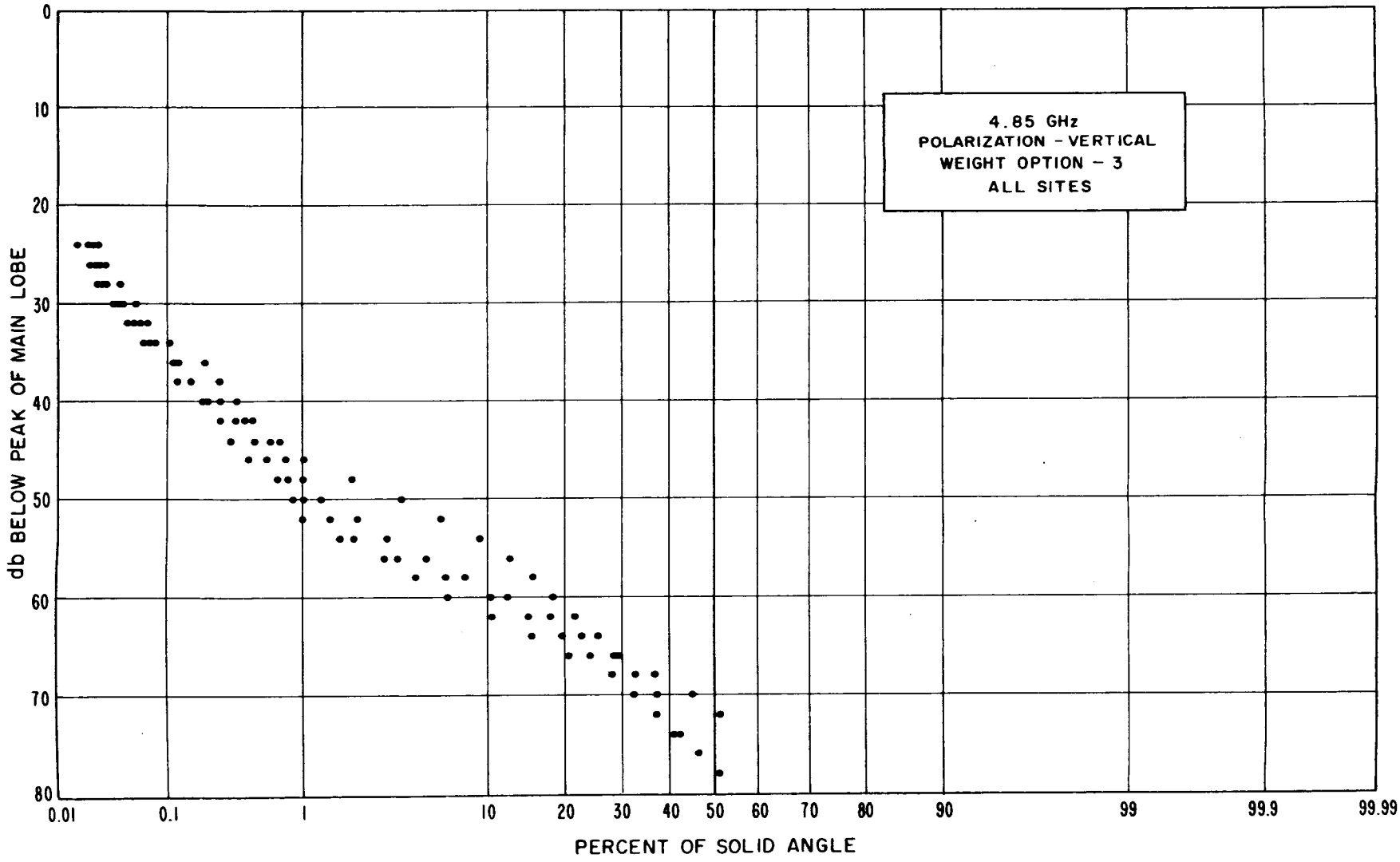

Figure 52

B- 48999

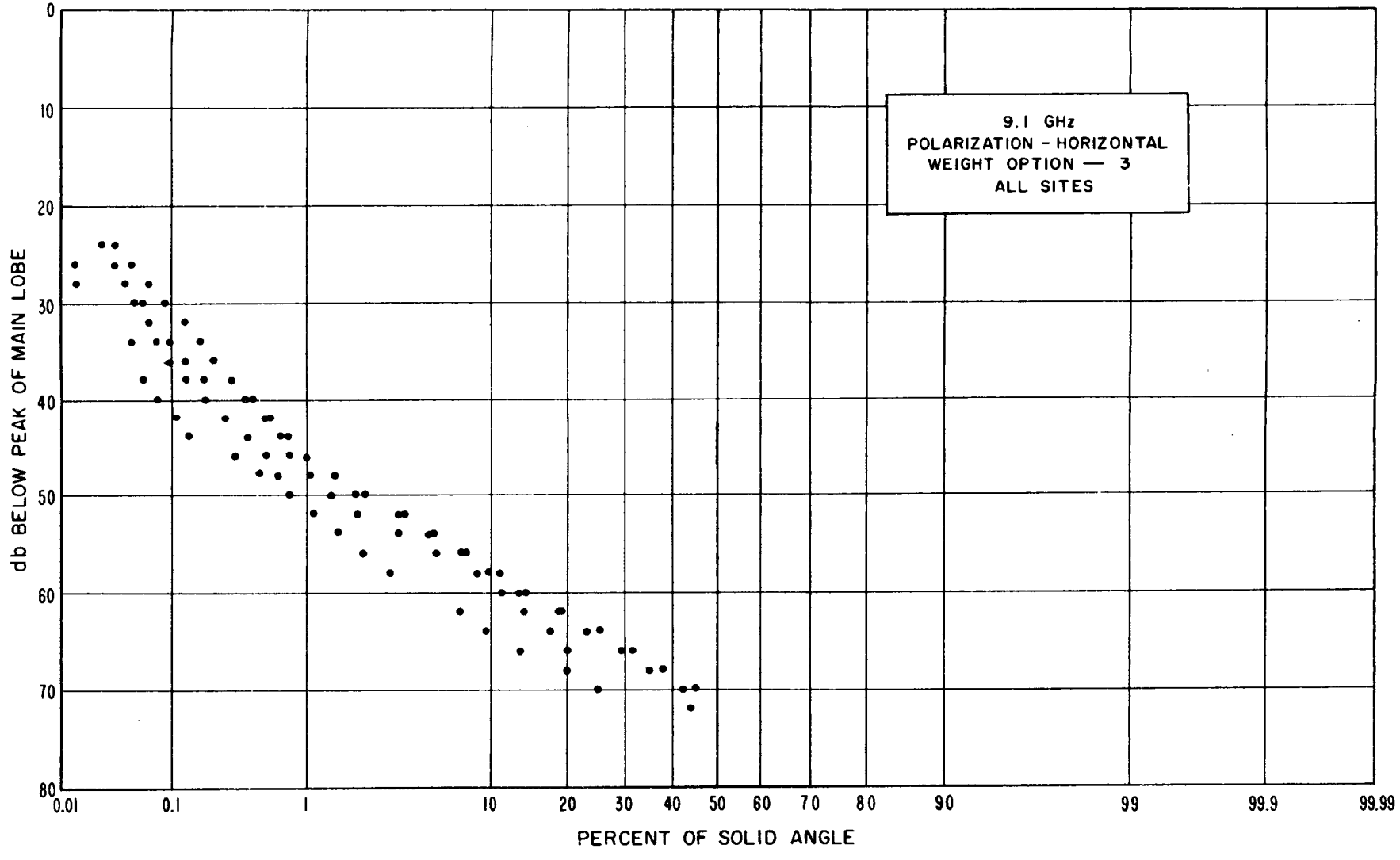
9.1 GHz
POLARIZATION - HORIZONTAL
WEIGHT OPTION — 3
ALL SITES
db BELOW PEAK OF MAIN LOBE
0
10
20
30
40
50
60
70
80
0.01
0.1
1
10
20
30
40
50
60
70
80
90
99
99.9
99.99
PERCENT OF SOLID ANGLE

Figure 53

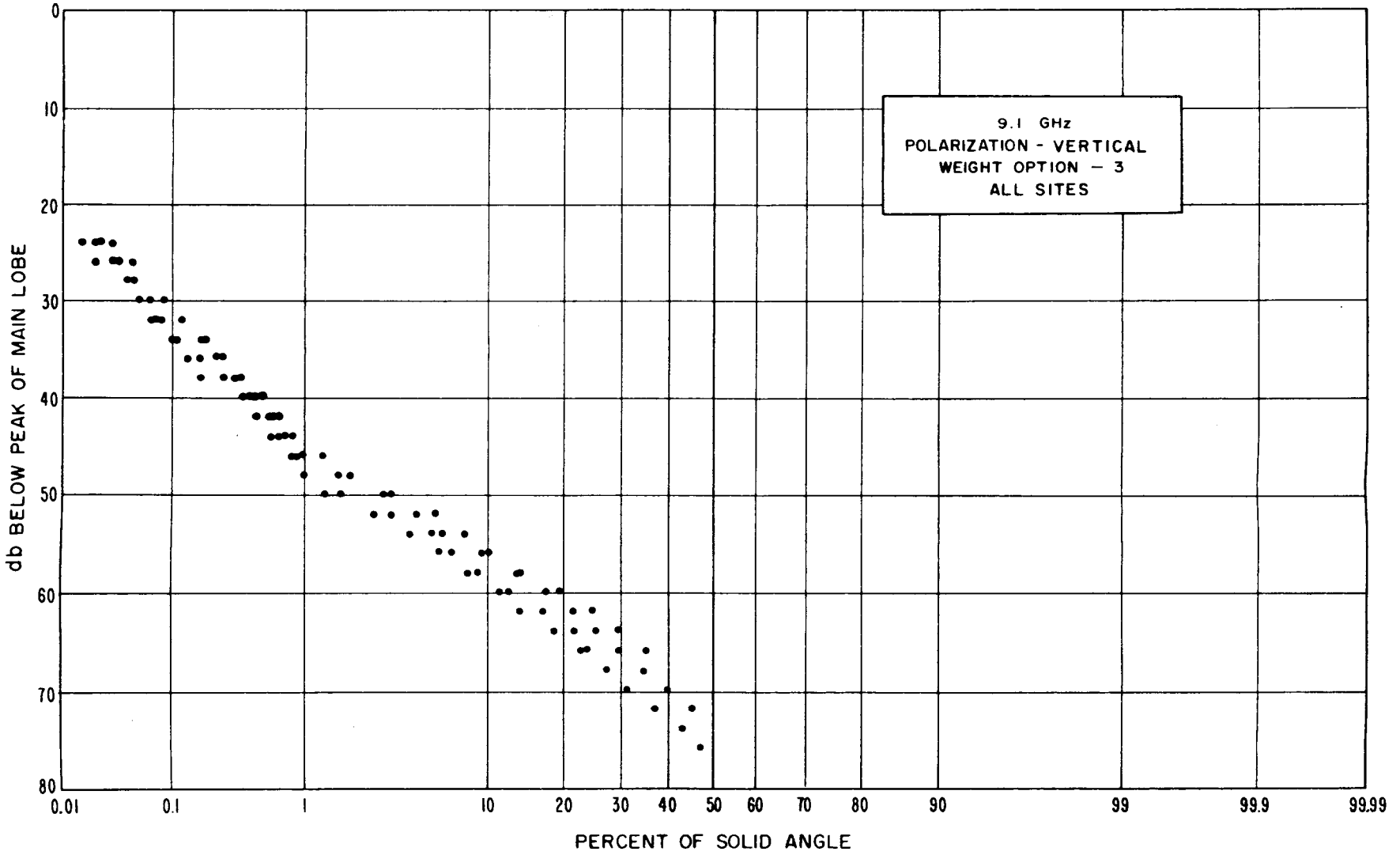
9.1 GHz
POLARIZATION - VERTICAL
WEIGHT OPTION — 3
ALL SITES
db BELOW PEAK OF MAIN LOBE
0
10
20
30
40
50
60
70
80
0.01
0.1
1
10
20
30
40
50
60
70
80
90
99
99.9
99.99
PERCENT OF SOLID ANGLE

Figure 54

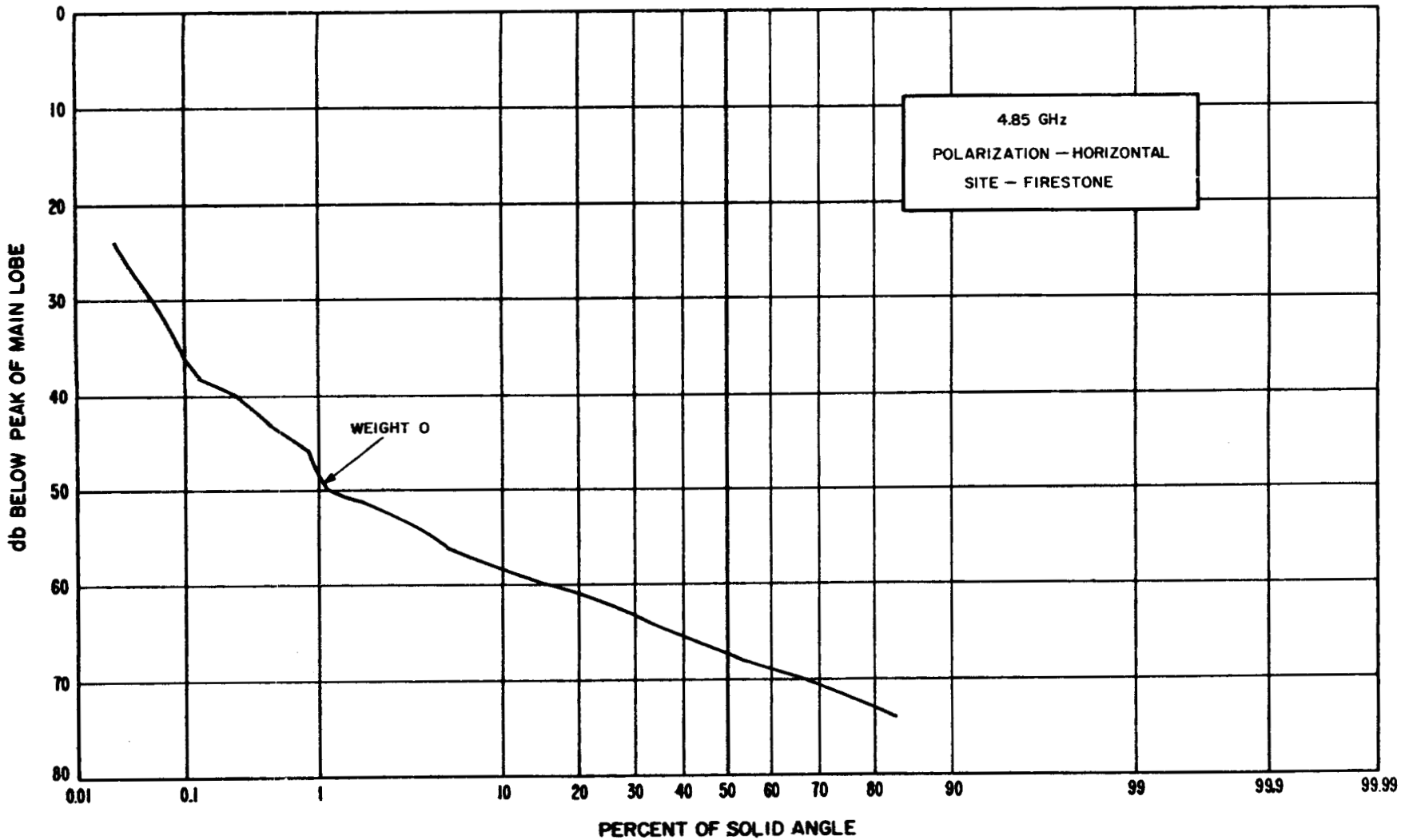
4.85 GHz
POLARIZATION — HORIZONTAL
SITE — FIRESTONE
WEIGHT 0
db BELOW PEAK OF MAIN LOBE
0
10
20
30
40
50
60
70
80
0.01
0.1
1
10
20
30
40
50
60
70
80
90
99
99.9
99.99
PERCENT OF SOLID ANGLE

Figure 55

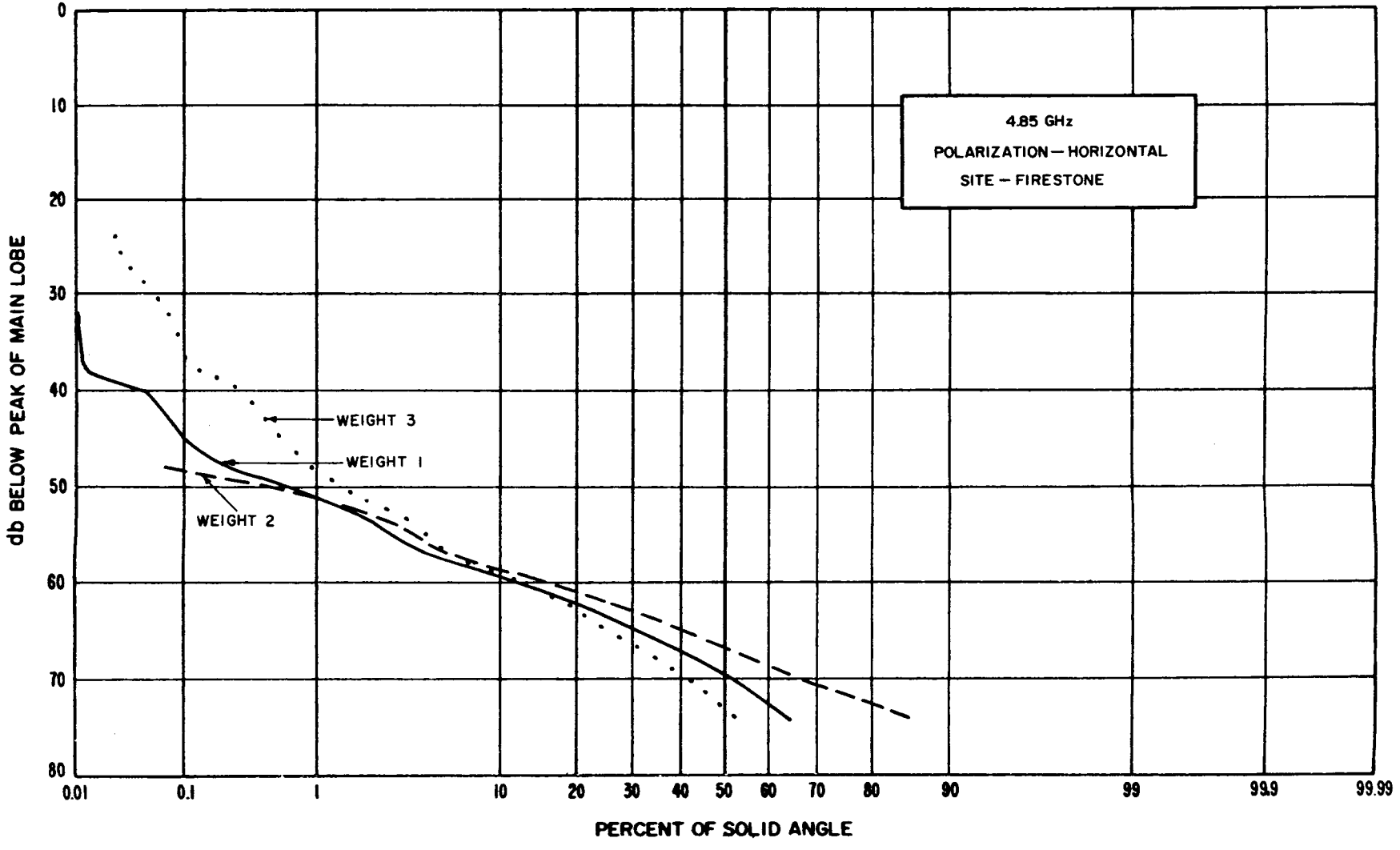

Figure 56

B-49199

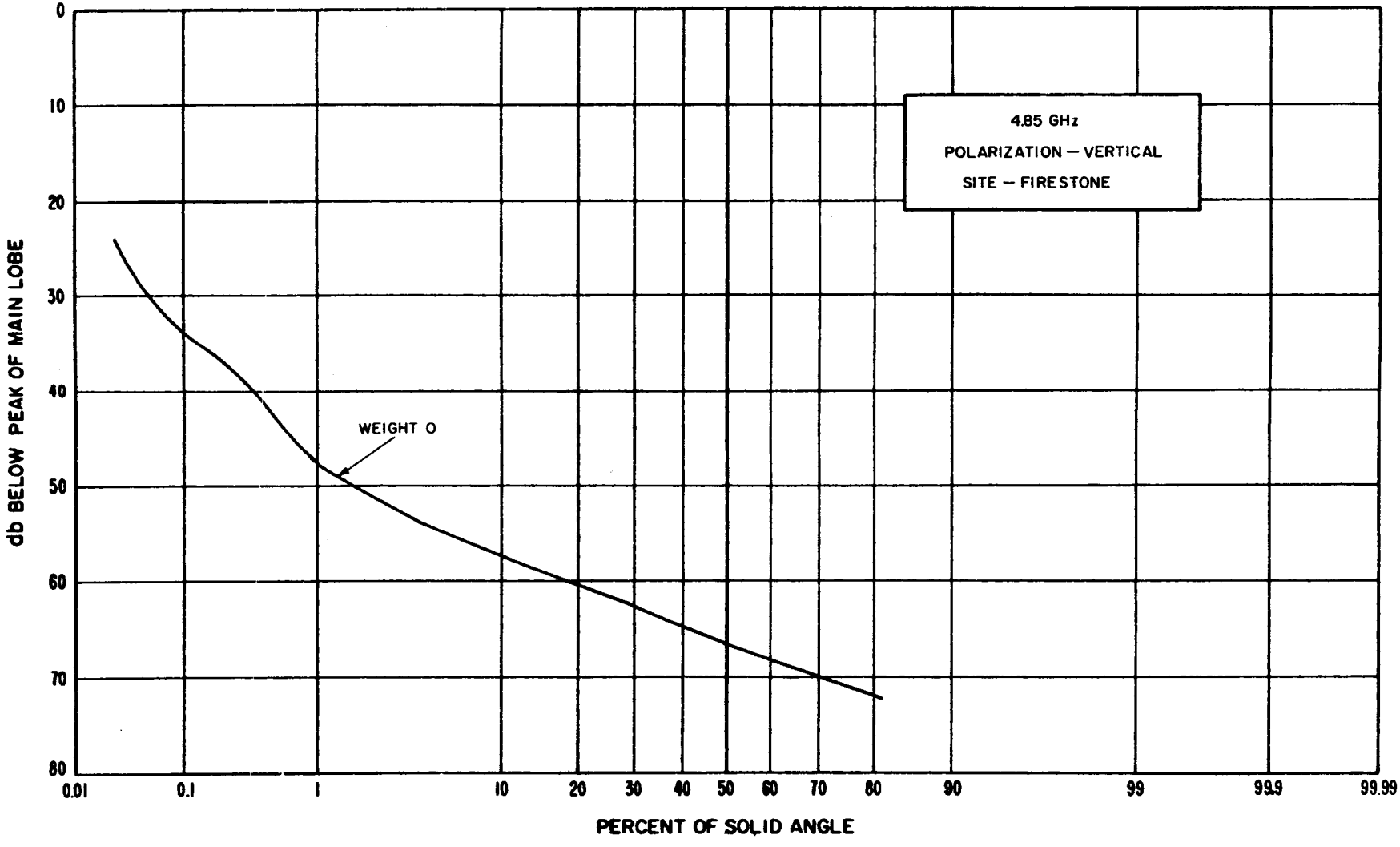
4.85 GHz
POLARIZATION — VERTICAL
SITE — FIRESTONE
WEIGHT O
db BELOW PEAK OF MAIN LOBE
0
10
20
30
40
50
60
70
80
0.01
0.1
1
10
20
30
40
50
60
70
80
90
99
99.9
99.99
PERCENT OF SOLID ANGLE

Figure 57

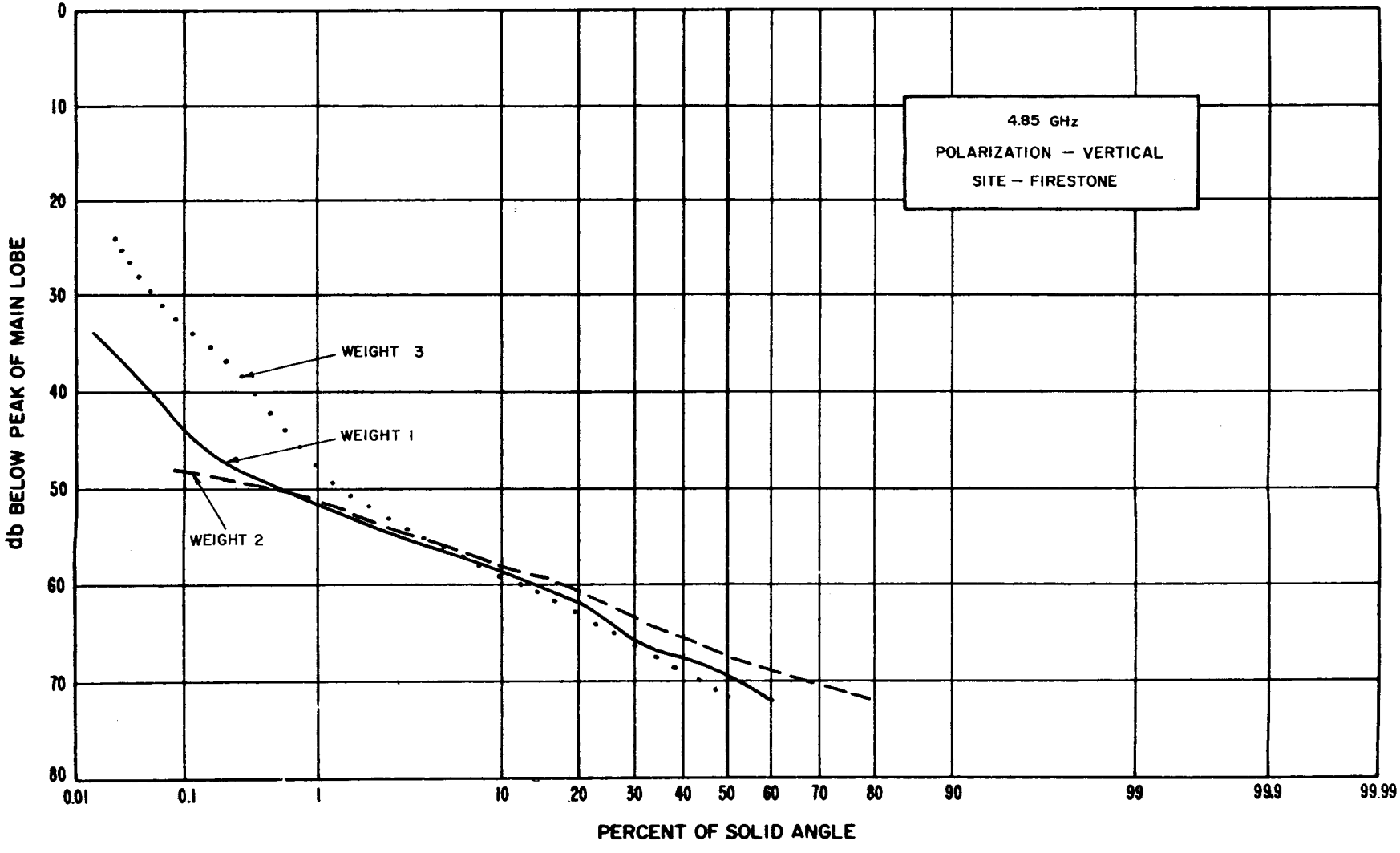

Figure 58

B- 49197

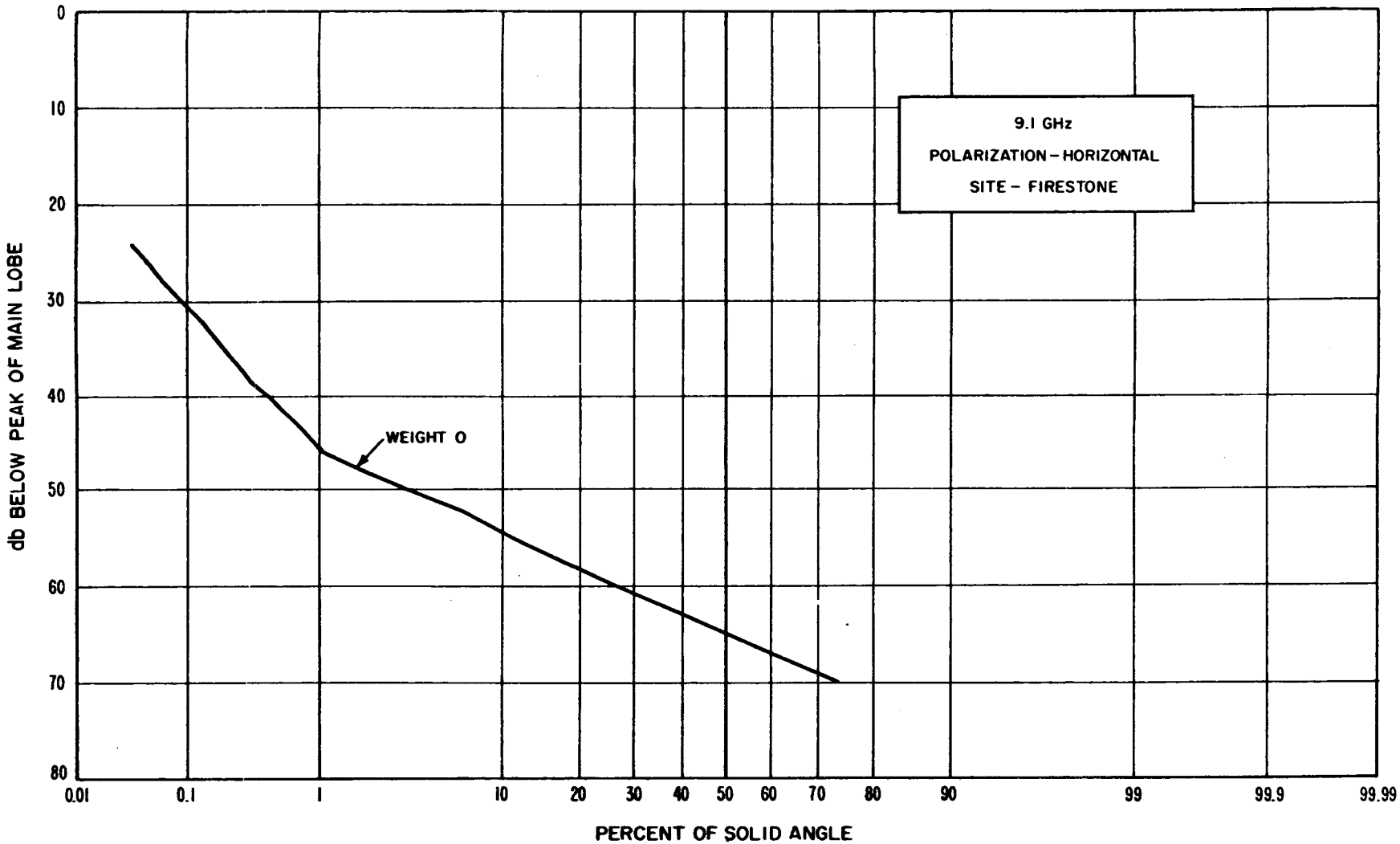

Figure 59

B- 49204

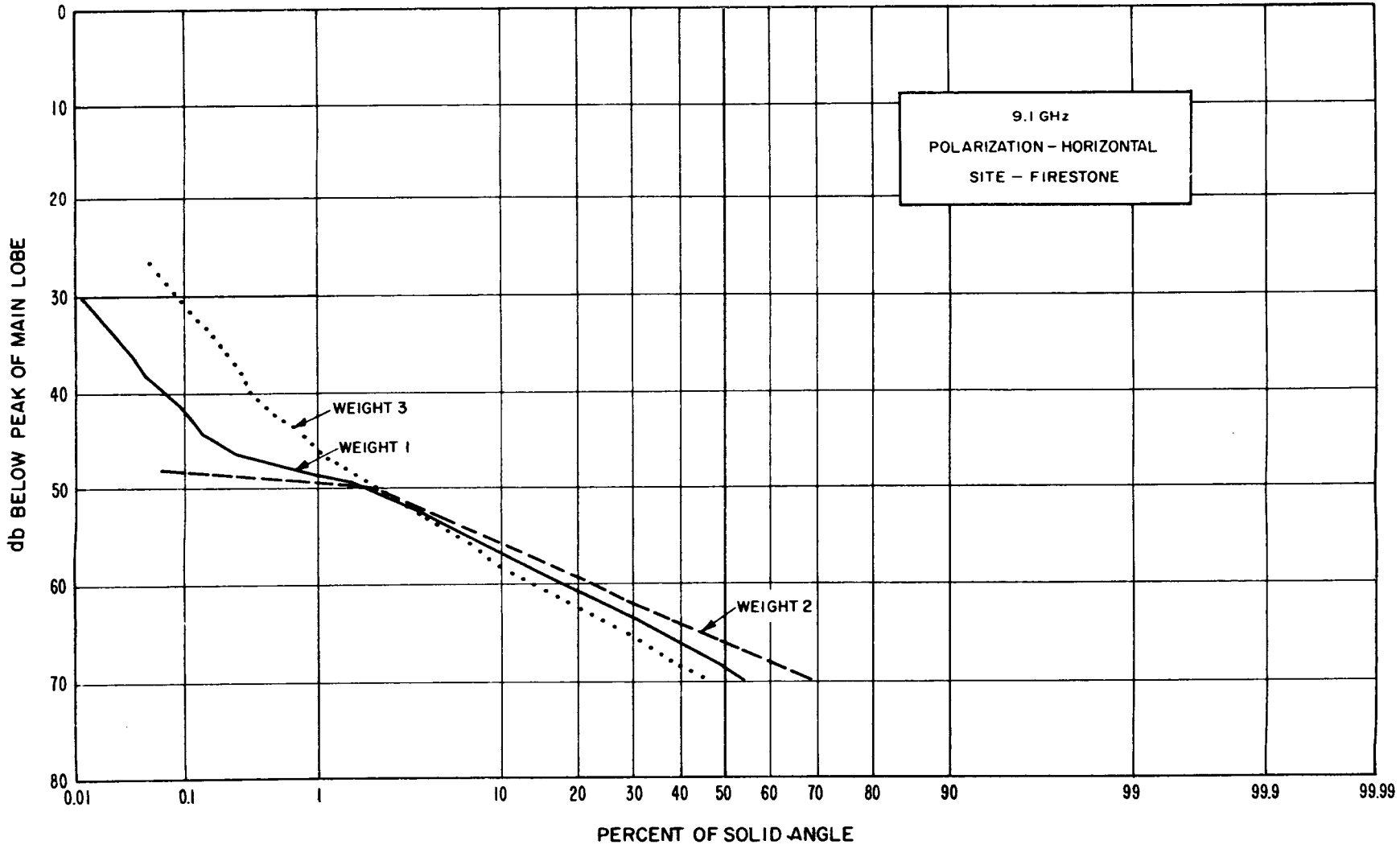

Figure 60

B-49203

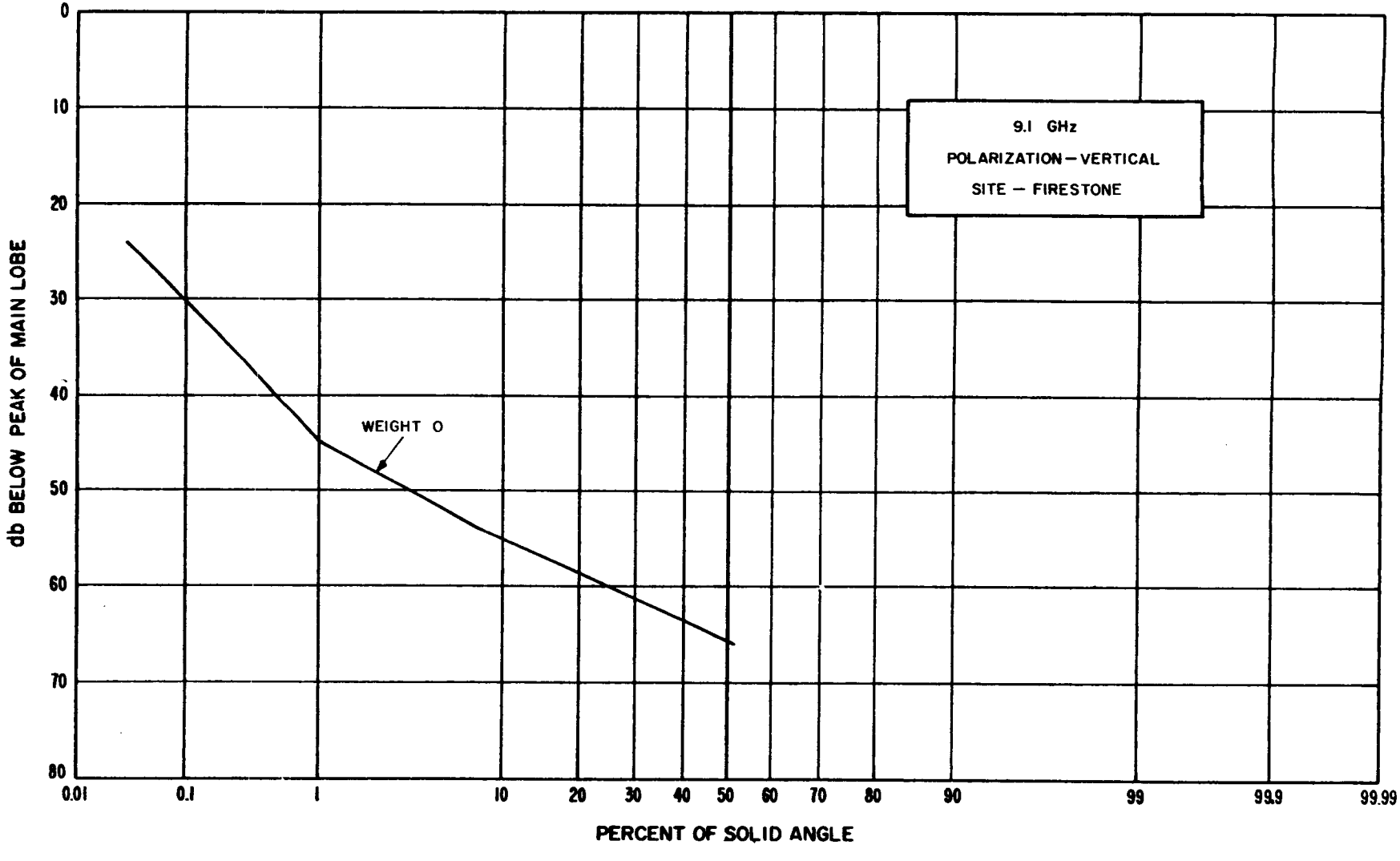
9.1 GHz
POLARIZATION — VERTICAL
SITE — FIRESTONE
WEIGHT O
db BELOW PEAK OF MAIN LOBE
0
10
20
30
40
50
60
70
80
0.01
0.1
1
10
20
30
40
50
60
70
80
90
99
99.9
99.99
PERCENT OF SOLID ANGLE

Figure 61

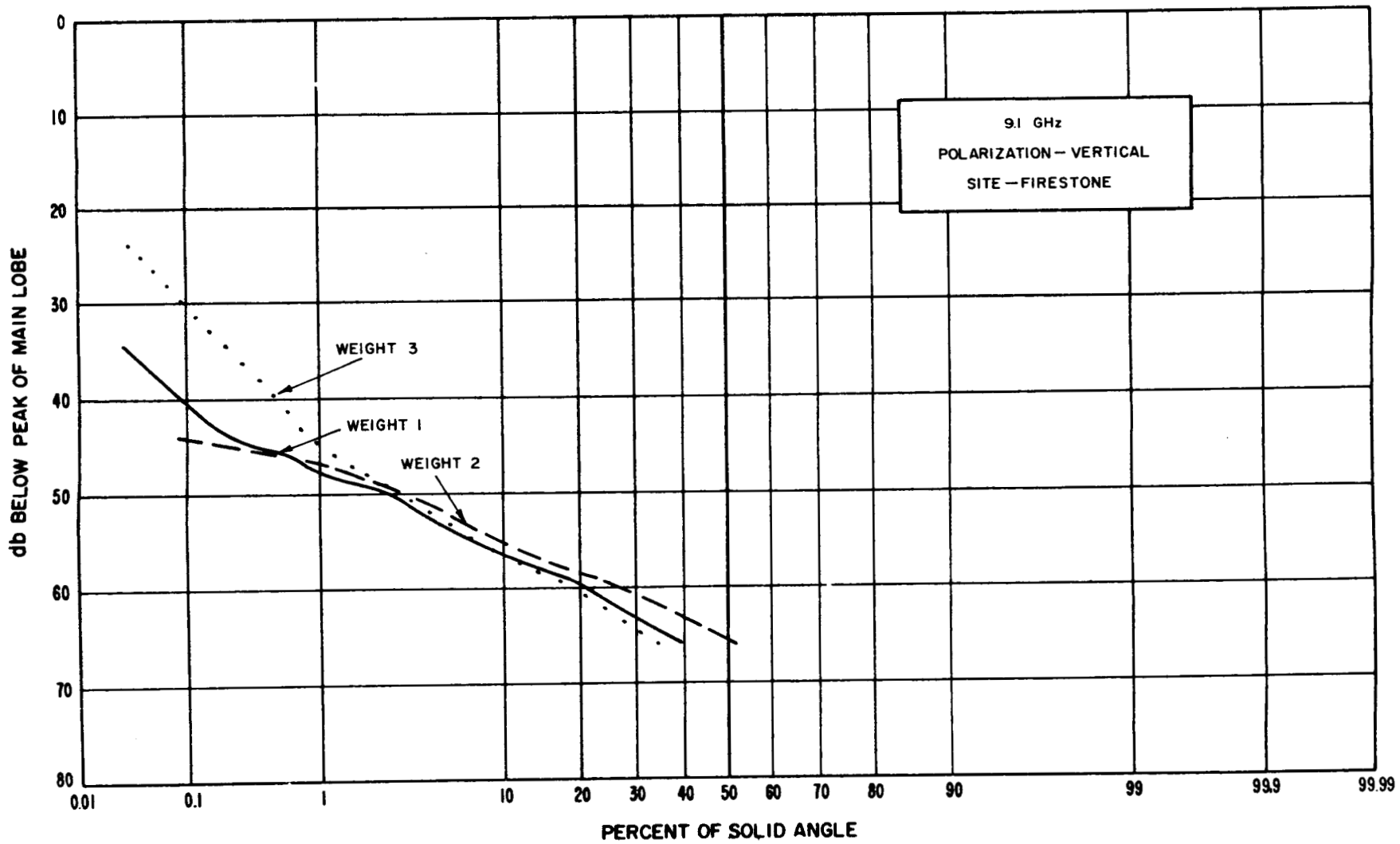

Figure 62

B-49201

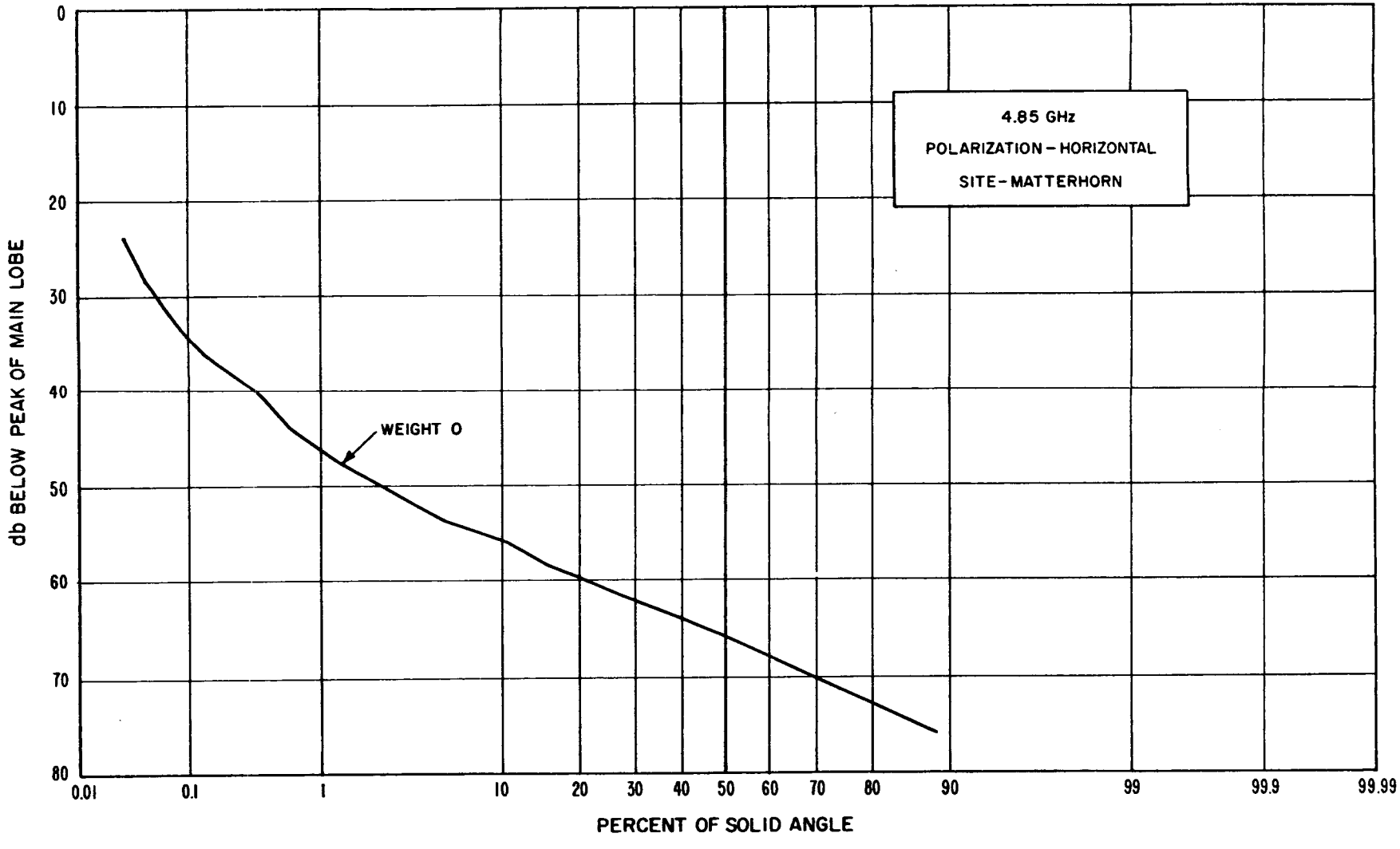

Figure 63

B-49210

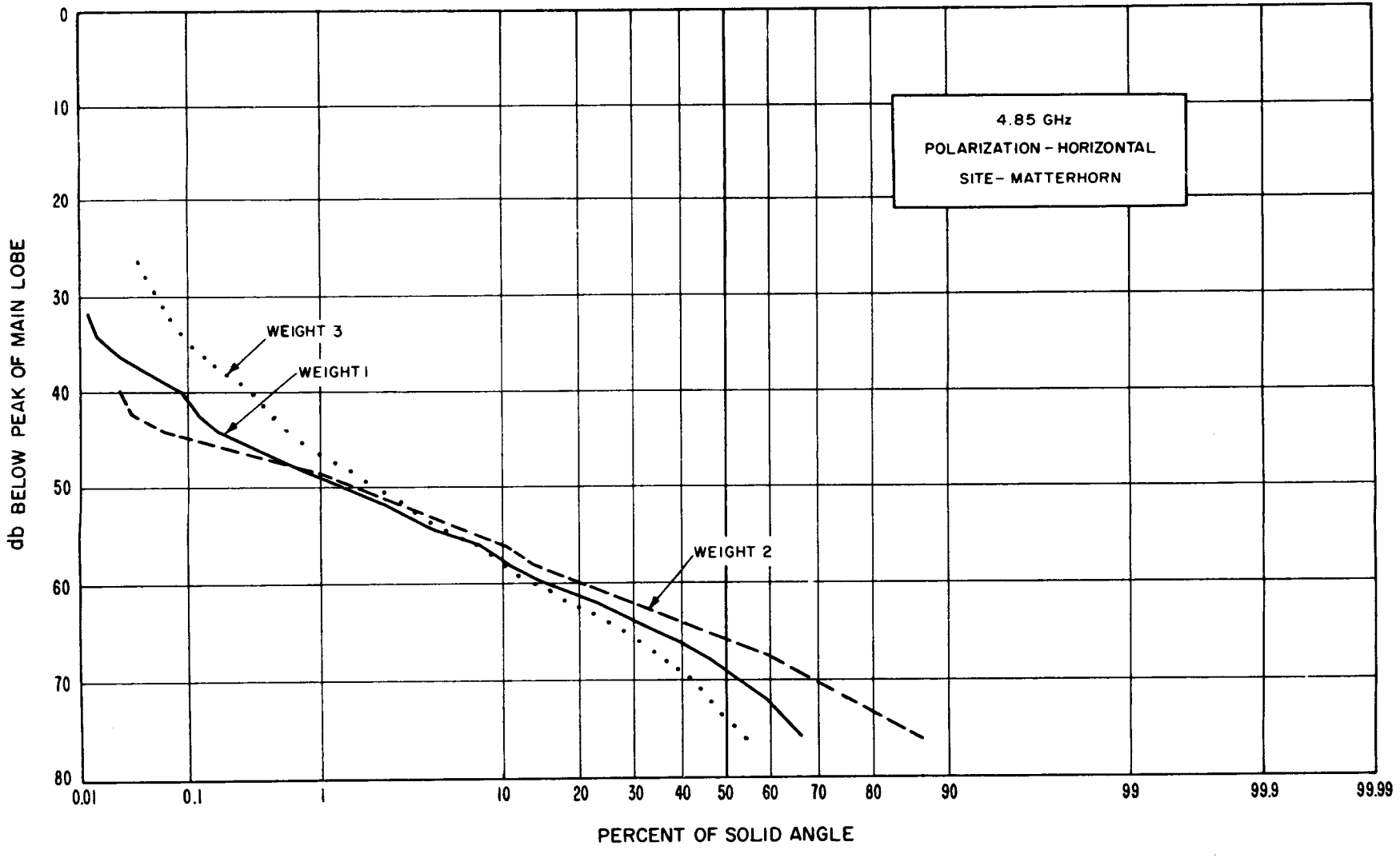

Figure 64

B-49209

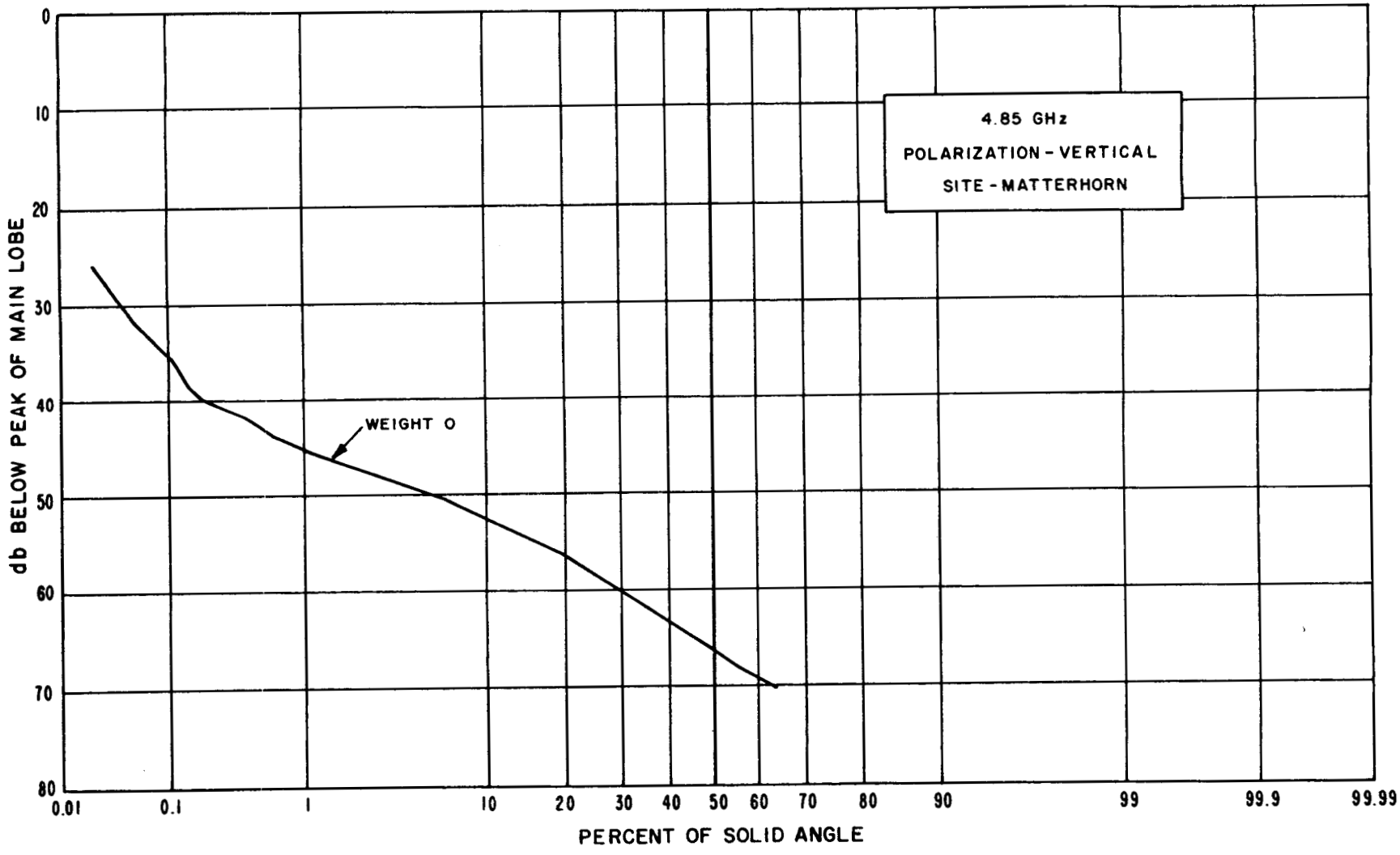

Figure 65

B-49208

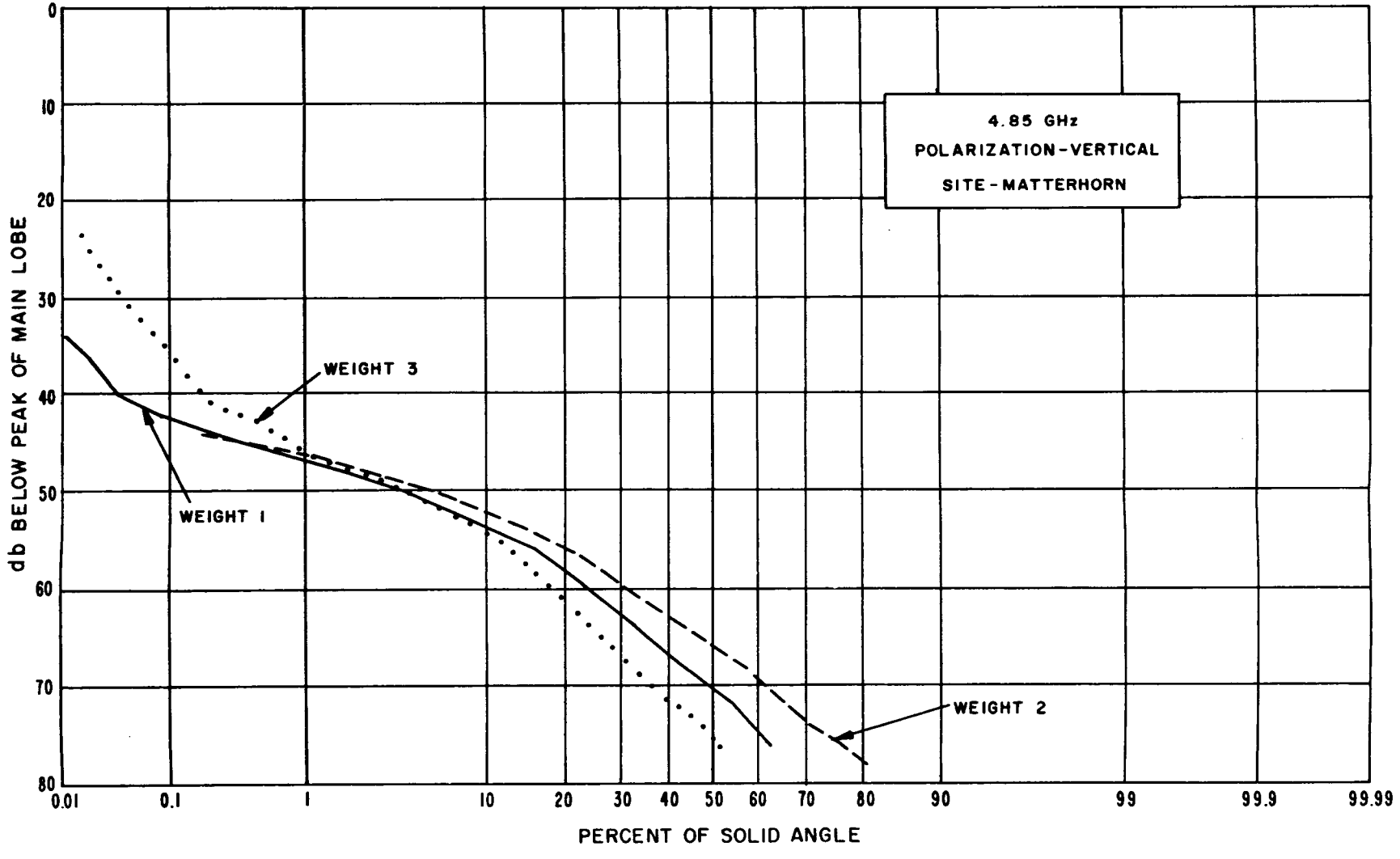

Figure 66

B-49207

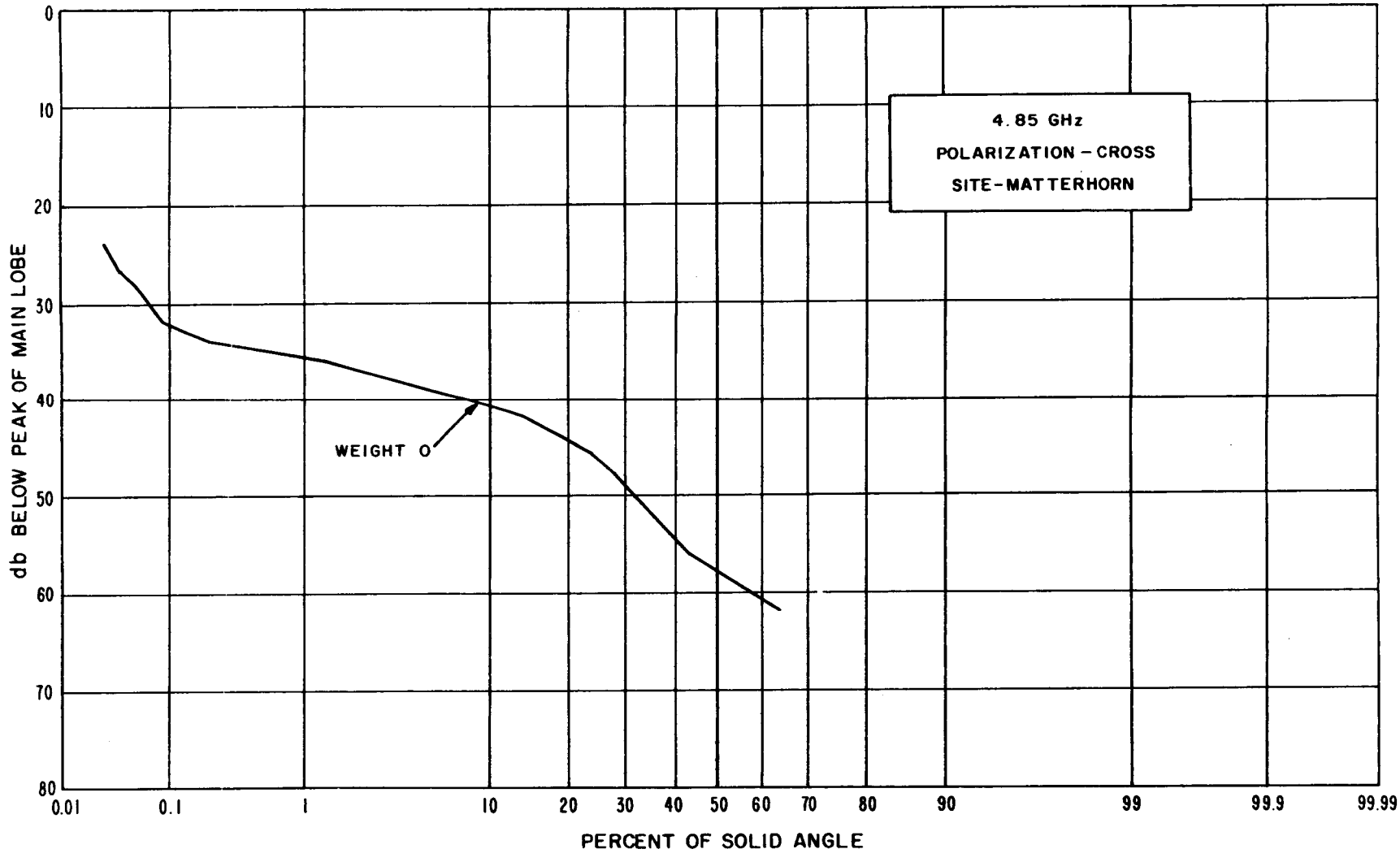
4.85 GHz
POLARIZATION – CROSS
SITE-MATTERHORN
WEIGHT O
db BELOW PEAK OF MAIN LOBE
PERCENT OF SOLID ANGLE
0
10
20
30
40
50
60
70
80
0.01
0.1
1
10
20
30
40
50
60
70
80
90
99
99.9
99.99

Figure 67

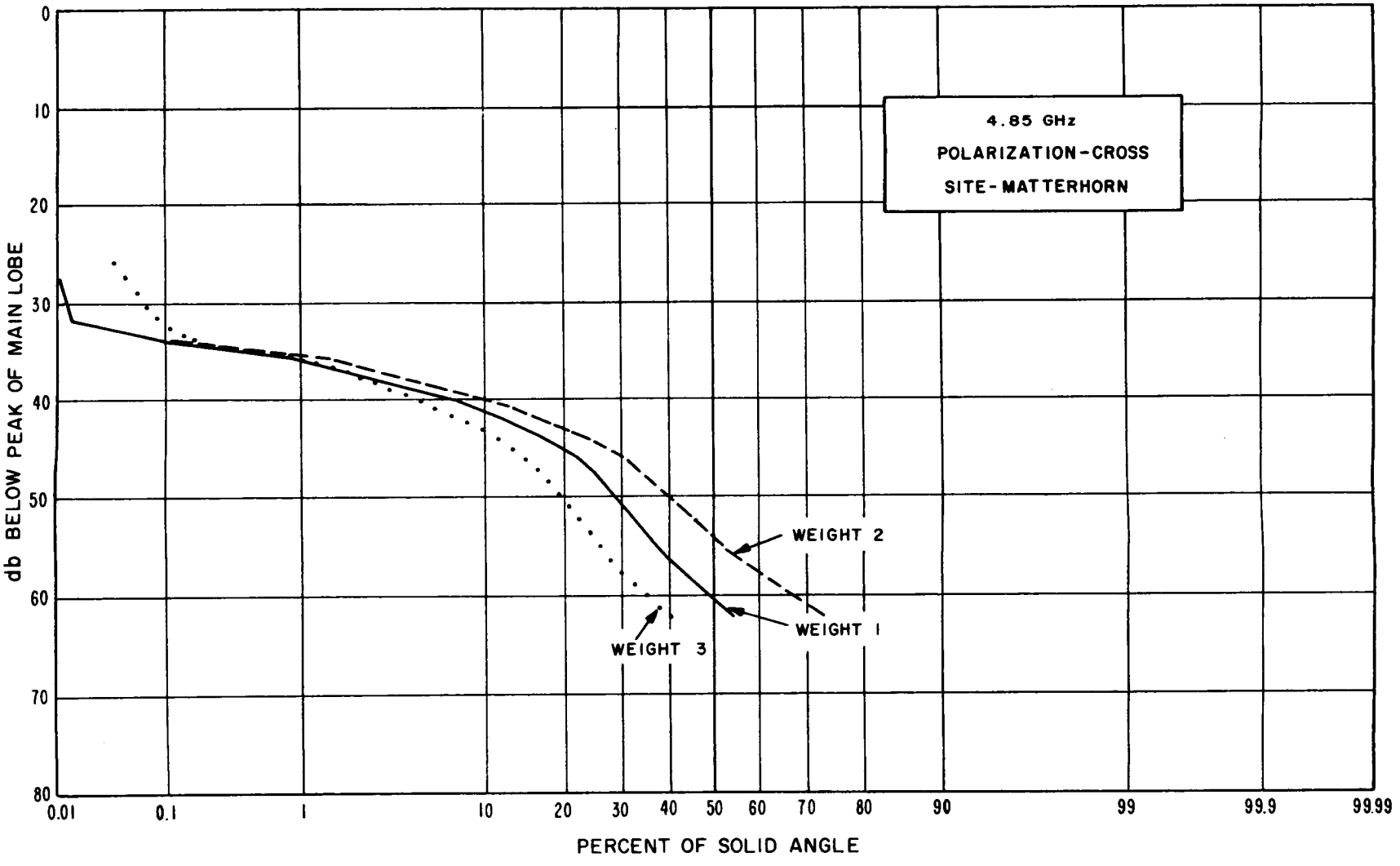

Figure 68

B-49205

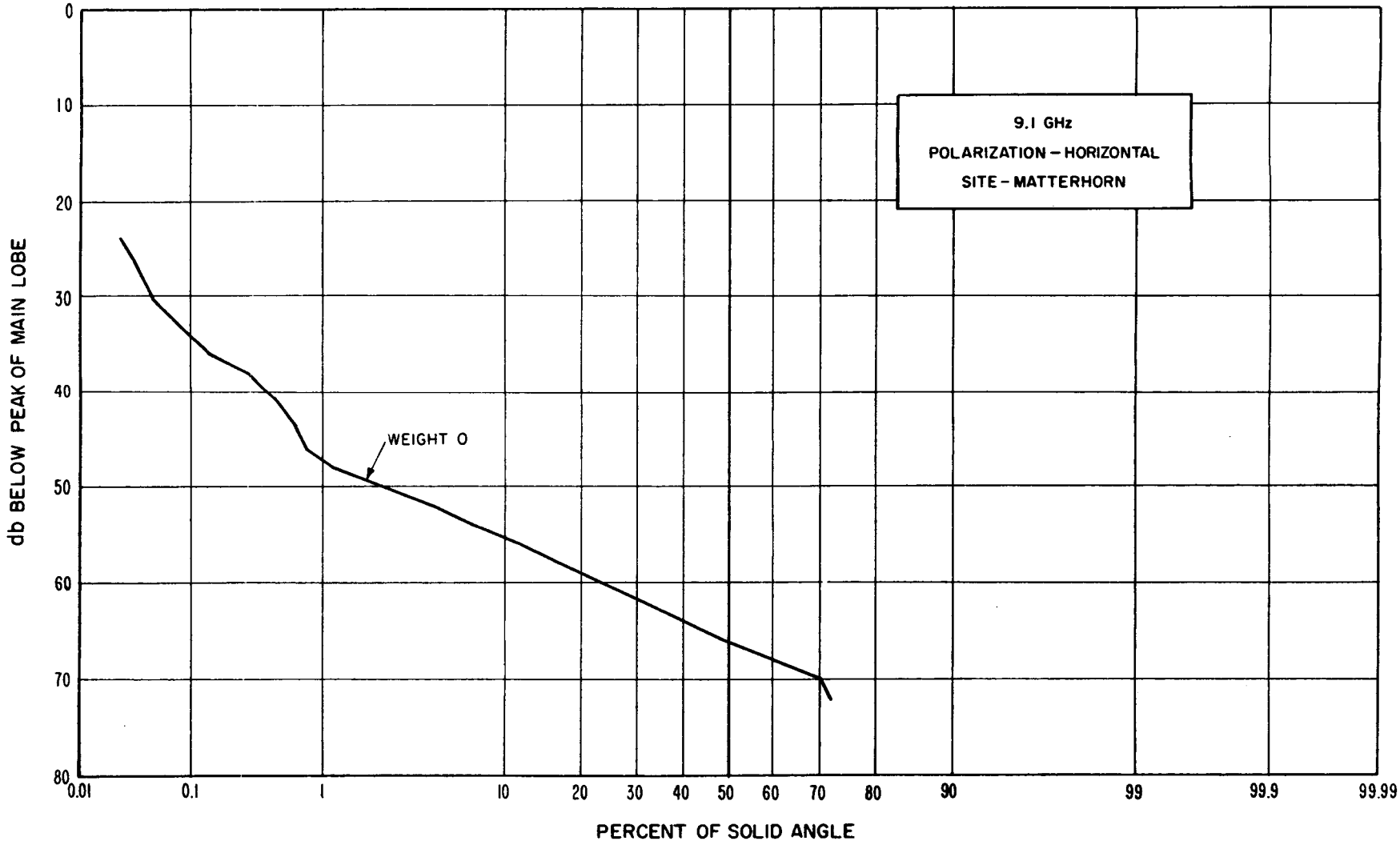
9.1 GHz
POLARIZATION – HORIZONTAL
SITE – MATTERHORN
WEIGHT 0
db BELOW PEAK OF MAIN LOBE
0
10
20
30
40
50
60
70
80
0.01
0.1
1
10
20
30
40
50
60
70
80
90
99
99.9
99.99
PERCENT OF SOLID ANGLE

Figure 69

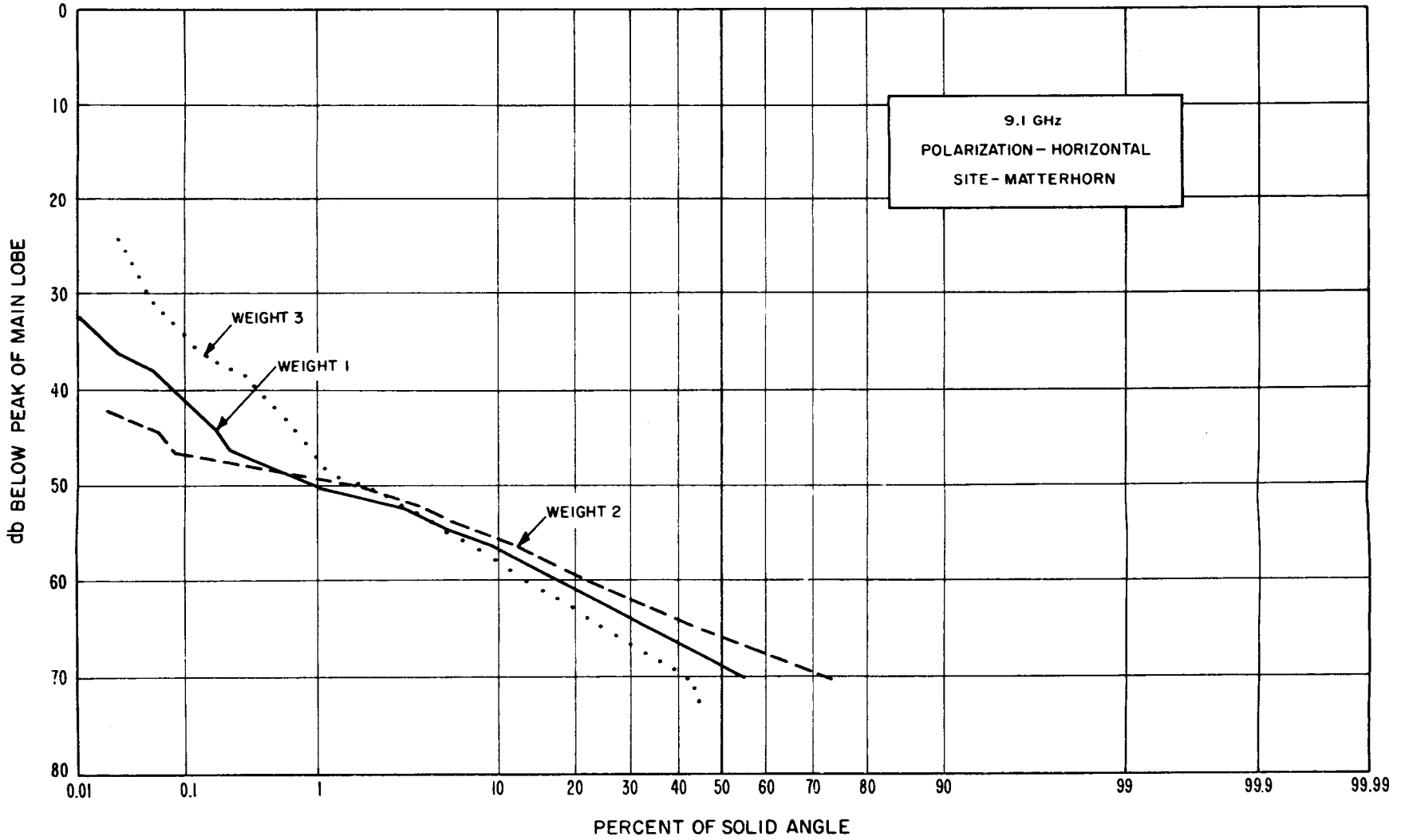

Figure 70

B- 49213

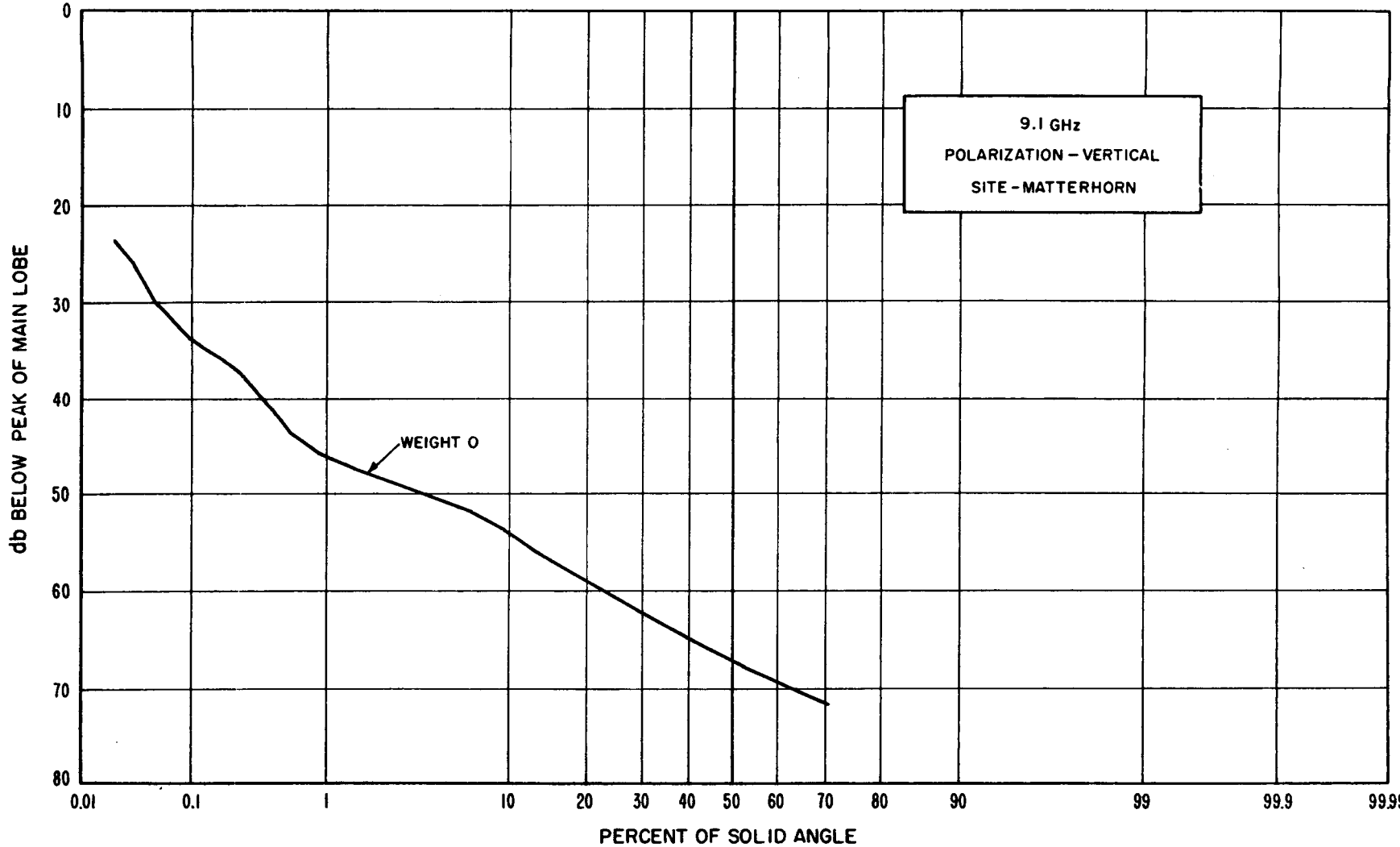

Figure 71

B- 49212

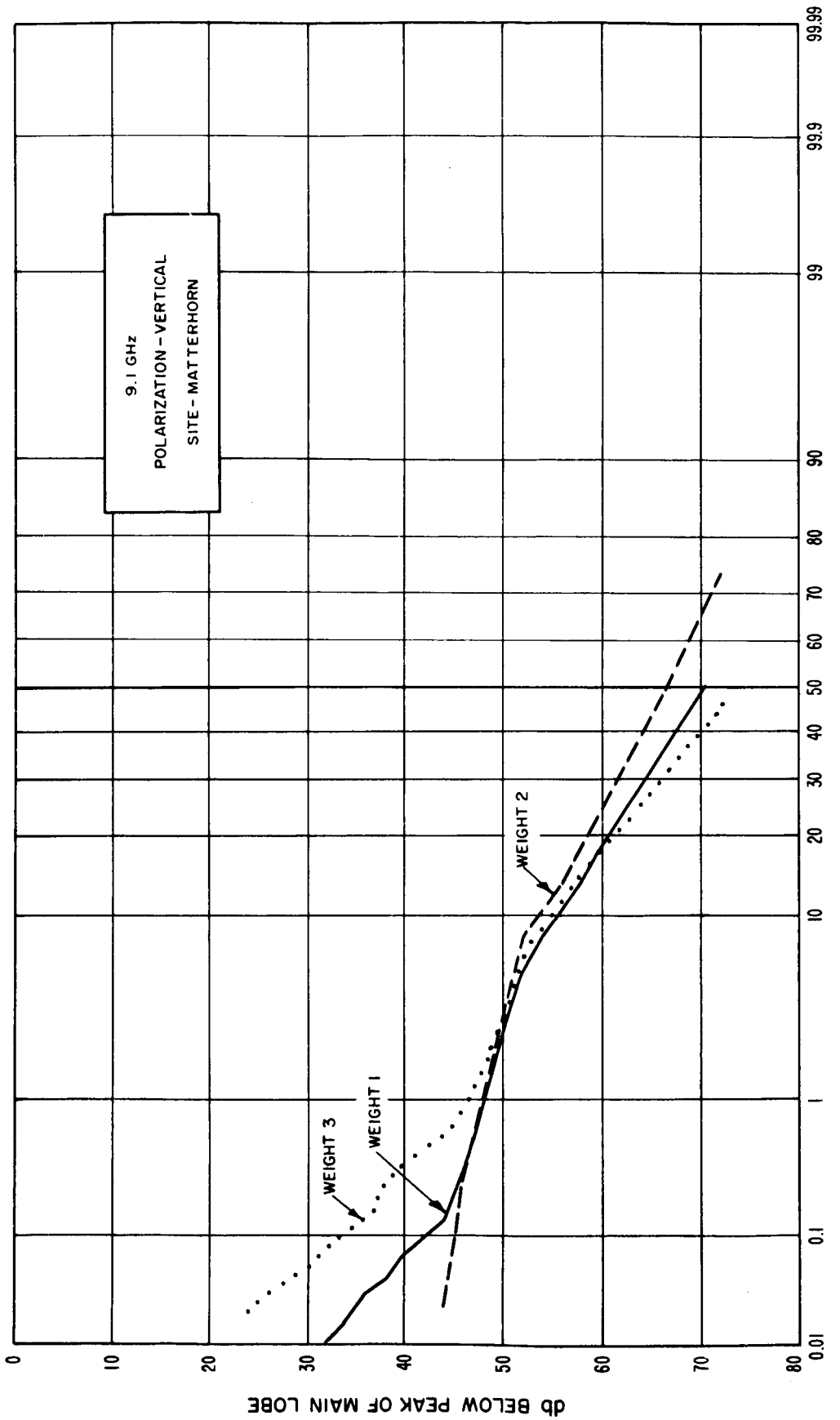

8-49211

Figure 72

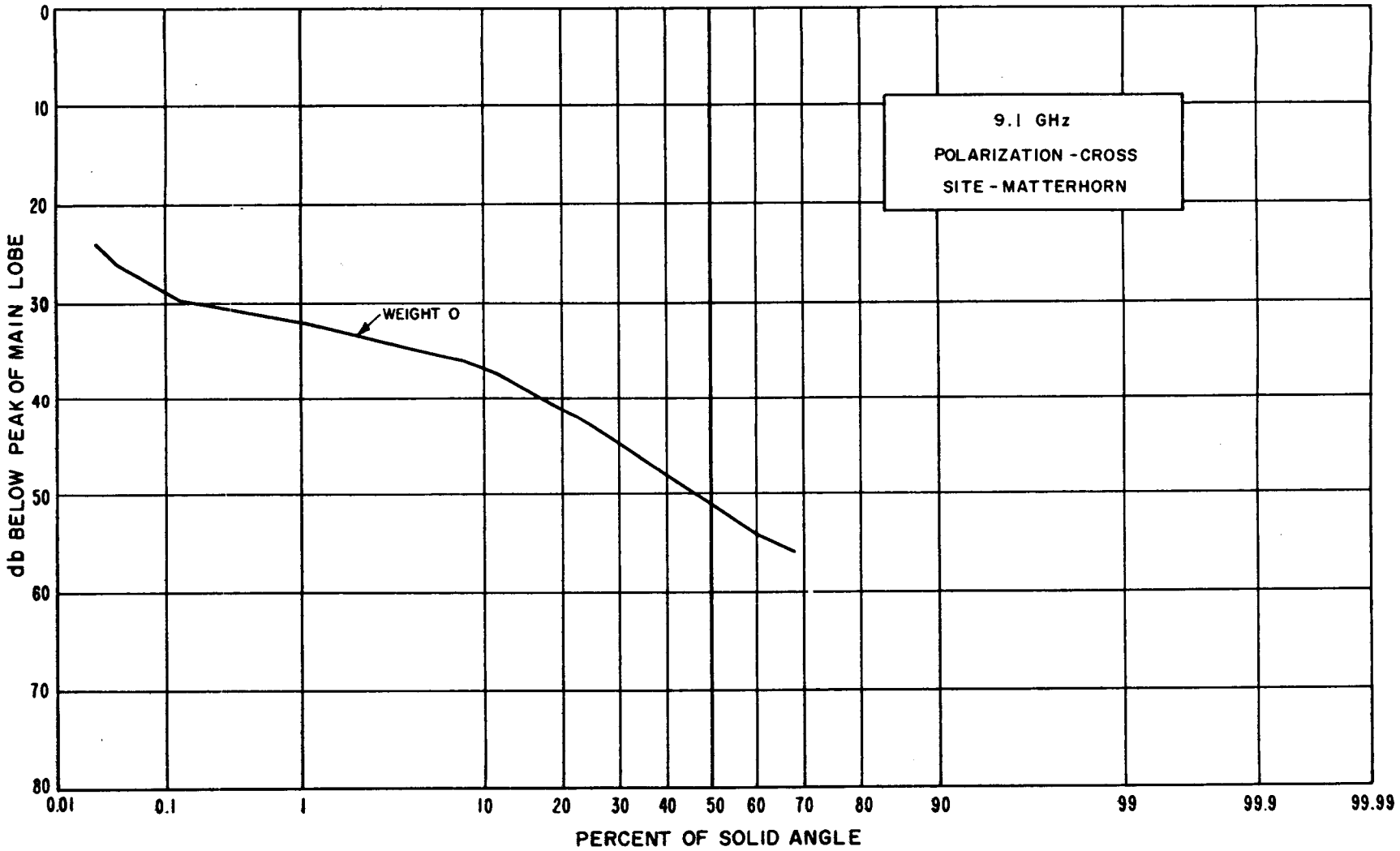

Figure 73

B- 49216

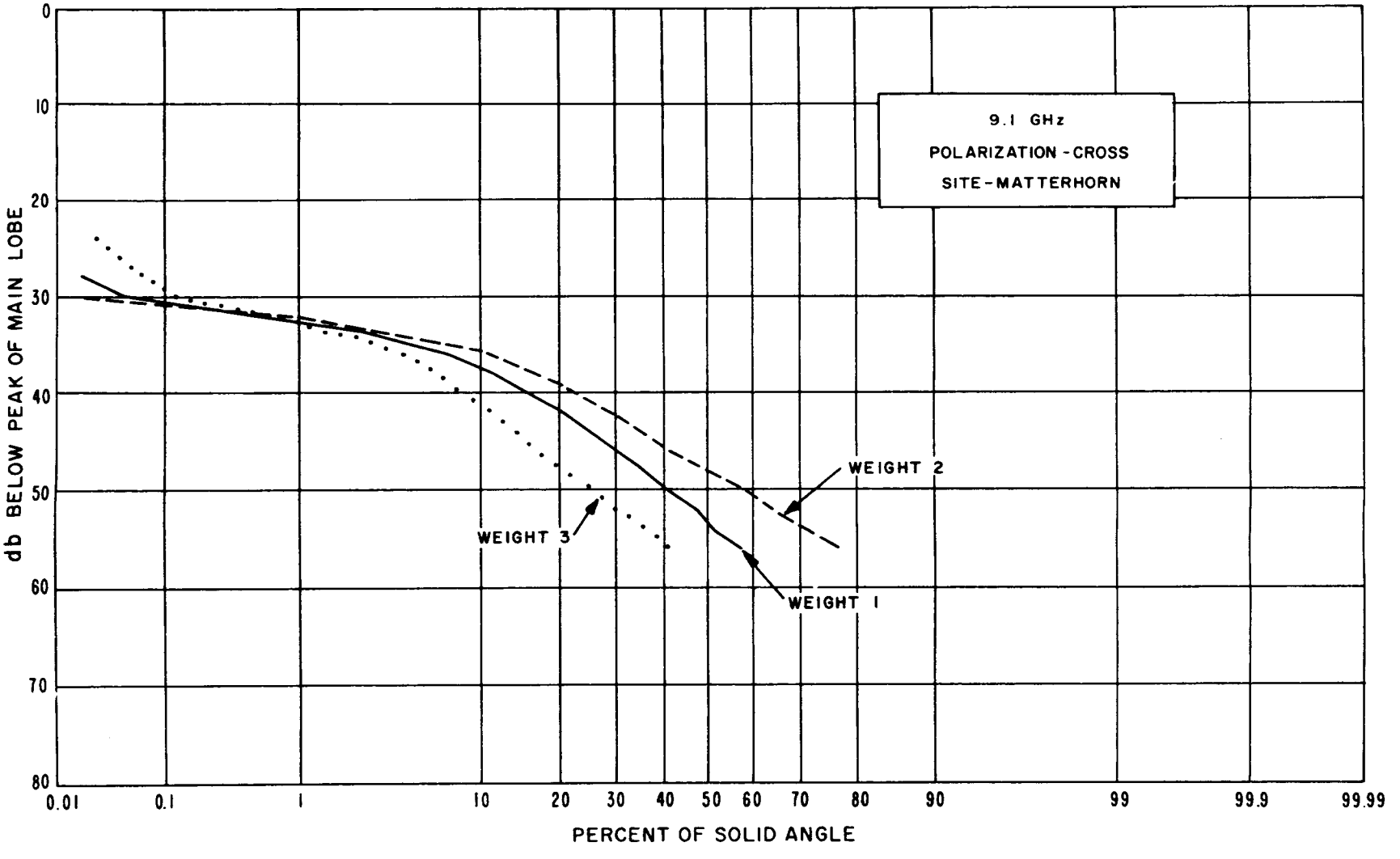

Figure 74

B-49215

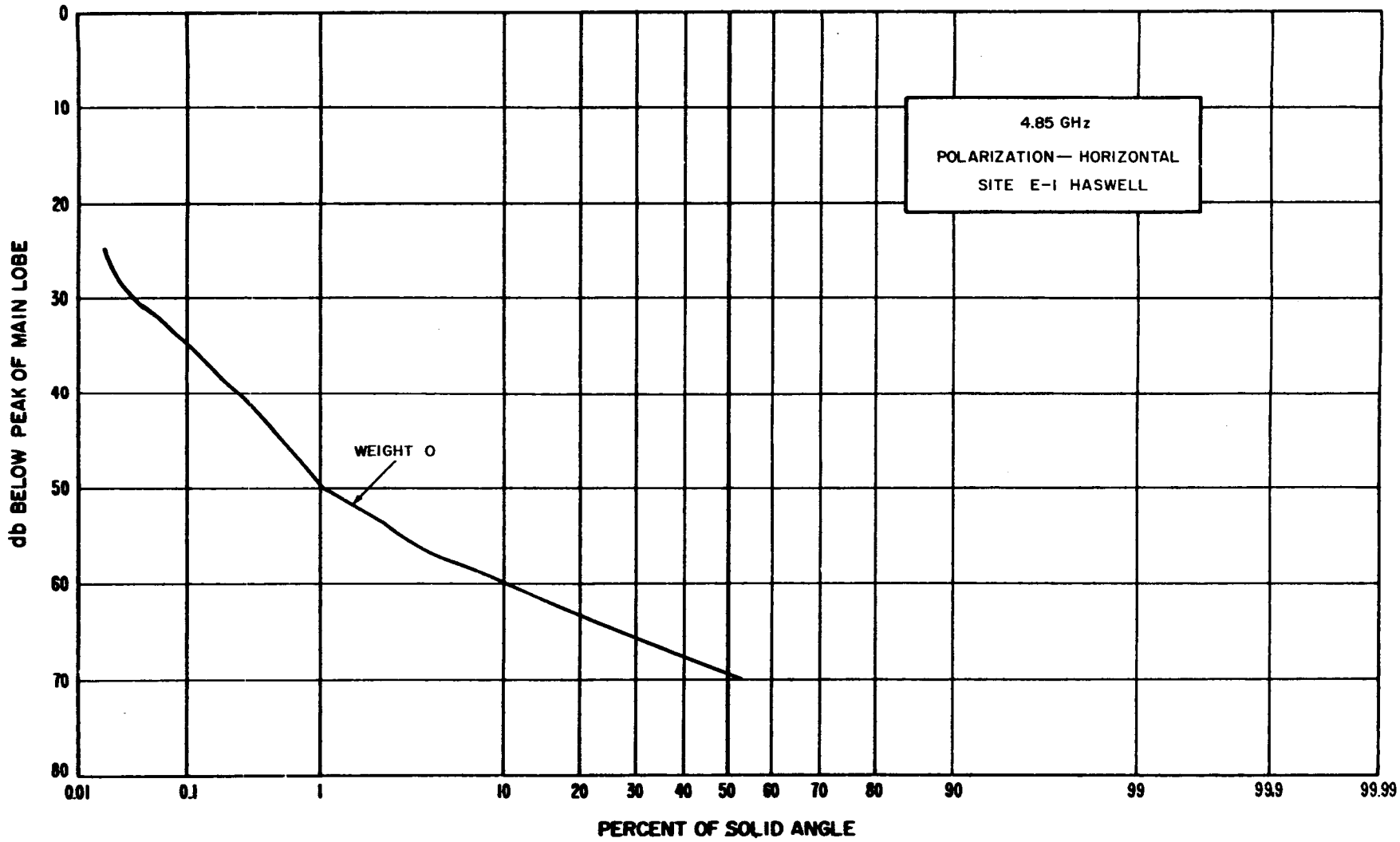

Figure 75

B- 49192

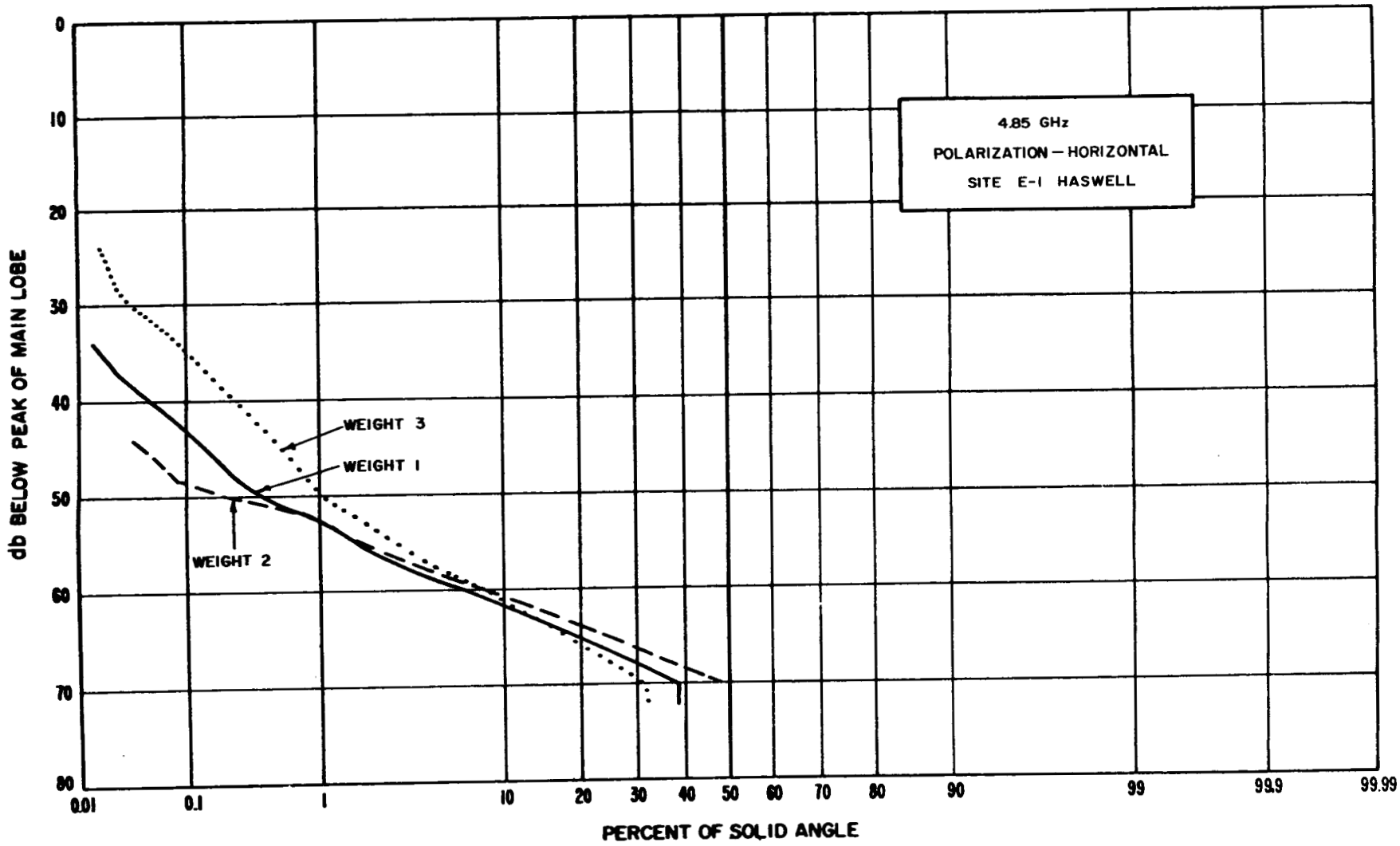

Figure 76

B- 49191

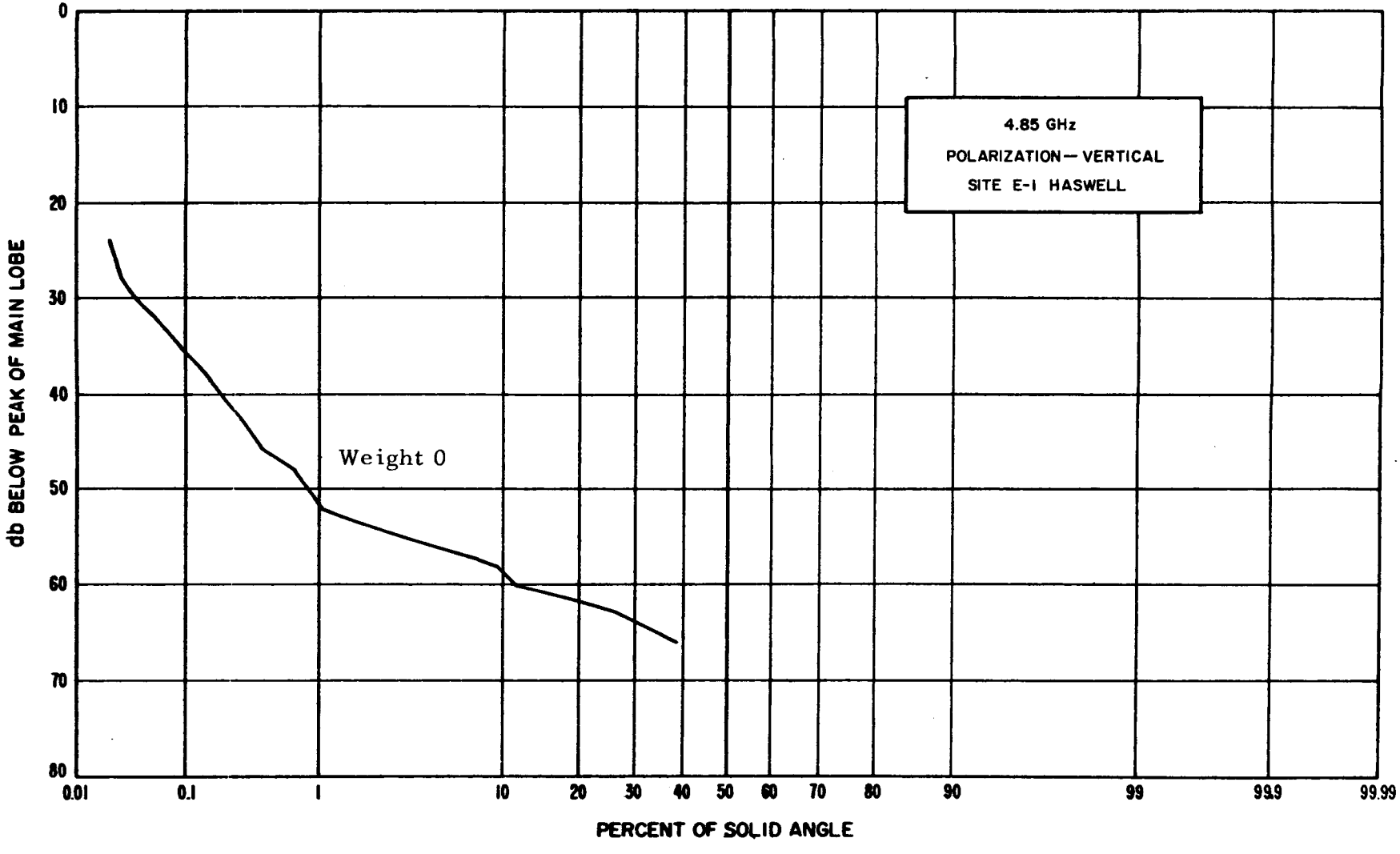
4.85 GHz
POLARIZATION — VERTICAL
SITE E-1 HASWELL
Weight 0
db BELOW PEAK OF MAIN LOBE
PERCENT OF SOLID ANGLE
0
10
20
30
40
50
60
70
80
0.01
0.1
1
10
20
30
40
50
60
70
80
90
99
99.9
99.99

Figure 77

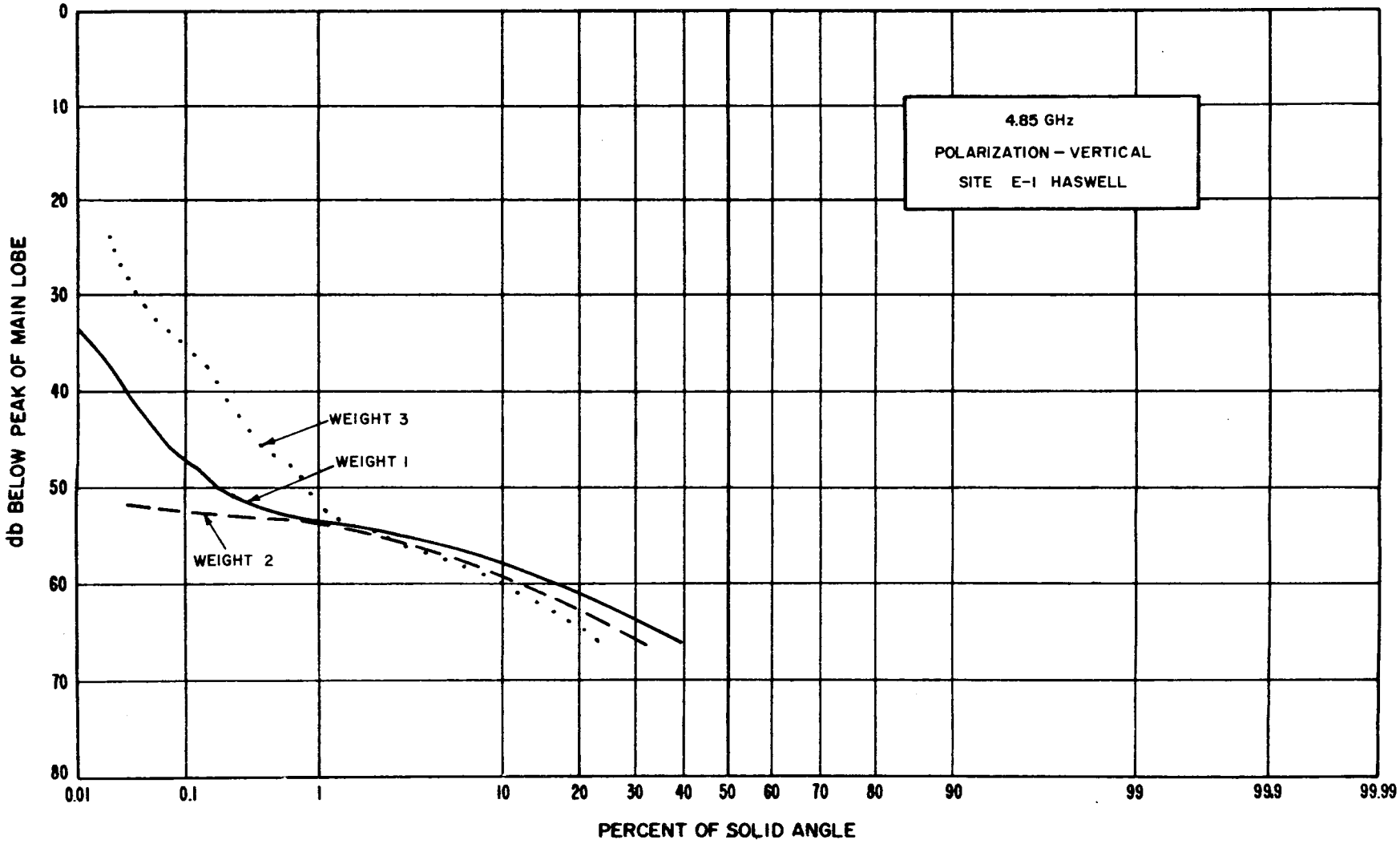

Figure 78

8- 49189

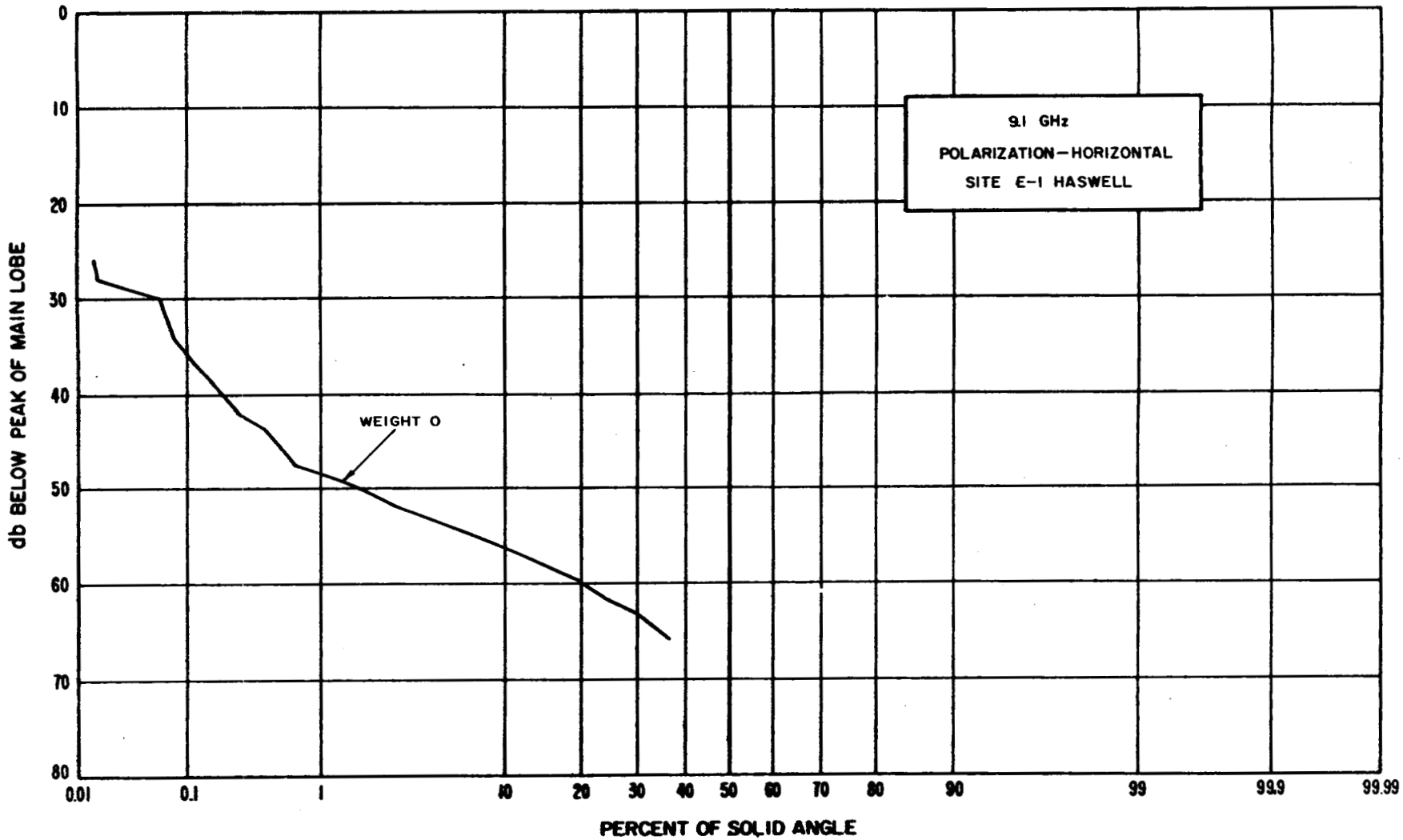

Figure 79

B- 49195

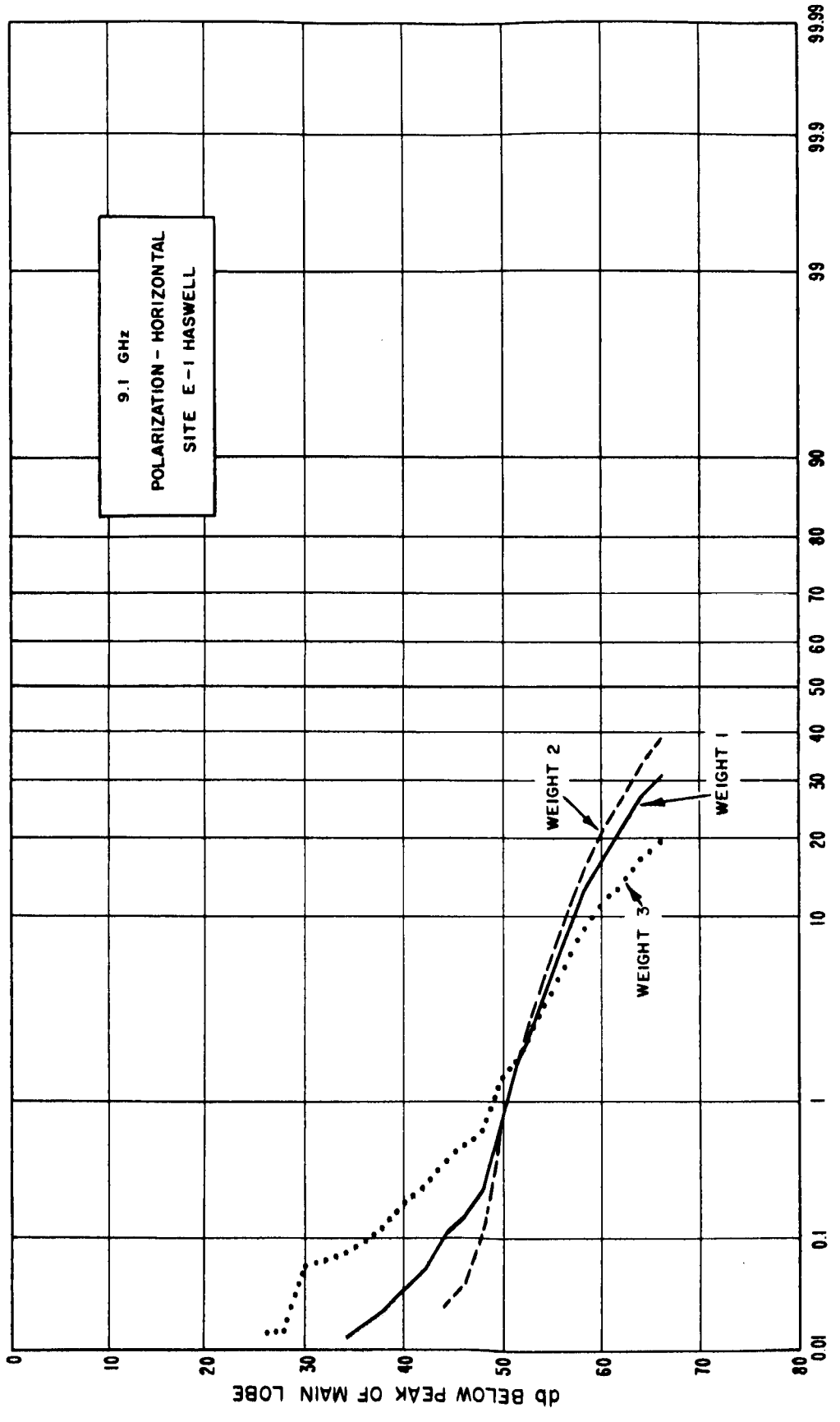

B-49196

Figure 80

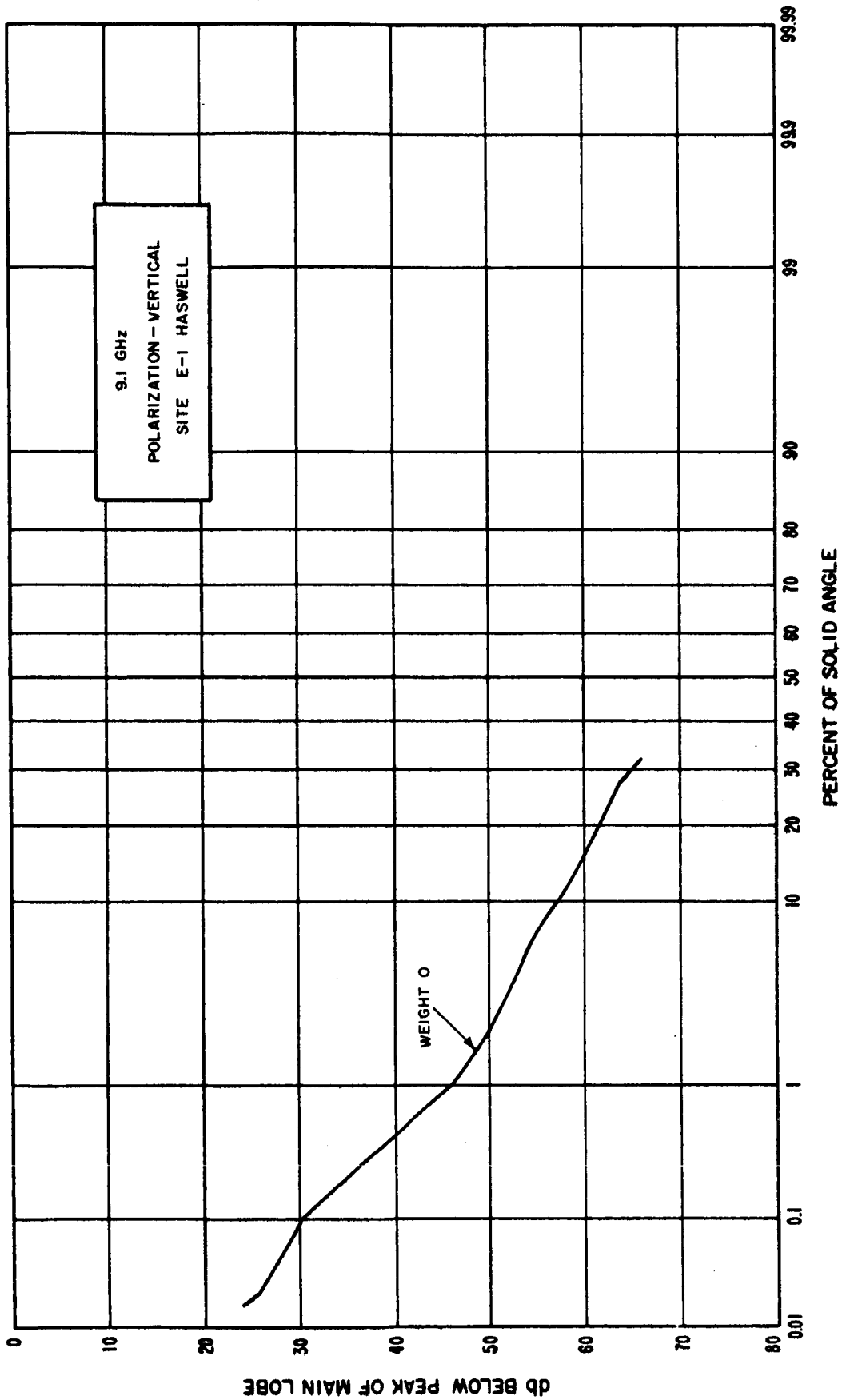

B-49194

Figure 81

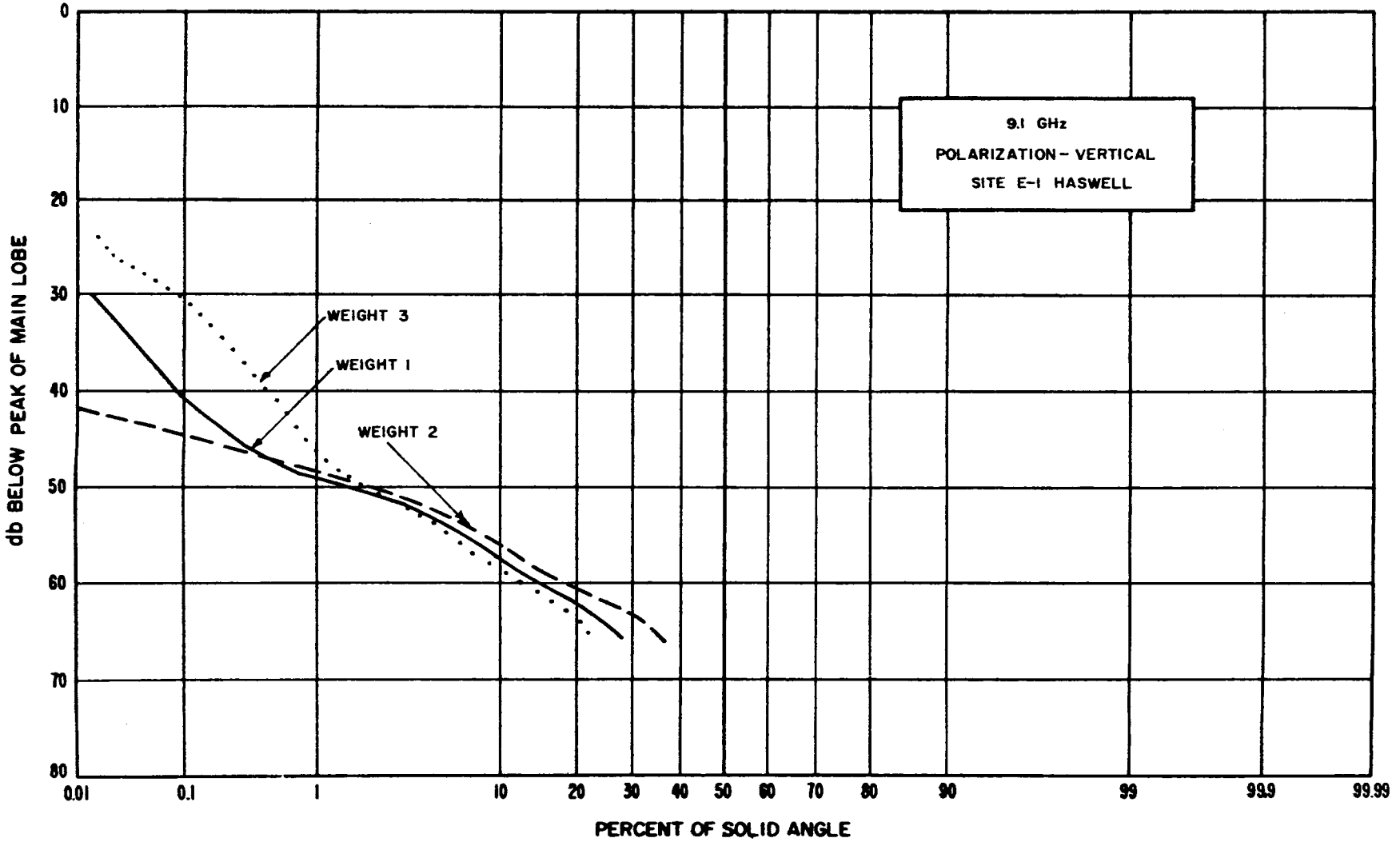

Figure 82

B- 49193

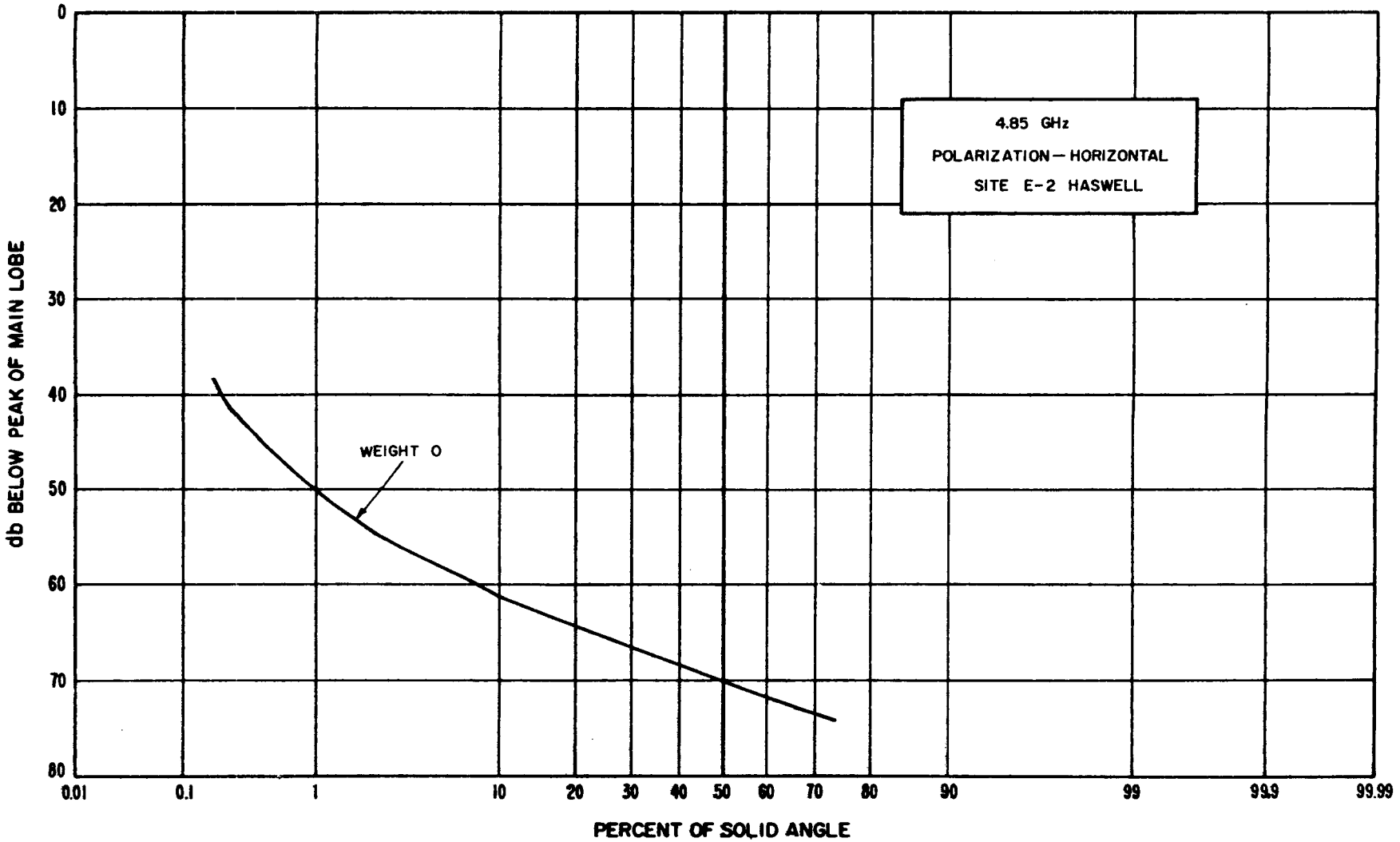

Figure 83

B-49184

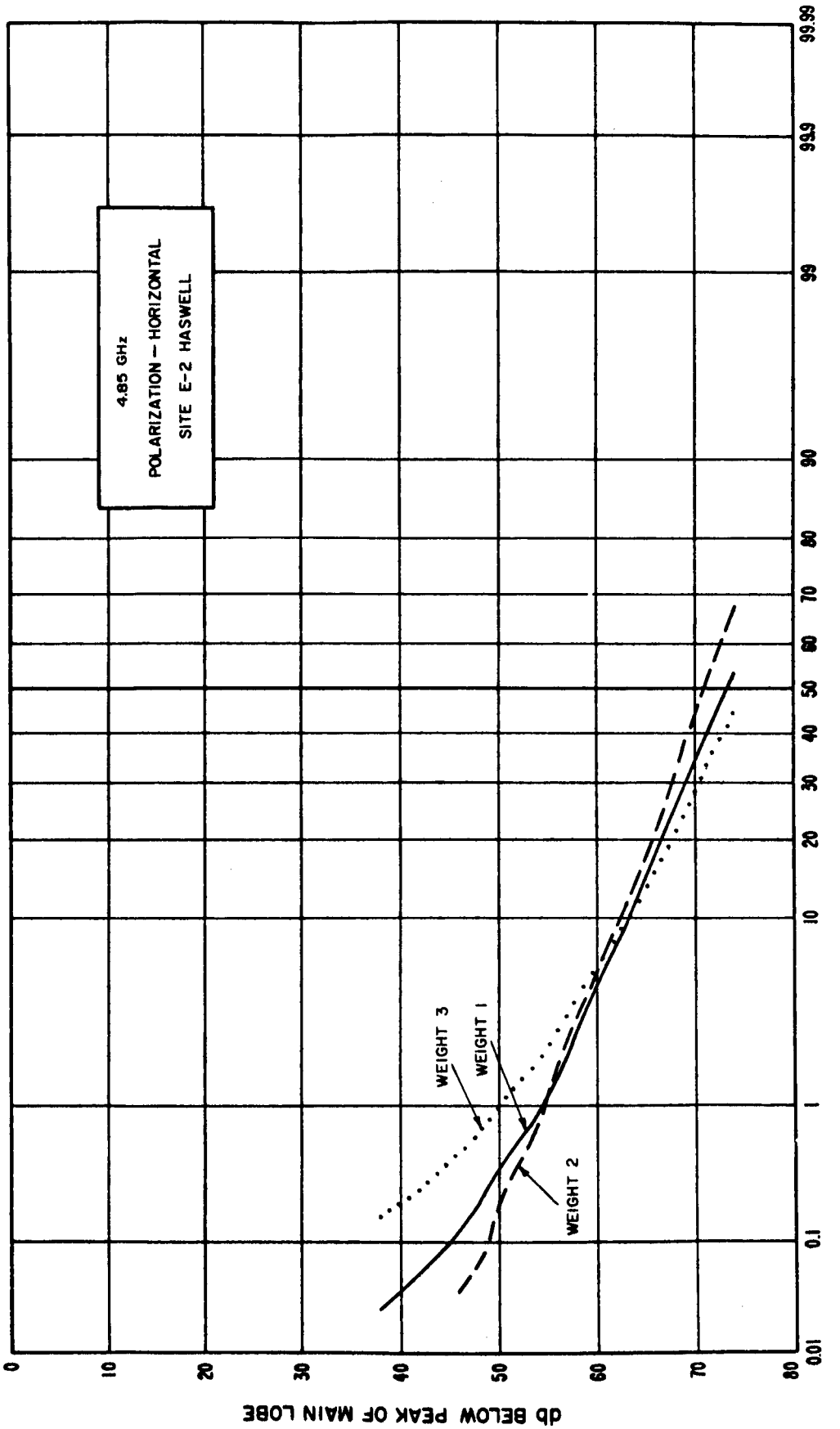

B- 49182

Figure 84

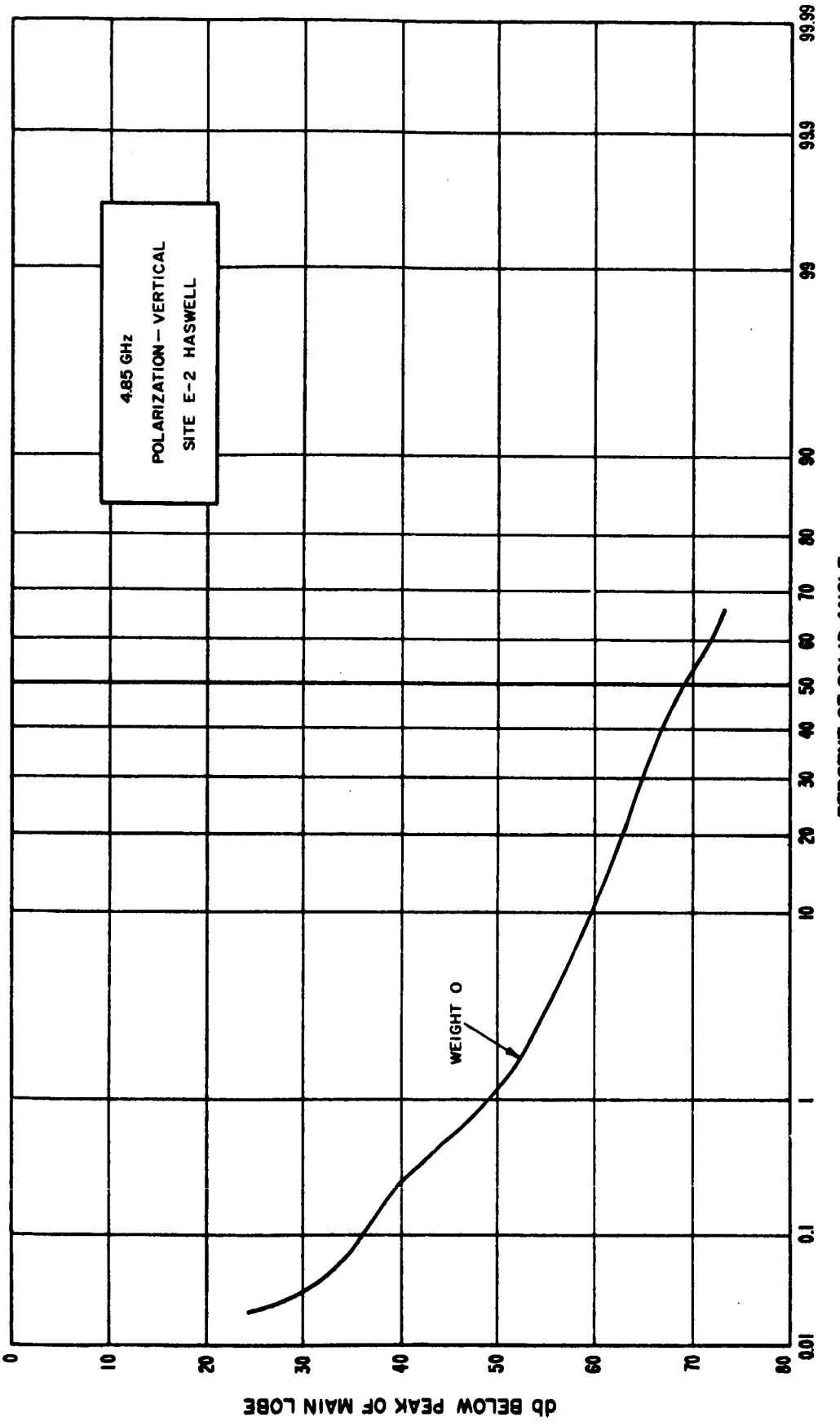

Figure 85

B- 49181

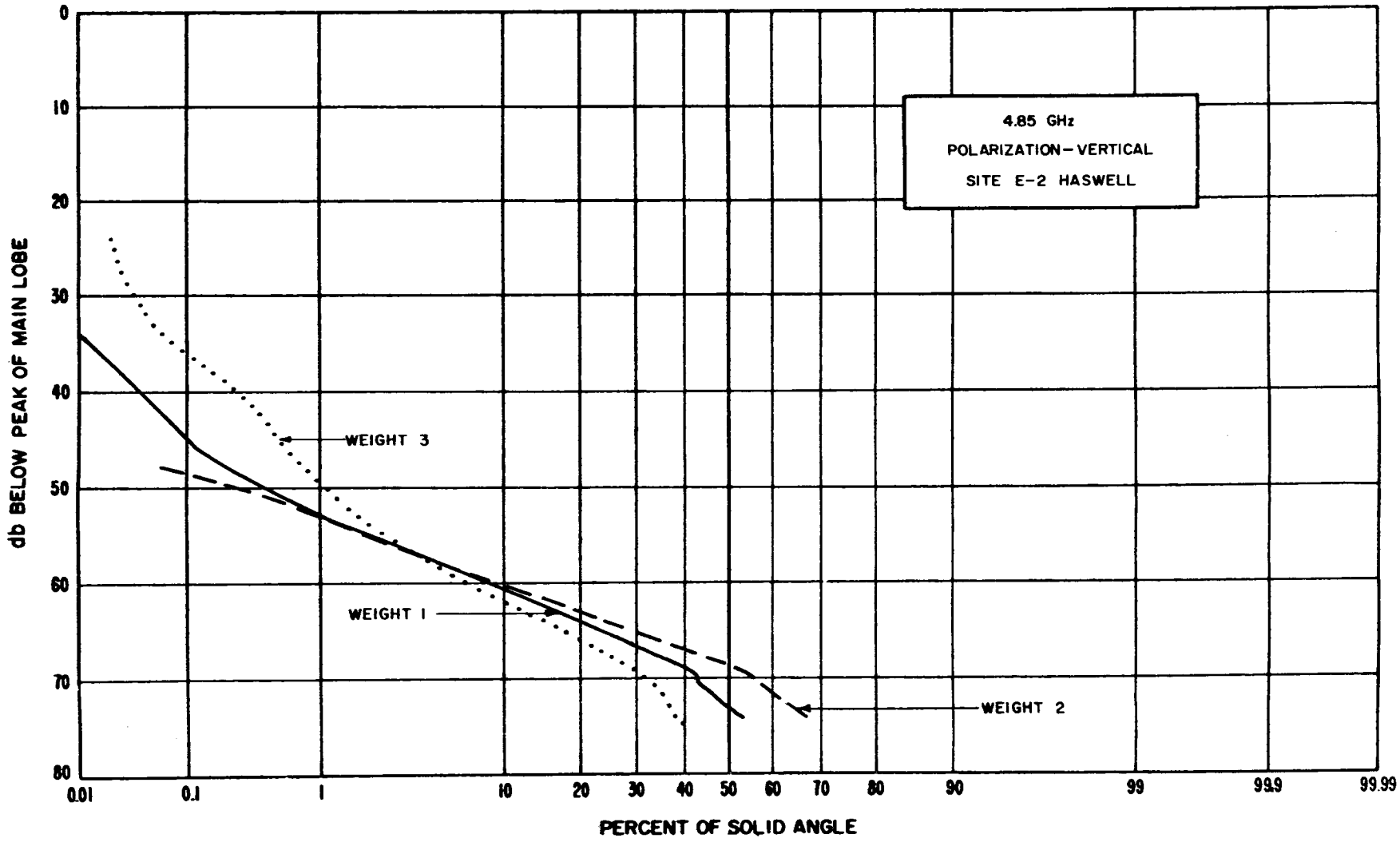

Figure 86

B- 49183

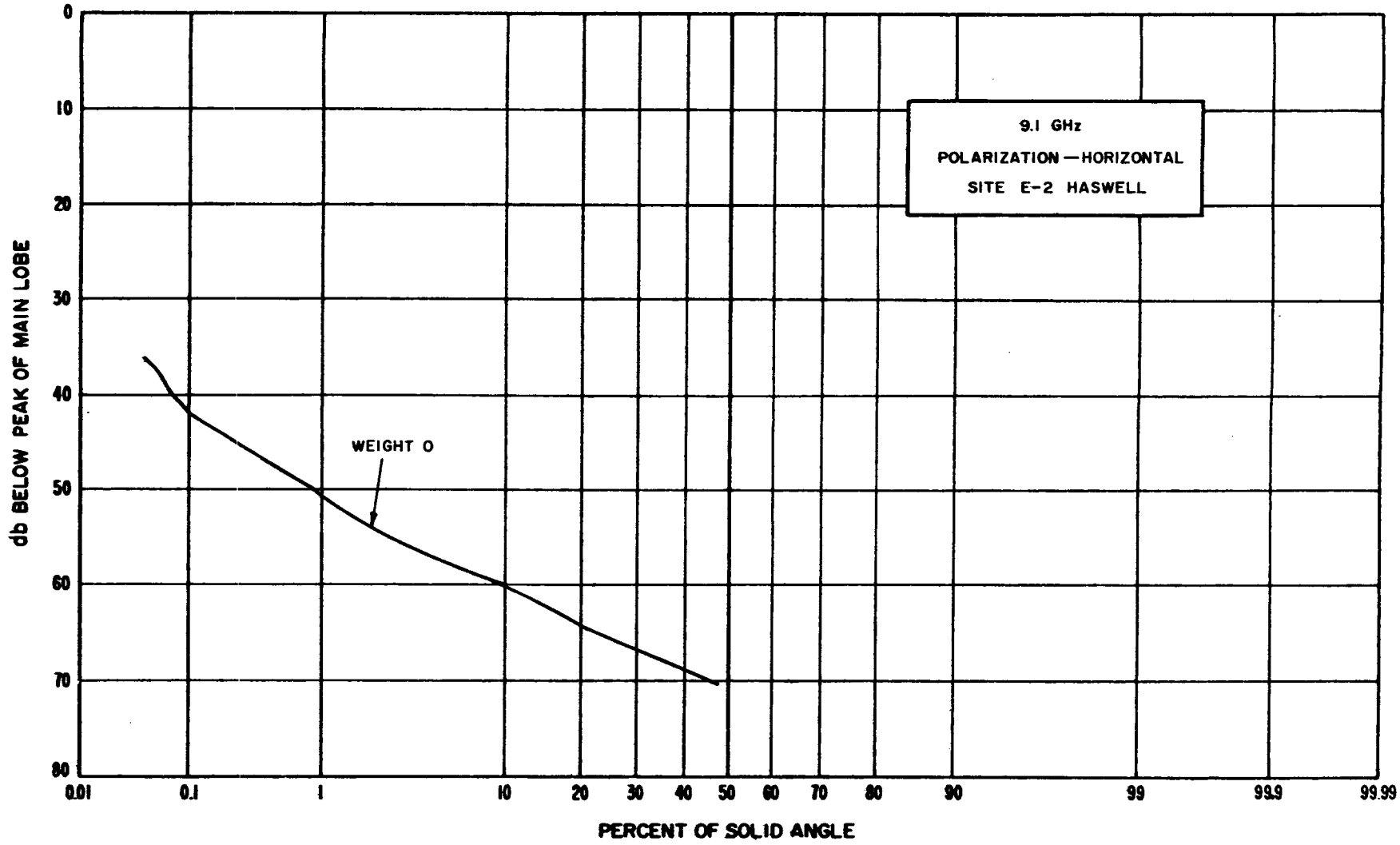
9.1 GHz
POLARIZATION — HORIZONTAL
SITE E-2 HASWELL
WEIGHT O
db BELOW PEAK OF MAIN LOBE
PERCENT OF SOLID ANGLE
0
10
20
30
40
50
60
70
80
0.01
0.1
1
10
20
30
40
50
60
70
80
90
99
99.9
99.99

Figure 87

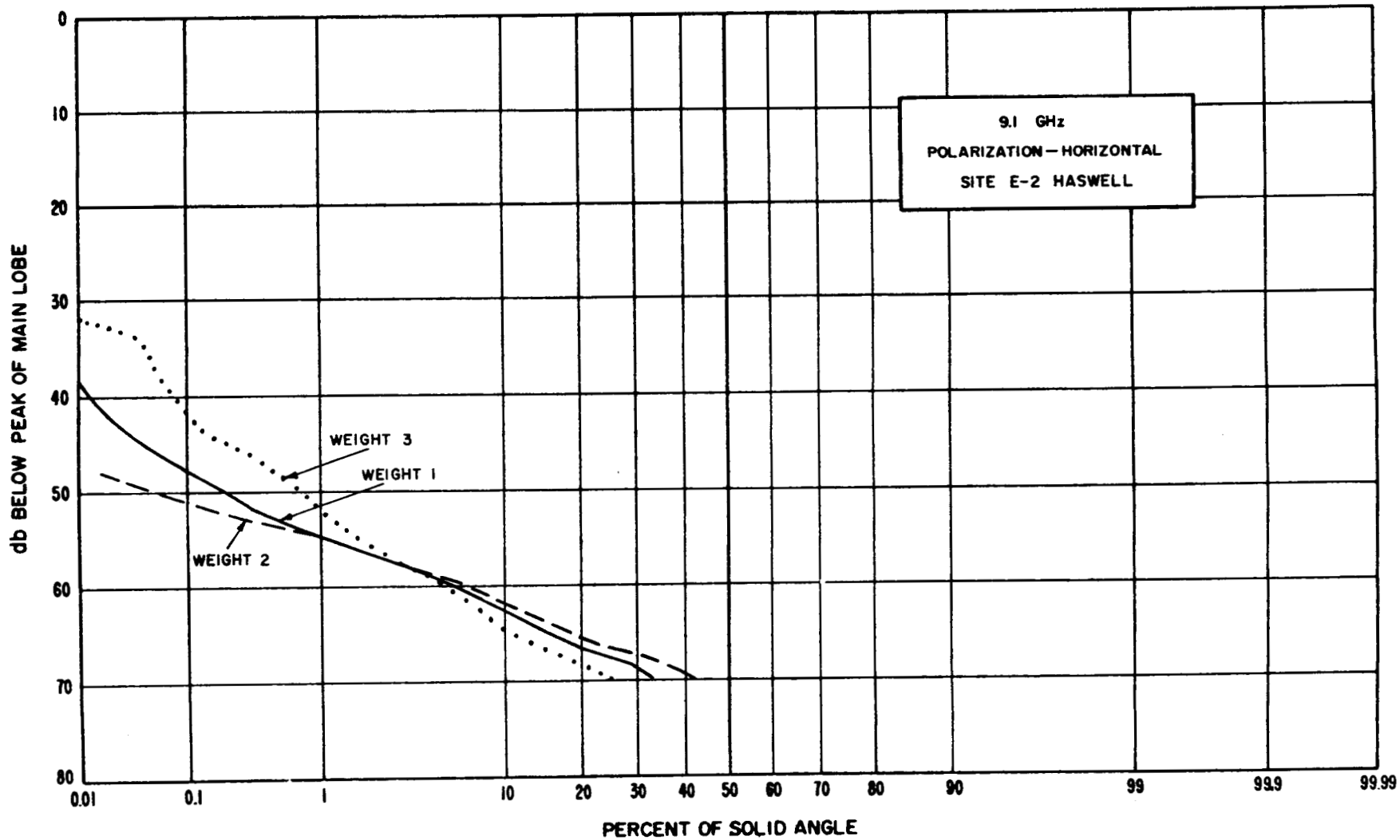

Figure 88

B- 49185

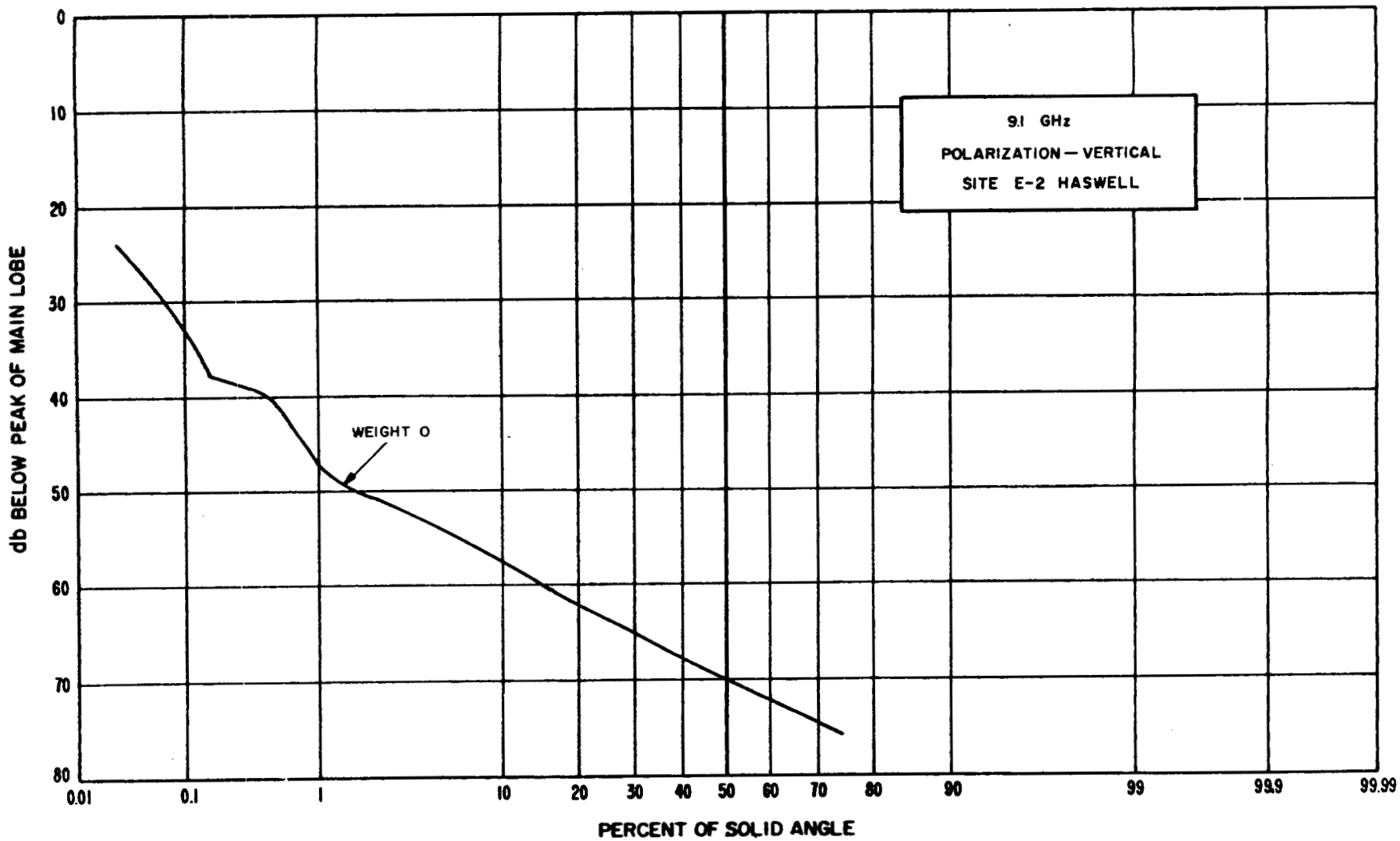

Figure 89

B- 49188

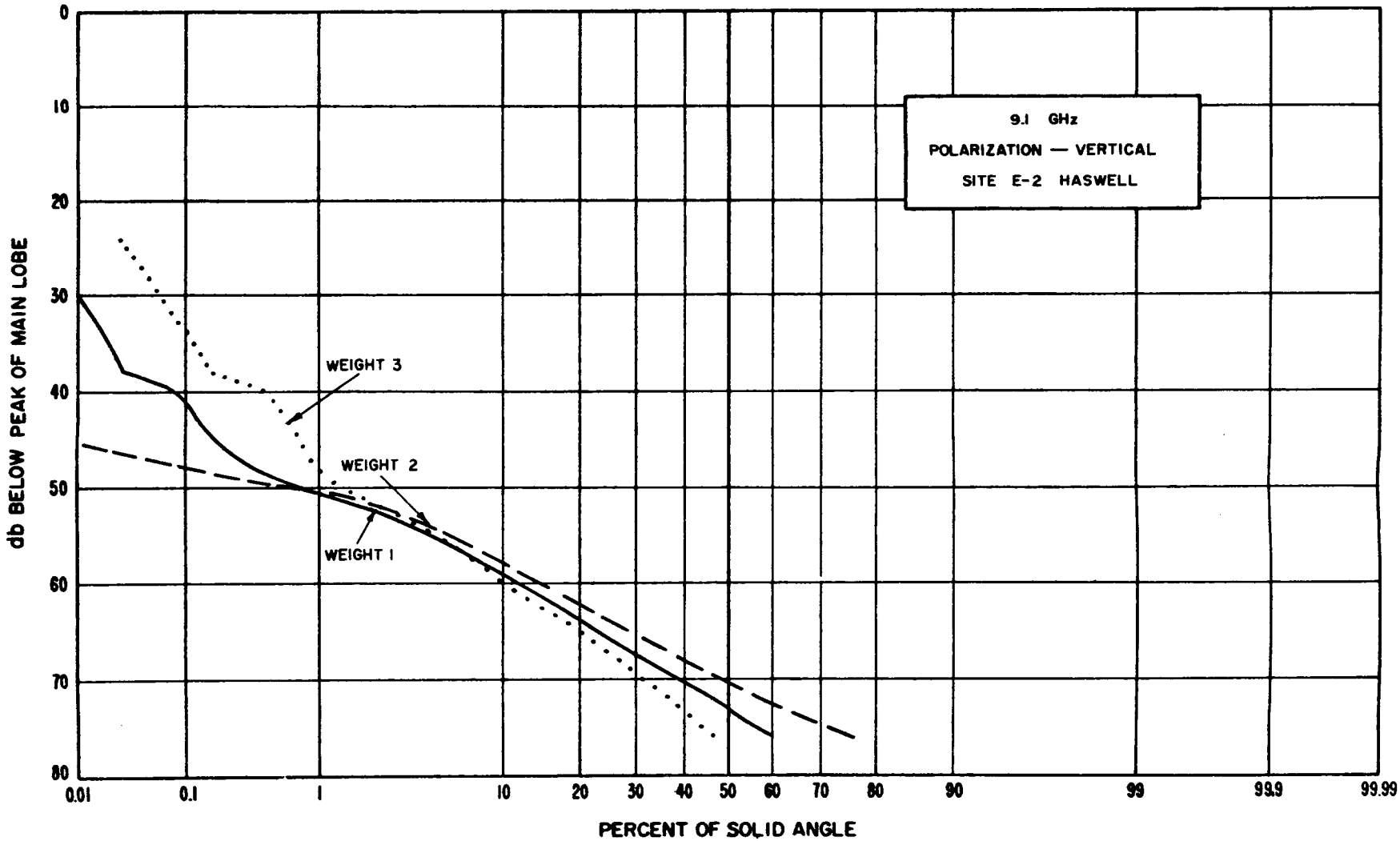

Figure 90

B- 49187

APPENDIX A

Consider the case of interference from a terrestrial microwave link affecting an earth station at an earth-space service. This case involves the same orientations and assumptions as case (b) of CCIR Study Group IV Document No. 45 [1962a]. The ratio R_u of signal power to interfering signal power at the receiving antenna terminals is given by the following expression:

$$R_u = P_{tw} - L_w - (P_{tu} - L_u) \tag{1}$$

where

$$L_u = L_{bu} - G_{tu} - G_{au} \tag{2}$$

P_{tw} = power of wanted transmitter

L_w = wanted signal transmission loss

P_{tu} = power of unwanted transmitter

L_u = unwanted signal transmission loss

G_{au} = random variable relative gain of the earth-space antenna

G_{tu} = relative gain of unwanted signal antenna

L_{bu} = basic transmission loss of unwanted signal path.

G_{au} is stated as a normally distributed random variable in terms of median value relative to isotropic and standard deviation taken from Table 5. Since Table 5 gives median gain relative to main lobe gain, G_{au} is increased by 52 db in the 9.1 GHz case to change the reference to isotropic.

Combining (1) and (2)

$$R_u = P_{tw} - L_w - P_{tu} + L_{bu} - G_{tu} - G_{au} \qquad (3)$$

It is assumed in this example that modulation and bandwidth of the desired and interferring signals are similar. The following numerical values are assumed:

P_{tw} = 1 watt (+30 dbm)

L_w $\overline{L_w}$ = 150 db; σ_{Lw} = 3 db

R_{ur} = 40 db for required error rate

P_{tu} = 100 mw (+ 20 dbm)

L_{bu} $\overline{L_{bu}}$ = 170 db; $\sigma_{L_{bu}}$ = 3 db

G_{au} $\overline{G_{au}}$ = -21 (-73 + 52) db; $\sigma_{G_{au}}$ = 10 db

G_{tu} = 0 db

$\overline{R_u}$ = + 30 dbm - 150 - 20 dbm + 170 + 21 - 0 = 51 db

Assuming that the variables are independently and normally distributed, when standard deviations are included

$$\sigma_{Ru} = (\sigma^2_{Lw} + \sigma^2_{L_{bu}} + \sigma^2_{G_{au}})^{1/2} \qquad (4)$$

$$\sigma_{Ru} = (3^2 + 3^2 + 10^2)^{1/2} = 10.9 \text{ db} \qquad (5)$$

This calculation assumes the basic transmission losses can be approximated by normal distributions and that all earth-space antenna tracking angles are equally likely in time. The ratio of signal power, R_u, will then be a normally distributed random variable with mean value 51 db and standard deviation 10.9 db. This distribution will provide a signal ratio of 40.1 db (51 - 10.9) or greater 84% of the time.

If R_{ur} of 40 db is required to be available 99.5% of the time, $\overline{R_u}$ must be increased by using greater physical separation between the earth station and terrestrial microwave antenna.